Universität Rostock Traditio et Innovatio

Aus der Professur für Bodenphysik
der Agrar- und Umweltwissenschaftlichen Fakultät

Seawater effects on water flow and solute mobility in peat soils

Kumulative Dissertation
zur Erlangung des akademischen Grades
Doktor der Agrarwissenschaften (Dr. agr.)

an der Agrar- und Umweltwissenschaftlichen Fakultät
der Universität Rostock

vorgelegt von Dipl.-Hydrol. Lennart Gosch
wohnhaft in Rostock

Rostock, 2021

https://doi.org/10.18453/rosdok_id00003385

Gutachter

Prof. Dr. Bernd Lennartz	Universität Rostock
PD Dr. Stefan Forster	Universität Rostock
Prof. Dr. Stephan Glatzel	Universität Wien

Eingereicht am: 08. März 2021

Verteidigt am: 28. Oktober 2021

CONTENTS

I LIST OF FIGURES

II LIST OF TABLES

III LIST OF SYMBOLS AND ABBREVIATIONS

$\varnothing$	Diameter of soil sample *(cm)*	p	Atmospheric pressure *(Pa)*
A	Cross-section of a soil sample *(cm²)*	Pe	Peclet number *(-)*
ADE	Advection-dispersion equation	PR	Pump rate *(mL h^{-1})*
BTC	Breakthrough curve	PV	Pore volume (-)
c	Concentration *(mg L^{-1})*	q	Water flux *(cm d^{-1})*
C/N	Ratio of carbon to nitrogen *(-)*	Q	Water flow *(cm^3 d^{-1})*
CDOM	Colored dissolved organic matter	R	Retardation factor *(-)*
CEC	Cation exchange capacity *(mmol kg^{-1})*	R_{gas}	Gas constant (8.314 Pa m^3 K^{-1} mol^{-1})
D	Effective dispersion coefficient *(cm^2 h^{-1})*	SAR	Sodium adsorption ratio *(-)*
DIC	Dissolved inorganic carbon *(mg L^{-1})*	SGD	Submarine groundwater discharge
DOC	Dissolved organic carbon *(mg L^{-1})*	SRB	Sulfate-reducing bacteria
DOM	Dissolved organic matter	t	Time *(h or d)*
dwt	dry weight	T	Temperature *(°C or K)*
EA	Electron acceptor	v	Average pore water velocity *(cm h^{-1})*
EC	Electrical conductivity *(mS cm^{-1})*	V	Volume of soil sample *(cm^3)*
F_{gas}	Water/headspace gas flux *(µmol m^{-2} d^{-1})*	V_h	Volume of the headspace *(m^3)*
FTR	Flow-through reactor	z	Distance *(cm)*
g	Gravitational acceleration (≈ 9.81 m s^{-2})	α	Exchange rate coefficient *(d^{-1})*
h	Hydraulic head *(cm)*	β	Fraction of the mobile water content *(-)*
k	Intrinsic hydraulic permeability *(m^2)*	θ_{mo}	Mobile water content *(cm^3 cm^{-3})*
K	Hydraulic conductivity *(cm d^{-1})*	λ	Dispersivity *(cm)*
K_i	Initial saturated hydraulic conductivity *(cm d^{-1})*	μ	First-order transformation rate constant *(h^{-1})*
K_s	Saturated hydraulic conductivity *(cm d^{-1})*	μ_f	Viscosity of a fluid *(kg m^{-1} s^{-1})*
L	Length of soil sample *(cm)*	ρ_b	Bulk density *(g cm^{-3})*
LOI	Loss on ignition *(%)*	ρ_f	Density of a fluid *(kg m^{-3})*
n	Number of samples	ρ_s	Particle density *(g cm^{-3})*
MIM	Mobile-immobile model	Φ	Total porosity *(-)*
OM	Organic matter	ω	Exchange coefficient between mobile and immobile regions *(-)*

IV SUMMARY

The climate change-induced sea-level rise exposes more and more low-lying coastal areas to an increased temporary or permanent seawater influence. The resulting soil salinization has distinct consequences for organic peat soils, whose physicochemical properties are more likely to change during seawater inflow than they would for mineral soils. The high ion load of seawater including sodium (Na^+), chloride (Cl^-) and sulfate (SO_4^{2-}) affects the organic peat matrix leading to potential changes in water flow, solute transport and solute release.

This thesis aimed to reveal and quantify the seawater effects on these peat soil processes using different laboratory flow-through experiments. Therefore, intact soil cores were taken from drained fens, which represent the most common peatland type in the southern Baltic Sea region. The peat cores were exposed to fresh, brackish or ocean water treatments and parameters of water flow, solute transport and solute release were monitored. Additionally, sea-exposed peat from a coastal fen was included in the experiments to explore its solute exchange behavior as a marine sediment as well as potential long-term seawater effects.

The peat's saturated hydraulic conductivity (K_s), the key soil parameter for water flow, showed a decreasing trend with test time and was not affected by a change of water salinity. This was unexpected as previous studies on bog peat reported a salinity-induced increase of K_s, which was attributed to a chemical pore dilation. Presumably, the non-occurrence of the pore dilation is linked to the tested peat's chemistry and could be due to elevated iron contents, which are often featured by drained fens. Iron oxides may interfere with salinity-induced precipitation processes and delay an increase in K_s and thus a more widespread distribution of sea salts in the peatland.

In terms of solute transport, all peats exposed to saline conditions showed typical non-equilibrium flow patterns analogue to freshwater conditions. Sulfate transport resembled bromide transport and thus had a conservative (i.e. non-reactive) character. Sulfate reduction required an input solution additionally enriched in acetate, which served as a labile organic carbon source for sulfate-reducing bacteria. Even then sulfate reduction only occurred after a lag time of 17 days, which may be attributed to an initial inhibitory iron reduction. With the beginning of sulfate reduction, an increased release of dissolved carbon, nitrogen and

phosphorus was observed, which demonstrates the risk for nutrient release in case of peat decomposition.

The release of dissolved organic carbon (DOC) slightly increased with rising water salinity, which — just like the decrease in K_s — contradicts results of previous studies, which reported an abrupt decrease in DOC release after a rise in salinity. It stands to reason that this fact is likewise related to the peat's chemistry and could be attributed to anion exchange processes that may occur on organometallic complexes. Conversely, the sea-exposed peat released during alternating saltwater-freshwater inflows more DOC and also more carbon dioxide (CO_2) and methane (CH_4) under less saline conditions, underlining the peat's potential as carbon source for the marine environment in case of freshwater submarine groundwater discharge (SGD).

Overall, short-term seawater effects on water and matter fluxes in peat depend on the environmental conditions, which are in turn strongly affected by the peatland's land-use history, and therefore differ considerably among peatlands. The interaction of geochemical and hydrophysical soil properties determines the mobility of solutes. Initial leaching and desorption processes and, later on, an enhanced, sulfate-related decomposition of organic matter may lead to nutrient emission into adjacent aquatic ecosystems. However, the analysis of the sea-exposed peat indicated that in case of long-term seawater submergence most of the geochemical and hydrophysical peat properties may remain rather unaffected.

V ZUSAMMENFASSUNG

Der klimawandelbedingte Anstieg des Meeresspiegels setzt immer mehr tiefliegende Küstengebiete einem erhöhten temporären oder dauerhaften Meerwassereinfluss aus. Die daraus resultierende Bodenversalzung hat spezifische Auswirkungen für organische Torfböden, deren physikochemische Eigenschaften durch Meerwasserzufluss stärkeren Veränderungen unterworfen sind als es für mineralische Böden der Fall ist. Die hohe Konzentration an Salzionen wie Natrium (Na^+), Chlorid (Cl^-) und Sulfat (SO_4^{2-}) beeinflusst die organische Torfmatrix, was zu Änderungen des Wasserflusses sowie des Transports und der Freisetzung gelöster Stoffe führen kann.

Ziel dieser Doktorarbeit war es, Meerwassereffekte auf diese Torfbodenprozesse mithilfe verschiedener Säulenexperimente in Laborversuchen aufzuzeigen und zu quantifizieren. Dafür wurden ungestörte Bodenproben in entwässerten Niedermooren genommen, die in der südlichen Ostsee-Region den häufigsten Moortyp darstellen. Die Proben wurden einem Zufluss von Süß-, Brack- oder Meerwasser ausgesetzt und Parameter hinsichtlich Wasserfluss, Stofftransport und Stofffreisetzung messtechnisch überwacht. Zusätzlich wurde meerexponierter Torf aus einem Küstenniedermoor in die Experimente integriert, um sein Stoffaustauschverhalten als marines Sediment sowie potenzielle Langzeitmeerwassereffekte zu untersuchen.

Die gesättigte hydraulische Leitfähigkeit (K_s), der wichtigste Bodenparameter für den Wasserfluss, zeigte für die in dieser Arbeit untersuchten Niedermoortorfe während der Messung einen abnehmenden Trend und keine Abhängigkeit vom Salzgehalt des Wassers. Dies war unerwartet, da frühere Studien an Hochmoortorf von einem steigernden Effekt einer erhöhten Salinität auf K_s berichten, der einer chemischen Porenaufweitung zugeschrieben wurde. Das Ausbleiben dieses Effektes ist vermutlich auf die Torfchemie zurückzuführen und könnte mit dem für entwässerte Niedermoore typischen erhöhten Eisengehalt zusammenhängen. Eisenoxide können sich störend auf salinitätsbedingte Fällungsprozesse auswirken und somit einen Anstieg von K_s und damit eine umfänglichere Verteilung der Seesalze im Moor verzögern.

Hinsichtlich des Stofftransports zeigten alle untersuchten Torfe unter Salzwasserbedingungen typische Ungleichgewichts-Strömungsmuster, wie sie auch unter Süßwasserbedingungen beobachtet werden. Der Sulfattransport

ähnelte dem Bromidtransport und war folglich als konservativ, d.h. nicht reaktiv, einzustufen. Eine Sulfatreduktion setzte nur bei einer Eingangslösung ein, die mit Acetat angereichert war, welches den sulfatreduzierenden Bakterien als leicht verfügbare Kohlenstoffquelle dient. Selbst in diesem Fall trat die Sulfatreduktion nur mit einer Verzögerungszeit von 17 Tagen ein, was auf eine anfänglich hemmende Eisenreduktion zurückzuführen sein könnte. Mit dem Eintreten der Sulfatreduktion wurde eine verstärkte Freisetzung von gelöstem Kohlenstoff, Stickstoff und Phosphor beobachtet, was das Risiko für Nährstoffaustrag im Fall von Torfzersetzung aufzeigt.

Die Freisetzung von gelöstem organischem Kohlenstoff (DOC) nahm mit steigender Salinität etwas zu, was — analog zu den Ergebnissen für K_s — früheren Studien widerspricht, nach denen die DOC-Freisetzung mit steigender Salinität abrupt abfällt. Es liegt nahe, dass dieser Umstand ebenfalls mit der Torfchemie zusammenhängt und ihm Anionen-Austauschprozesse an metallorganischen Komplexen zugrunde liegen könnten. Dagegen setzte der meerexponierte Torf bei wechselndem Salz- und Süßwasserzufluss mehr DOC und auch mehr Kohlenstoffdioxid (CO_2) und Methan (CH_4) unter salzarmen Bedingungen frei, was seine potenzielle Wirkung als Kohlenstoffquelle für die marine Umwelt im Fall von süßwassergespeisten submarinem Grundwasseraustritt (SGD) hervorhebt.

Insgesamt hängen kurzfristige Meerwasserauswirkungen auf Wasser- und Stoffflüsse im Torf von den Umweltbedingungen im Moor ab, welche stark von der Landnutzung beeinflusst werden, wodurch die Auswirkungen sich je nach Standort stark voneinander unterscheiden können. Dabei bestimmt das Zusammenspiel von geochemischen und hydrophysikalischen Bodenparametern die Mobilität gelöster Stoffe. Anfängliche Auswaschungs- und Desorptionsprozesse und eine später einsetzende sulfatbasierte Zersetzung von organischem Material können zu Nährstoffaustrag in angrenzende aquatische Ökosysteme führen. Allerdings deutet die Analyse des meerexponierten Torfes darauf hin, dass im Fall einer langfristigen Überflutung mit Meerwasser die meisten geochemischen und hydrophysikalischen Torfparameter weitgehend unbeeinflusst bleiben.

1 INTRODUCTION

The global climate change induces a rise of sea-level as well as an increased frequency and level of storm surges (Sterr, 2008). Recent projections of sea-level rise show a world-wide average of 0.63–1.32 m by 2100 and 1.67–5.61 m by 2300, relative to 1986–2005 (Horton et al., 2020), and an accelerating tendency (Nerem et al., 2018). The effect will hit areas with a subsidizing and receding coastline like the southern part of the Baltic Sea hardest (Harff et al., 2017) and expose low-elevation coastal regions to an increased seawater impact in form of submergence, more frequent flooding and saltwater intrusion in aquifers (Nicholls and Cazenave, 2010; Sterr, 2008).

Seawater inflow in terrestrial soils entails an increasing salinity and a changing composition of the dissolved substances of the pore water, which alters the soil's biogeochemistry (Herbert et al., 2015; Tully et al., 2019). This has ramifications for all soil components, but specifically for the organic matter (OM), which is permanently subject to decomposition processes (Paul, 2016; Rath and Rousk, 2015; Sahrawat, 2003). The salinization of wetlands with organic soils such as peat can lead to a severe degradation of the ecosystem (Herbert et al., 2015) and may alter the geochemical and hydrophysical properties of the peat profoundly. Compared to their mineral counterparts peat soils store large amounts of carbon and nitrogen, which renders them highly relevant for the nutrient balance of downstream aquatic ecosystems. Coastal peatlands represent a potential source for lateral nutrient fluxes towards the sea, which can be problematic for surface waters, which are already affected by eutrophication, like it is the case for the Baltic Sea (HELCOM, 2018). Increasing seawater effects on water flow, solute transport and solute release in peat, which govern subsurface exchange processes, may modify the peatland's role regarding water and matter fluxes (Succow and Joosten, 2001).

According to a geographic assessment by Henman and Poulter (2008), approximately 150.000 km² of coastal freshwater peatlands worldwide are below 5-m elevation, i.e. in the range of the projected sea-level rise by 2300. Peatlands also seam the coastline of the North and Baltic Sea (Figure 1.1), but so far, little scientific attention has been given to the interaction between them and the adjacent shallow sea, although the interaction will most likely intensify in the future. The interdisciplinary research project "*Baltic TRANSCOAST - The German*

Baltic Sea Coast as Terrestrial-Marine Interface of Water and Matter Fluxes" launched by the University of Rostock and the Leibniz Institute for Baltic Sea Research Warnemünde (IOW) and funded by the Deutsche Forschungsgemeinschaft (DFG, Grant number "GRK 2000") targets to fill this gap. This thesis is part of the project and addresses the seawater effects on the peat as a water and solute transmitting medium, which plays a key role for the occurring exchange processes between the terrestrial and marine environment such as seawater intrusion and submarine groundwater discharge (SGD), i.e. the inflow of freshwater and recirculated seawater in the shallow coastal waters.

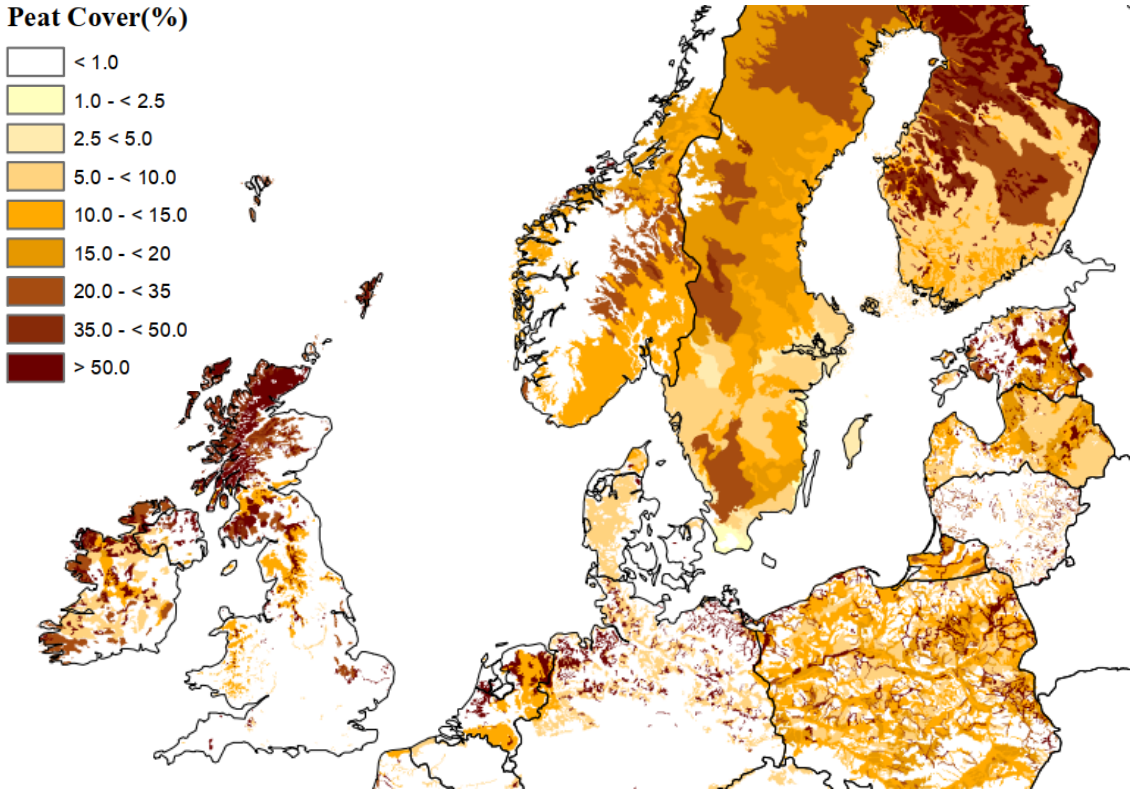

Figure 1.1: Map section from Montanarella et al. (2006): Distribution of peatlands in the North and Baltic Sea region. Edited by R. Hiederer, European Commission, 2010.

1.1 Mires and peat

Pristine peatlands, generally termed "mires" in Europe, are wetlands, in which the long-term average of the water table is close to the land surface. Their characteristic feature is the formation of peat, an organic substrate consisting of partly-decomposed plant material. The permanent waterlogging reduces the supply of oxygen (O_2), which diffuses much slower from the atmosphere through

water saturated soils than through dry soils (Succow and Joosten, 2001). Under these anoxic conditions the microbial consortium acting as decomposers has to rely on less-energy providing electron acceptors than O_2, which slows down the decomposition (i.e. mineralization and humification) of the dead plant material (Göttlich, 1990). The waterlogged conditions also drastically reduce the abundance of shredding invertebrates such as mites, which is why botanical macroremains can be preserved in the peat (Göttlich, 1990; Succow and Joosten, 2001). However, peat formation is a very slow process and amounts mostly to about 1 mm per year (Charman, 2002). A wide range of impact factors affect the peat formation such as plant community (i.e. the decay resistance of the plant material), hydrologic conditions and water chemistry.

In German soil science a peatland is defined as an area with a prevailing peat horizon containing ≥ 30 % dry weight of organic matter with a thickness ≥ 30 cm (Ad-hoc-Arbeitsgruppe Boden, 2005; IPS, n.d.). According to Succow and Joosten (2001) peatlands can be divided into different “hydrogenetic” peatland types. The most important distinction is made between bogs (rainwater-fed peatlands) and fens (groundwater-fed peatlands). A large number of bogs is located in high northern latitudes with a plant community generally characterized by mass occurrence of peat mosses (*Sphagnum*). This plant genus is well adapted to the acidic rainwater regime and possesses hyaline cells, which can store water for low precipitation periods. Large fens are situated in the floodplains, where they form the interface between upland areas and surface waters. Because of the geogenic impact, fens are less nutrient-deficient than bogs, have a more neutral soil *pH* and a plant community mostly dominated by graminoids or brown mosses.

Depending on the plant material it is derived from, peat can look very different and can be classified in various peat types according to the visible botanical macroremains (Meier-Uhlherr et al., 2011). While in bog peat mostly *Sphagnum* pieces can be found (Figure 1.2 a), in fen peat generally the underground parts (roots, rhizomes) of plants such as sedges or reed are preserved (Figure 1.2 b and c). Furthermore, the appearance of the peat is heavily affected by the degree of decomposition; in highly decomposed peat macroremains may be absent and a peat type classification is no longer possible (Figure 1.2 d). The degree of decomposition is mostly determined in the field with the method according to von Post (1922) with which the peat is attributed to a degree of decomposition between 1–3 (poorly-decomposed), 4–7 (moderately-decomposed) and 8–10

(highly-decomposed) based on visible features of a squeezed peat sample and the colour of the outcoming water.

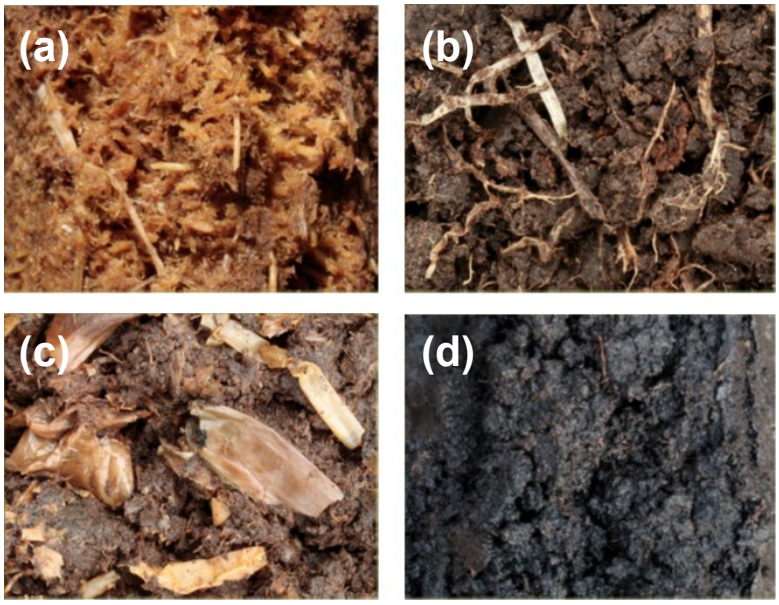

Figure 1.2: Photos of different peat types taken from Meier-Uhlherr et al. (2011). (a) Sphagnum moss peat, (b) sedge peat, (c) reed peat, (d) highly-decomposed peat.

Due to the peat's high OM content, it has properties that are substantially different from mineral soils. The OM consists primarily of carbon (~ 50–60 %), while the remaining parts comprise primarily oxygen and hydrogen, but also smaller amounts of other elements such as nitrogen or phosphorus (Göttlich, 1990). The ratio of carbon to nitrogen (C/N) is an indicator for the degree of decomposition, as it decreases with enhanced decomposition. The C/N is generally higher for bog peat (50 to 100) than for fen peat (15 to 35) due to a higher nitrogen content in fen peat (up to 4 %) caused by nutrient input from the mineral catchment of the fen (Göttlich, 1990).

Because organic matter has a lower particle density ($\rho_s \approx 1.4$ g cm^{-3}) than mineral soil components such as quartz ($\rho_s = 2.65$ g cm^{-3}), the bulk density ρ_b of peat is generally lower than for mineral soils and can range between 0.01 and 0.76 g cm^{-3} (Liu and Lennartz, 2019a). Another reason for the lower ρ_b is the high total porosity (Φ) of peat, which ranges between 62.0 and 98.6 % (Liu and Lennartz, 2019a). As the partly decomposed plant material can appear in many different forms the pore network in peat is particularly complex and susceptible to changes. This leads to a high spatial variability (horizontally and vertically) of soil properties in peat, i.e. specifically its pore network-related, hydrophysical properties.

1.1.1 Importance of peatlands for landscape water and matter balance

Due to the peat's specific soil properties, peatlands have a particular effect on water and matter fluxes in the landscape. They possess a high water storage capacity and fulfill a buffer function in the landscape water balance. However, most of the storage is static instead of dynamic (Succow and Joosten, 2001), which is why their potential to mitigate flood events and reduce flood risks depends on the respective site characteristics such as topography or soil moisture status (Acreman and Holden, 2013). The accumulation of the organic peat material renders peatlands to the globally most important soil carbon stock. While covering only 4 million km² (3 % of the earth's land surface), peatlands store about one-third of the global soil carbon (Joosten and Clarke, 2002). Thus, their carbon sink function is highly relevant for the atmospheric carbon balance and addressing the issue of climate change. For fens, which receive water from mineral catchments, solutes in the runoff are retained due to sorption and degradation processes within the peat as porous and water-saturated medium (Succow and Joosten, 2001). Hence, fens fulfill a filter function in the landscape matter balance, e.g. for dissolved nutrients and pollutants, which reduces nutrient loads to surface waters.

However, the aforementioned ecosystem services get lost when the peatlands are artificially drained. In Europe enhanced efforts were made in the 1970s to intensively drain peatlands for agricultural use and for the exploitation of peat as a fossil fuel (Holden et al., 2004). In Central Europe this development has led to a vast destruction of the pristine peatlands — in Northeastern Germany most of the fens (> 95%) have been drained (Succow and Joosten, 2001). In drained peatlands, the water table is lowered leading to a transition from an anoxic to an oxic milieu. Under these conditions, the peat accumulation stops and instead the peat is aerobically decomposed. Drainage-induced peat oxidation paired with peat compaction leads to land subsidence of approximately 1 cm a^{-1} (Hoogland et al., 2012). The extent of land subsidence can be seen very impressively in the example of the Netherlands, where, due to peatland drainage, about one third of the land area is nowadays below sea level (Hoogland et al., 2012). A large part of the carbon stored in the degrading peat is released as carbon dioxide (CO_2); one hectare of drained peatland in Germany emits around 28 t CO_2 per year (Tiemeyer et al., 2016). The entirety of all drained peatlands in Germany (12,550 km²) (Tanneberger et al., 2017) accounts for approximately 5 % of the country's

greenhouse gas emissions (Tiemeyer et al., 2017a). Furthermore, the degrading peat releases solutes such as dissolved organic carbon (DOC) and ammonium (NH_4^+) (Zak and Gelbrecht, 2007), which can easily be mobilized and transported to aquatic ecosystems. Overall, the consequences of the extensive drainage of peatlands have huge environmental implications. For this reason, there have been increased efforts to rewet peatlands in recent years to restore their biodiversity and/or their carbon and nutrient sink function. As these ecosystem services highly depend on the peat's soil functions of storing, transmitting and retaining water and solutes, attention needs to be paid to the peat's properties and potential alterations due to seawater effects.

1.1.2 Seawater impact in coastal peatlands

Unlike terrestrial peatlands, coastal peatlands can be exposed to seawater incursions in form of flooding, backflow in rivers or intrusion in the groundwater as well as atmospheric salt deposition leading to a natural salinization of a peatland's hydrosphere. The average ocean water salt content (~ 3.5 %) is much higher than the average salt content commonly observed in freshwater ecosystems (e.g. 0.35 % in Chambers et al. (2011)). The salt content in the Baltic Sea as a brackish ecosystem is lower than the average ocean water salt content — in the southern Baltic Sea the average water salinity ranges between 0.6 and 1.6 % (Feistel et al., 2010).

In addition to salt, seawater flooding also carries dissolved oxygen and sediments into the peatland. Peatlands that formed under the impact of seawater flooding (so-called "coastal flooding mires") contain therefore rather decomposed and mineral-rich peats, with peat horizons often separated in the soil profile by silt deposits. Along the coastline of the Baltic Sea approximately 21,000 ha of this type of fen can be found, but are often artificially separated from the sea by dikes (Succow and Joosten, 2001).

Although the majority of the salt content in seawater is formed by sodium (Na^+) and chloride (Cl^-), a long-term effect on the peat soil particles can be expected due to another ion abundant in seawater with particular biogeochemical importance: sulfate (SO_4^{2-}). Sulfate can serve as an electron acceptor in mineralization processes under anoxic conditions and therefore can prolong the decomposition of organic matter. The sulfate-reducing bacteria (SRB) produce sulfide (HS^-), which can react with iron to form iron sulfide (FeS), which precipitates as black mud. An

increased sulfate reduction and iron sulfide formation can lead to different nutrient limitation conditions, since iron oxyhydroxides tend to bind phosphorus in soils and sediments, but release it when they form iron sulfide instead (Weston et al., 2006). Overall, the sulfur cycle in peatlands is very complex as sulfur exists in wetlands in many different organic and inorganic forms and can be oxidized and reduced multiple times within the wetland (Mandernack et al., 2000). In other terrestrial coastal ecosystems (such as saltmarshes and mangroves), sulfate reduction has been shown to represent the dominant mineralization process with 40-90 % of the total C mineralization (Chambers et al., 2014).

Increased SO_4^{2-} concentrations also impact the emission of the greenhouse gas methane (CH_4), which is of great importance for climate change mitigation, because wetlands represent the major natural source for CH_4 (Dean et al., 2018). Active SRB may contribute to lowering CH_4 emissions as they are, to a certain extent, competing with methanogens for available carbon sources, i.e. low molecular weight DOC compounds such as acetate (Weston et al., 2011). Furthermore, anaerobic methanotrophic archaea can use SO_4^{2-} for the oxidation of CH_4 (Boetius et al., 2000). However, coastal peatlands may nevertheless emit CH_4 if suitable carbon sources are not sufficiently limited or are even increased by saltwater inflow due to desorption of DOC (Weston et al., 2011) or when rewetting is mainly accomplished by SO_4^{2-}-poor freshwater inflow (Koebsch et al., 2019).

Just like their inland counterparts, a large proportion of coastal peatlands were drained and put into intensive agricultural use and, additionally, diked to prevent the temporary seawater inundations. Drainage of coastal peatlands can lead to the development of acid sulfate soils caused by the oxidation of FeS, which results in SO_4^{2-} formation and a decrease of *pH* (Portnoy and Giblin, 1997; van Diggelen et al., 2020). The input of high amounts of SO_4^{2-} in adjacent freshwater surface waters can be problematic since SO_4^{2-} reduction in anoxic sediments can, as mentioned above, induce phosphorus mobilization.

After the realization that peatlands provide important ecosystem services, in some coastal peatlands dikes are being removed within the framework of nature conservation projects to intentionally expose the peatland to seawater impact and restore the natural seawater regime (Ostseestiftung, 2016; Portnoy and Giblin, 1997). Some studies suggest that restored, near-natural coastal peatlands might grow together with the sea-level and thus contribute to climate change adaption (Weston et al., 2011). However, for tidal freshwater wetlands Neubauer and Craft

(2009) stated an actual decrease in soil accretion following salinization presumably due to reduced plant productivity and increased soil metabolism, which can also stimulate a large nutrient release (Portnoy and Giblin, 1997).

1.2 Peat soil processes and expected seawater effects

Like their mineral counterparts peat soils can be considered a three phase porous medium consisting of the components air, water and soil particles, in which water (including the dissolved substances) and air move through the pore network formed by the soil matrix. Due to the peat's specific geophysical and -chemical properties, peat soil processes are more prone to be altered under seawater impact than they would for mineral soils. In the following, water flow, solute transport and solute release in peat as well as expected changes during seawater inflow are described.

1.2.1 Water flow

Under saturated conditions, the aqueous phase constitutes up to 90 % of the peat soil volume, which underlines the importance of water fluxes in peatlands. A (laminar) water flow Q (cm³ d^{-1}) through a cross-section area A (cm²) can be described with an equation generally referred to as Darcy's Law (see e.g. Charman, 2002), which also applies to peat soils:

$$\frac{Q}{A} = q = -K_s \cdot \left(\frac{\delta h}{\delta L}\right) \quad (1)$$

with q as the water flux (cm d^{-1}), K_s as saturated hydraulic conductivity (cm d^{-1} or m s^{-1}), ∂h as pressure head difference (cm) and ∂L as length of the soil sample (cm). The ratio of ∂h and ∂L is commonly termed "hydraulic gradient". The variable in this equation is ∂h, while K_s is generally considered a constant soil hydraulic parameter, which depends on the intrinsic hydraulic permeability k (m²) of the soil and the viscosity μ_f (kg m^{-1} s^{-1}) and density ρ_f (kg m^{-3}) of the fluid as well as the gravitational acceleration g (≈ 9.81 m s^{-2}):

$$K_s = k \cdot \frac{\rho_f \cdot g}{\mu_f} \quad (2)$$

Under natural conditions K_s is constantly subject to slight changes since temperature and salinity affect μ_f and ρ_f of water. The order of magnitude of k (and

consequently K_s) is determined by the pore network characteristics, such as diameter, shape, number, orientation and continuity of the pores (Rezanezhad et al., 2009). Thus, K_s of peat depends on factors affecting the pore network such as peat type, degree of decomposition or bulk density. Average K_s values for different peat types are shown in a meta study by Liu and Lennartz (2019a). They found an average K_s value of 22 cm d^{-1} for sedge fen peat and a very high variance indicated by a standard deviation of 159 cm d^{-1} and a minimum and maximum of 0.04 and 1739 cm d^{-1}, respectively.

While in mires K_s generally decreases with depth as the peat is more decomposed and compacted in deeper soil horizons, in drained peatlands the upper peat horizon often is the one most decomposed and may therefore hamper water inflow (e.g. when water is dammed up in the ditches to resaturate the peatland) (Succow and Joosten, 2001; Zeitz and Velty, 2002). Further processes that change the pore network and consequently K_s are root penetration (K_s ↑), the formation of shrinkage cracks paired with high wetting resistance (K_s ↑) (Miegel et al., 2016) and bioclogging (K_s ↓) (Kleimeier et al., 2014).

In case of seawater inflow salinity-induced coagulation of the OM may affect K_s. The coagulation can be caused by cation bridging by polyvalent ions such as Ca^{2+} or Mg^{2+} (Tiemeyer et al., 2017b) and can be enhanced by large amounts of monovalent cations such as Na^{+}, which reduce the charge density of the organic molecules and therefore reduce the repulsions forces (Kalbitz et al., 2000; Strehse et al., 2018). Ours et al. (1997) observed an increase of K_s during flow of chloride solutions through bog peat (Figure 1.3) and attributed this to a chemical pore dilation caused by coiling of the humic acids at the edges of the pores. The K_s-increasing effect of an increased ionic strength and a reduced *pH* was later confirmed by several other laboratory and mesocosm studies on bog peat (Comas and Slater, 2004; Kettridge and Binley, 2010; van Dijk et al., 2017). To date, studies on fen peat are scarce but needed to validate the processes' occurrence for different peat types.

When measuring K_s, it is important to note if the samples were taken vertically or horizontally. Particularly in case of less decomposed peat, the plant residues in the peat may cause anisotropic behavior. Most studies on fen peat report that the vertical K_s is higher than the horizontal K_s (Kruse et al., 2008; Wang et al., 2020). This has implications for the exchange processes, since in case of a higher vertical K_s water flow towards the groundwater prevails while a higher horizontal K_s

may promote the water flow towards a draining ditch system (Miegel et al., 2016). However, a recent study within *Baltic TRANSCOAST* showed that the anisotropy has less effect on solute transport and release than on K_s (Wang et al., 2020).

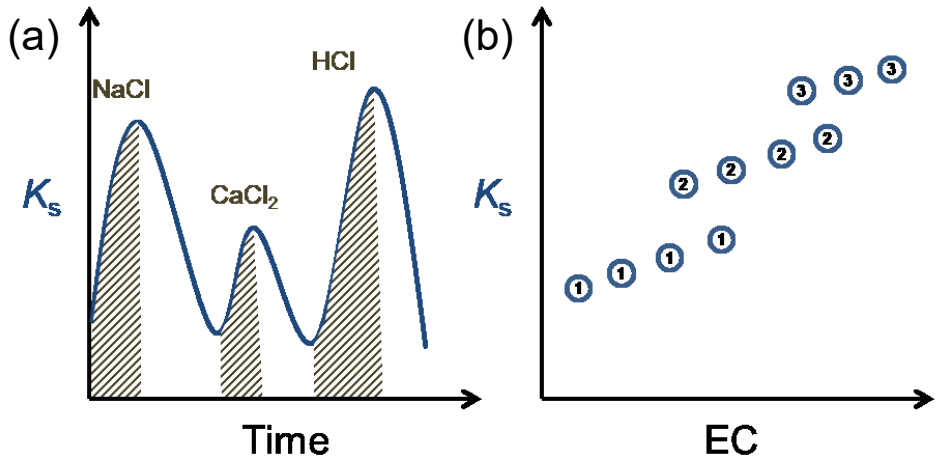

Figure 1.3: Illustration of an increase of the saturated hydraulic conductivity (K_s) of bog peat with rising water salinity observed by Ours et al. (1997) and Kettridge and Binley (2010). (a) Finding by Ours et al. (1997) that K_s increases during through-flow of NaCl, $CaCl_2$ and HCl solutions (indicated by hatched area), while it decreases during through-flow of deionized water (non-hatched area). (b) Observed relation between K_s and electrical conductivity (*EC*) of the outflow during K_s test in Kettridge and Binley (2010). The circles represent single measurements of K_s on the same peat sample, but on different days (indicated by numbers) of the experiment.

1.2.2 Solute transport

Pore water acts as solvent and transport medium for various substances in the soil. In case of seawater inflow major concentrations of sodium (Na^+) and chloride (Cl^-), but also of calcium (Ca^{2+}), magnesium (Mg^{2+}), potassium (K^+), sulfate (SO_4^{2-}) and hydrogencarbonate (HCO_3^-), enter the peatland (Sigg and Stumm, 2011). Each solute is subject to different transport processes in the soil; the most important ones are advection, dispersion, diffusion, adsorption and degradation. Their combined solute transport can be described mathematically with the advection dispersion equation (ADE). For one-dimensional, steady-state conditions the ADE is (Radcliffe and Simunek, 2010):

$$R\frac{\partial c}{\partial t} = D\frac{\partial^2 c}{\partial z^2} - v \cdot \frac{\partial c}{\partial z} - \mu c \qquad (3)$$

with the variables *t* (h) *as* time, *c* (mg L^{-1}) as concentration and *z* (cm) as distance and the parameters *v* (cm h^{-1}) as average pore water velocity (advection),

D ($cm^2\ h^{-1}$) as effective dispersion coefficient (dispersion and diffusion), R (-) as retardation factor (adsorption) and μ (h^{-1}) as first-order transformation rate constant (degradation). To obtain these parameters, inverse modeling with the help of a breakthrough curve (BTC), i.e. the concentration of a tracer at a certain depth plotted as a function of time, can be carried out. For this purpose, generally solutes considered inert (i.e. only advection, dispersion and diffusion are relevant so that R = 1 and μ = *0)* like bromide (Br^-) or chloride (Cl^-) are used (e.g. Baird and Gaffney (2000)). However, for most solutes moving in peat, adsorption and/or degradation need to be taken into account.

Due to a large amount of carboxylic and phenolic OH-groups, soil organic matter is mainly negatively charged, which is why cations in particular tend to interact with the peat soil matrix via surface adsorption. They are more attracted to the edges of the pores, while anions are being repulsed and tend to be found in the center of the pores, where the pore water velocity is higher (Hillel, 1998). Thus, for cations in peat R is generally > 1; reported values for sodium (Na^+) are in the range of 1.22 to 3.07 (Rezanezhad et al., 2012; Simhayov et al., 2018; McCarter et al., 2018). However, the cation adsorption is reversible — the differently charged cations can replace each other. Thus, when other cations like K^+ or NH_4^+ are present in the pore water, R values of Na^+ may decrease to 1.01 – 1.98 (McCarter et al., 2018). The cation exchange capacity (*CEC*) of peat is generally high (McCarter et al., 2018) and was reported to range between 960 and 1430 mmol kg^{-1} for fen peat (Rydelek et al., 2016). The *CEC* of peat depends on the amount and kind of cations as well as the functional groups in the peat matrix and increases with increasing *pH* due to variable charges (Succow and Joosten, 2001) and decreasing *EC* due to the uncoiling of humic acids leading to an increase of sorbing surface (Caron et al., 2015). It is also generally higher for highly-decomposed peat than for poorly-decomposed peat, because of the increased specific surface area of more decomposed peat (Ottow, 2011).

Batch experiments have shown no or only weak adsorption of anions on peat, for example chloride (Cl^-) for which McCarter et al. (2018) stated R = 1.07 with an increasing tendency at higher Cl^- concentrations. Weak anion adsorption may be associated with positively charged amino groups, whose anion adsorption capacity increases with decreasing *pH* (Ottow, 2011). This indicates that this process primarily takes place under acidic conditions rendering it more important for bog peat than for fen peat. Anion mobility in peat is especially interesting for SO_4^{2-} due

to its relevance for decomposition processes. However, systematic studies on sulfate mobility in peat are lacking.

In peat soils, measured BTCs can often not be simulated adequately with the ADE in form of Equation 3 due to an early breakthrough, i.e. C/C_0 = 0.5 (step input) or a peak arrival time (pulse input) at less than one pore volume (PV), and tailing of the curve (Baird and Gaffney, 2000; Rezanezhad et al., 2017). This phenomena, also observed in mineral soils (Gerke and van Genuchten, 1993), is generally attributed to the occurrence of preferential flow, also referred to as physical non-equilibrium flow, due to a heterogeneity of the pore network. To depict this anomalous behavior in solute transport models van Genuchten and Wierenga (1976) developed the mobile immobile model (MIM) also known as dual-porosity approach. This approach divides the pore network into a mobile zone, where water and solute transport takes place (also referred to as active porosity) and an immobile zone, which only serves as solute sink or source though solute-exchange via diffusion (also referred to as inactive porosity). The diffusion of solutes in the immobile zone leads to a mechanical retardation of the solute, whose effect on the BTC is similar to the adsorption in the peat. The ADE can be expanded for the non-equilibrium flow with “mo” and “im” referring to the mobile and immobile zone, respectively (Toride et al., 1999):

$$\beta R \frac{\partial c_{mo}}{\partial t} = \frac{1}{Pe} \frac{\partial^2 c_{mo}}{\partial z^2} - \frac{\partial c_{mo}}{\partial z} - \omega(c_{mo} - c_{im}) - \mu_{mo} c_{mo} \quad (4)$$

$$(1-\beta) R \frac{\partial c_{im}}{\partial t} = \omega(c_{mo} - c_{im}) - \mu_{im} c_{im} \quad (5)$$

with the two dimensionless parameters β and ω, which are used to parametrize the non-equilibrium conditions, and Pe as the Peclet number ($Pe = v \times L/D_e$), which indicates if advection or dispersion prevails. If no adsorption occurs or the adsorptions sites are assumed to be equally distributed in the mobile and immobile region, the parameter β represents the fraction of the mobile water content ($\beta = \theta_{mo}/\theta$) (Radcliffe and Simunek, 2010). The second parameter ω is the mass transfer coefficient for the transfer between the two phases ($\omega = \alpha_s \times L/q$, with α_s as the exchange rate coefficient (s^{-1})). Generally, values for β and ω range between 0.3 to 1 and 0.1 to 5, respectively. A low β indicates the existence of macropores, i.e. preferential flow, while a low ω indicates a very slow solute

exchange between the mobile and immobile zones so that there is no equilibrium between the mobile and immobile zone (Radcliffe and Simunek, 2010).

Liu et al. (2017) tested the performance of equilibrium and non-equilibrium-models for BTCs of fen peat samples with different OM content. Only 10 % of the samples (all with OM content > 80 %) were simulated best with the “single-porosity” ADE. All peat samples with a low OM content showed non-equilibrium flow, characterized by early breakthrough and tailing (Figure 1.4). These BTCs were better simulated with a dual-porosity approach, with MIM parameter values for β and ω ranging between 0.48–0.86 and 0.02–0.46, respectively. The authors concluded that the pore network in more pristine peat is more continuous and that with an enhanced decomposition the proportion of dead-end pores increases. This could imply a reduced filter and buffer function of the degraded peat as solutes interact less with the soil matrix.

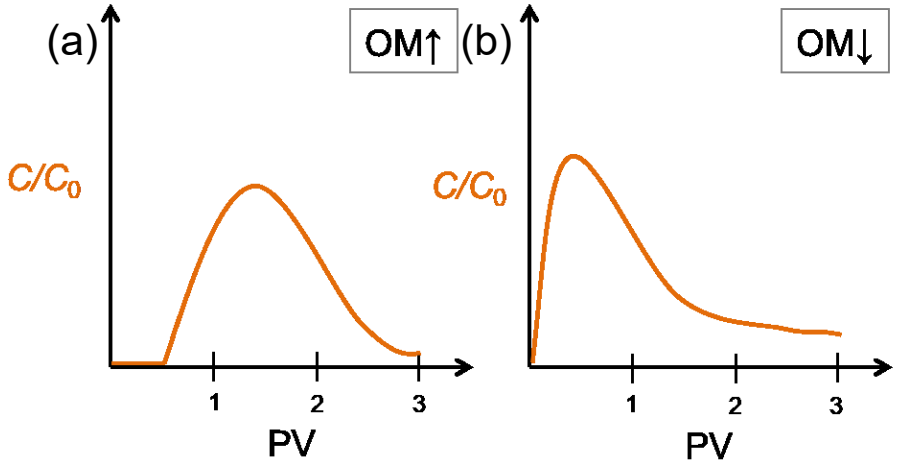

Figure 1.4: Illustration of breakthrough curves (BTC) of a tracer pulse input for fen peat following the results by Liu et al. (2016). PV = pore volume, C/C_0 = ratio of measured tracer concentration to tracer concentration in input solution. (a) BTC for a peat sample with a high organic matter (OM) content without preferential flow, which can be simulated with the advection-dispersion equation (ADE), (b) BTC for a peat sample with lower OM content with preferential flow characterized by early breakthrough and tailing, which cannot be simulated with the ADE, but with the mobile-immobile model (MIM).

However, Kleimeier et al. (2017) found a higher nitrate (NO_3^-) removal rate for degraded peat than for undegraded peat which they attributed to a higher percentage of immobile water fractions which supposedly acted as hotspots for the denitrification. This goes along with the assumption that microorganisms preferably reside in smaller pores (Watt et al., 2006) which tend to be part of the

immobile zone (Rezanezhad et al., 2017). The microorganisms also produce solutes by decomposing the OM, which leads to the release of solutes which originate from the peat.

1.2.3 Solute release

While mineral soils tend to release primarily inorganic products of weathering to the aqueous phase, peat soils release soluble end- and intermediate products of mineralization and humification of the OM. The common land-use sequence of pristine conditions, drainage and rewetting has far-reaching implications for the biogeochemistry of peatlands (Koebsch et al. 2019, van Diggelen et al. 2020) and complicates the assessment of salinity related changes of solute release.

Generally, peatlands represent a major source for dissolved organic carbon (DOC) or more generally dissolved organic matter (DOM) in surface water; Aitkenhead et al. (1999) found a correlation coefficient of 0.83 between DOC concentrations in Scottish streams and the peat cover (%) in their catchment. Because DOC fuels food webs, transports pollutants and limits light availability (Ardón et al., 2016), increased DOC concentrations can have a huge impact on aquatic ecosystems. In water for human use high DOC concentrations are problematic as the organic substances can react with chlorine and therefore reduce the elimination capacity regarding germs and lead to the formation of potential carcinogens like trihalomethanes (Worrall et al., 2007).

The DOM consists of different fractions of which some are rapidly degradable (labile fraction), some are degraded more slowly and some are recalcitrant, whereby the biodegradability generally decreases with an increasing proportion of aromatic structures (Marschner and Kalbitz, 2003). The DOM released from peat is usually classified as not easily degradable (Kalbitz et al., 2003). How much DOC is released from a peatland depends on a variety of environmental parameters such as water level as well as temperature, *pH* and *EC* (Worrall et al., 2007). Thus, DOC export can show a high temporal variability. Glatzel et al. (2003) measured DOC concentrations of 35-625 mg L^{-1} in natural, harvested and restored peat bogs and Schwalm and Zeitz (2015) observed a range of 4–123 mg L^{-1} at the outlet of a fen lysimeter. Although the drainage of peatlands leads primarily to a carbon loss in form of carbon dioxide emission (according to Chambers et al. (2014) ~ 95 %), drained peatlands and degraded peat also tend to release more DOC than pristine peatlands due to increased oxidation processes (Schwalm and

Zeitz, 2015). In the last decades, the DOC concentrations in surface waters in Europe and North America have increased (Monteith et al., 2007). The reasons for this development are still subject to debate, but identified stressors are the recovery of soils from atmospheric acid deposition, land-use change, increased nitrogen deposition and climate change (Meyer-Jacob et al., 2019).

The impact of the water salinity on solute release is shown by the processes that occur once the rivers reach the ocean. A part of the dissolved organic and inorganic substances from river water are precipitated in estuaries when the fresh water is mixed with seawater. Sholkovitz (1976) found that 3 to 11 % of riverine humic substances flocculated during estuarine mixing in a salinity range from 0 to 1.5 %. Together with salinity-induced desorption (DOC↑), coagulation processes (DOC↓) constitute the way how an increased water salinity directly affects DOC release (Reemtsma et al., 1999). Generally, the DOC release from peat decreases considerably and abruptly when water salinity is increased (Tiemeyer et al., 2017b), which has been shown not only for bog peat, but also for fen peat (Liu and Lennartz, 2019b) (Figure 1.5). But seawater inflow in a peatland can affect the release of DOC through various other mechanisms (Ardón et al., 2016), such as a decreased biomass production due to salt-damages to plants (DOC↓) or an increased mineralization of OM due to sulfate reduction (DOC↑). This might affect the nutrient supply of the marine biota as coastal wetlands represent a large source for terrestrially derived DOC for marine ecosystems, especially during storm events (Ardón et al., 2016).

During seawater inflow coastal peatlands can also act as a source for nitrogen (Ardón et al., 2013; Weston et al., 2006). Due to the high ionic strength of seawater and the high *CEC* of peat, seawater cations replace cations previously bound to the peat matrix, such as NH_4^+ (Liu and Lennartz, 2019b) (Figure 1.5). Due to a fertilization effect, the release of NH_4^+ can be particularly pronounced when the coastal peatland is currently drained or was drained in the past (Ardón et al., 2013). The release of NH_4^+ can potentially contribute to eutrophication of coastal waters, which naturally are often nitrogen-limited (Howarth and Marino, 2006). At the same time the release of organically bound nitrogen may be reduced (Ardón et al., 2013) as the same mechanisms apply as for DOC.

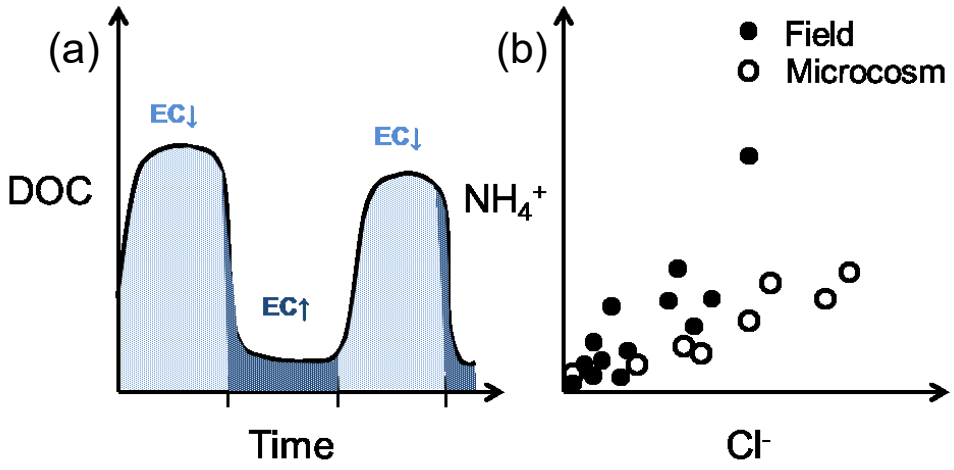

Figure 1.5: Illustration of (a) DOC release from peat with increasing electrical conductivity (EC) as observed by Liu and Lennartz (2019b) and (b) relationship between NH_4^+ and Cl^- in wetland surface water and a microcosm experiment by Ardón et al. (2013).

1.3 Objectives, hypotheses and outline of this thesis

The overall objective of this thesis was to study seawater effects on water flow, solute transport and solute release in (saturated) fen peats as the dominant peat substrate in the Baltic Sea region (Figure 1.6). Since seawater impact on peatlands can be temporary and/or persisting, short-term as well as long-term consequences were of interest. Seawater inflow in peat creates different biogeochemical conditions than they would prevail in a purely terrestrial site. This affects the pore water and may alter the hydrophysical parameters of the peat, which govern the water and solute exchange between peatlands and adjacent aquatic ecosystems such as the sea. The specific objectives and the associated hypotheses (marked in bold), which are based on the current state of research (see Chapter 1.2), were formulated as follows:

(i) Water flow: The most crucial hydraulic parameter for water flow is K_s, which has been shown to depend on water salinity for bog peat (Kettridge and Binley, 2010; Ours et al., 1997; van Dijk et al., 2017). Therefore, this thesis aimed at verifying and quantifying seawater effects on K_s of fen peat for different water salinities.

It was hypothesized that K_s of fen peat increases with increasing water salinity due to a chemical pore dilation effect.

(ii) Solute transport: Seawater inflow carries great amounts of seawater ions such as Na^+, Cl^- and SO_4^{2-} into the peatland. In terms of solute transport, this thesis focussed on SO_4^{2-}, which most likely affects the peat soil matrix and the pore network due to its function as electron acceptor, and seeked to study the transport properties of fen peat for different SO_4^{2-} concentrations.
It was hypothesized that the transport of seawater-derived SO_4^{2-} in fen peat differs from conservative anion transport (e.g. Br^-) due to its biogeochemical reactivity, but may still be characterized by physical non-equilibrium flow, notably in highly-decomposed peat.

(iii) Solute release: Due to its high OM content the release of solutes from peat is dominated by organic compounds measurable as DOC. This thesis aimed at verifying the negative correlation between DOC release and water salinity for seawater-exposed fen peat.
It was hypothesized that seawater inflow reduces the release of DOC from fen peat due to salinity-induced coagulation processes, although anion exchange processes can also lead to a desorption of DOC.

(iv) Long-term seawater effects: Sea-level will in some cases lead to a permanent inundation of previously terrestrial peat soil, turning it into a marine sediment exposed to impact factors such as increased water salinity, wave action, sediment transport, algae growth or bioturbation. This thesis strived to reveal potential long-term seawater effects on geochemical and hydrophysical peat properties and how peat acts as a coastal sediment in terms of exchange processes such as SGD.
It was hypothesized that due to seawater-induced intrusion of O_2 and SO_4^{2-} the peat is subject to enhanced decomposition-related changes, which may imply an enhanced physical non-equilibrium flow, and that peat deposits serve as long-term carbon source for the adjacent shallow sea.

The hypotheses were tested with several laboratory-based studies on fen peat. Compared to bog peat fen peat is less well-studied: a Scopus inquiry on 6 July 2020 resulted with 5.516 publications for “bog peat” and only 1.789 publications for

"fen peat". Therefore, the question arises whether the findings for bog peat can be transferred to fen peat. Samples for the experiments were taken at different locations, main sampling sites were *Pölchow*, a drained fen, which has not been affected by seawater inflow, and the *Hütelmoor*, a formerly drained but nowadays rewetted coastal fen directly at the Baltic Sea, which serves as mutual study site in *Baltic TRANSCOAST*.

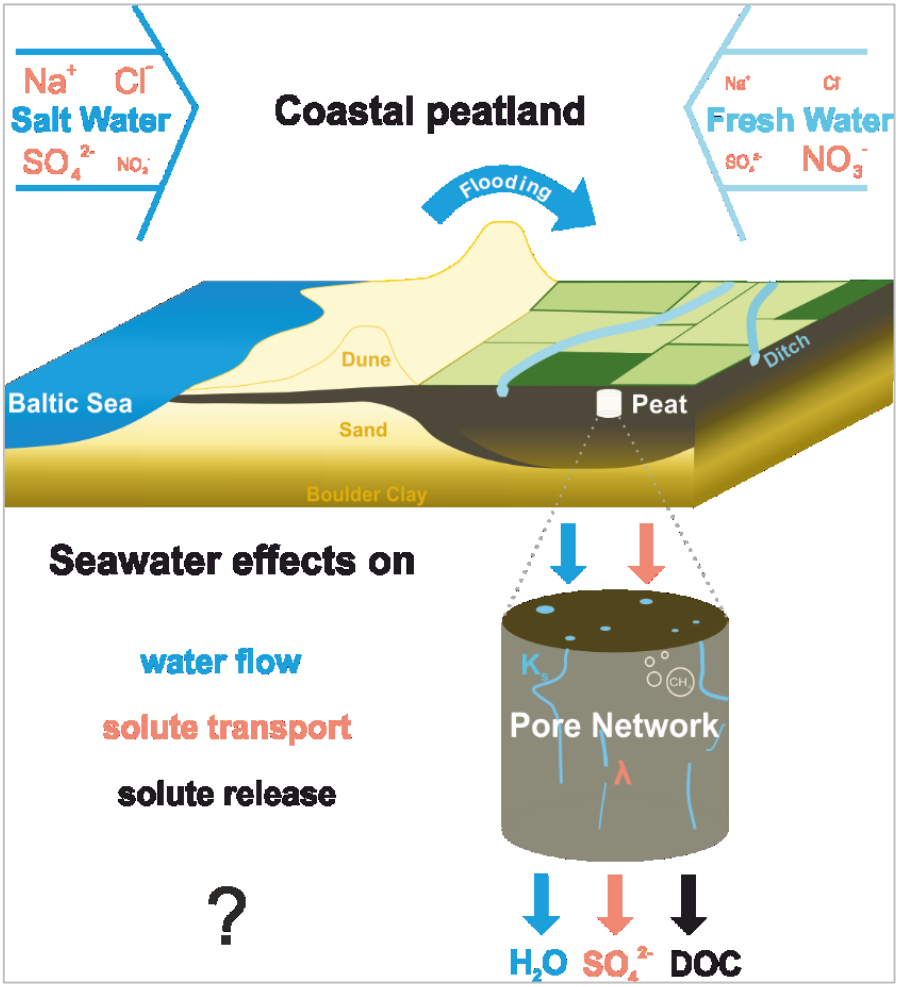

Figure 1.6: Graphical abstract of the objectives of this thesis illustrated by the example of the conditions in the *Hütelmoor*, a coastal fen separated from the Baltic Sea by coastal protection dunes and pervaded by ditches, which were used to drain the peatland but serve nowadays to rewet the site. However, since the experiments of this thesis were carried out at the point scale with peat samples from different sites, the results may apply to other peatlands as well. Illustration was edited by Miaorun Wang.

To address the hypothesis (iv), fen peat at the beach of the *Hütelmoor* (Figure 1.7) was sampled, which has been exposed to seawater for a long time. It may allow statements about long-term seawater impact and its function as a marine sediment

by comparing it to peat material of the same soil horizon, which is dune-protected and thus less seawater-affected, and permeable sandy sediments as the mineral counterpart at the beach (Schade, 2019).

Figure 1.7: Photo of the outcropping peat layer at the beach of the *Hütelmoor*. Photographer: Julia Westphal. For location of outcropping peat layer, which is temporarily covered by sand, see Figure 4.1.

The results of the laboratory studies were published in international, peer-reviewed journals. This cumulative thesis consists of three published articles, out of which two are first-authored (Gosch et al., 2018; Gosch et al., 2019) and one is co-authored (Kreuzburg et al., 2020). The following chapters contain these articles in chronological order:

Chapter 2:

Gosch, L., Janssen, M., Lennartz, B., 2018. Impact of the water salinity on the hydraulic conductivity of fen peat. Hydrol. Process. 32, 1214–1222. doi:10.1002/hyp.11478

Contribution L. Gosch: study design, field work, lab work, data analysis, manuscript writing & editing

Chapter 3:

Gosch, L., Townsend, H., Kreuzburg, M., Janssen, M., Rezanezhad, F., Lennartz, B., 2019. Sulfate mobility in fen peat and its impact on the release of solutes. Front. Environ. Sci. 7, 1–13. doi:10.3389/fenvs.2019.00189

Contribution L. Gosch: study design, field work, lab work, data analysis, manuscript writing & editing

Chapter 4:

Kreuzburg, M., Rezanezhad, F., Milojevic, T., Voss, M., Gosch, L., Liebner, S., Van Cappellen, P., Rehder, G., 2020. Carbon release and transformation from coastal peat deposits controlled by submarine groundwater discharge: a column experiment study. Limnol. Oceanogr. 65, 1116–1135. doi:10.1002/lno.11438

Contribution L. Gosch: field work, counseling, manuscript editing

The results are discussed jointly in **Chapter 5** and complemented by unpublished data collected for the constantly sea-exposed fen peat material from the beach of the *Hütelmoor* to bring further potential long-term effects of seawater exposure into the picture.

2 IMPACT OF THE WATER SALINITY ON THE HYDRAULIC CONDUCTIVITY OF FEN PEAT

Lennart Gosch, Manon Janssen and Bernd Lennartz

Faculty of Agricultural and Environmental Sciences, University of Rostock, Justus-von-Liebig-Weg 6, 18059 Rostock, Germany

Hydrological Processes (2018) 32: 1214–1222

Abstract

Coastal peatlands represent an interface between marine and terrestrial ecosystems; their hydrology is affected by salt and fresh water inflow alike. Previous studies on bog peat have shown that pore water salinity can have an impact on the saturated hydraulic conductivity (K_s) of peat because of chemical pore dilation effects. In this study, we aimed at quantifying the impact of higher salinities (up to 3.5% NaCl) on K_s of fen peat. Two experiments employing a constant-head upward-flow permeameter and differing in measurement and salinity change duration were conducted. Additionally, a third experiment to determine the impact of water salinity on the release of dissolved organic carbon (DOC) of the studied peat type was carried out. The results show a decrease of K_s with time, which does not depend on the water salinity but is differently shaped for different peat types. We assume pore clogging due to a conglomerate of physical, chemical, and biological processes, which rather depend on water movement rate and time than on water salinity. However, an increased water salinity did increase the DOC release. We conclude that salinity-dependent behavior of K_s is a function of peat chemistry and that for some peat types, salinity may only affect the DOC release without having a pronounced impact on water flow.

2.1 Introduction

The hydraulic conductivity of a soil (K) is a crucial parameter for the depiction of water flow and the associated solute transport. It depends on the generally fluctuating water content of the soil and therefore shows a high temporal variability under unsaturated conditions. Under saturated conditions, as often occurring in peatlands, K reaches its maximum - the saturated hydraulic conductivity (K_s). But this supposedly constant soil parameter is also subject to processes that let it vary over time. One known factor is the soil water chemistry, for which Edelstein et al. (2010) concluded that for soils that contain a fraction of clay K_s clearly depends on the electrical conductivity (*EC*) and the sodium adsorption ratio (*SAR*) of the penetrating water. The change of these parameters (low *EC*, high *SAR*) can lead to clay dispersion and/or clay swelling which in turn leads to the plugging of pores and therefore to a decrease of K_s. In studies on the impact of water salinity on K_s of mineral soils generally a decrease of K_s with time also for high *ECs* was observed, but the lower the *EC* and the higher the *SAR* the faster and more pronounced was the decrease of K_s.

However, Ours et al. (1997) observed an increase of K_s with time with increasing water salinity specific for peat soils. They carried out tracer experiments with chlorine compounds (HCl, $CaCl_2$, NaCl) to study the material properties of peat which govern the solute transport in the soil (hydraulic conductivity, effective porosity, dispersivity). Between the tracer applications they flushed the peat columns with deionized water. During this transitional phase K_s decreased substantially while it increased equally remarkably during the actual tracer throughflow. Assuming a reaction of the tracer with functional groups of the peat they hypothesized that humic acids of higher molecular weight at the edge of the peat fibers coiled and compacted and therefore enlarged the pores. This so-called chemical pore dilation was largely diminished for all tracers after one time flushing with $NaHCO_3$, which supposedly dissolved a part of the organic acids and led to a diminution of the potential pore dilation.

According to Ours et al. (1997) the presence of the pore dilation effect was confirmed by the fact that the outflow of the soil became clearer during tracer throughflow than during throughflow of deionized water. It is therefore likely that the pore dilation is associated with the turnover of dissolved organic carbon (DOC). The impact of water salinity on the export of DOC has lately been studied by Ardón et al. (2016), who found that salt water incursions in coastal peatlands

lead to a reduction of DOC export. Accordingly, Tiemeyer et al. (2017b) observed a strong decrease of DOC concentration after an increase of water *EC* from ~0.1 to 1 mS cm^{-1}.

Observations similar to those of Ours et al. (1997) regarding the increase of K_s with increasing salinity were made by Comas & Slater (2004) during their study of low-frequency electrical properties to derive the *EC* of the pore water from electrical measurements. They used different concentrations of NaCl and found a proportionality between the *EC* and K_s ($K_s \propto EC^{0.3}$). These findings impelled Kettridge & Binley (2010) to study the effect's relevance for laboratory K_s measurements. For these experiments often deionized water is used, which has a different water chemistry than the natural pore water. Pointing out that pore water of samples, which were saturated with deionized water is in fact a mixture of the latter and the original pore water, they measured K_s of peat samples with deionized water over shorter (1h) and longer (3d) periods. Alongside with the expectable decrease of *EC* in the effluent water they also observed a continuous distinct decrease of K_s (up to 95 %), whereby only in some cases a pronounced correlation between *EC* and K_s was observed. They attributed this decrease to the pore constriction effect (as the opposite of the pore dilation effect). In following experiments with water with NaCl (*EC* = 1 mS cm^{-1}) they observed a strong increase of K_s and therefore confirmed the existence of the chemical pore dilation. According to their findings the process also continues during periods with no water flow. Field measurements of K_s with a changing salinity have been carried out by van Dijk et al. (2017), who observed an increase of 280 % of K_s for an increase of the *EC* from approx. 0.9 to 9 mS cm^{-1}. They attributed the increase to the pore dilation and a decreased methane production due to sulfate reduction and an associated decrease of gas bubble formation.

In all the studies about the impact of water salinity on K_s of peat soils so far the substrate of study was *Sphagnum* peat originating from bogs. This kind of peatland is generally rainwater-fed and often faces maximally low salinity changes due to groundwater interaction. Fens on the opposite are often located in lowlands closer to the sea and are more likely to be actually subject to a greater change of salinity in times of flooding or saltwater intrusion into the groundwater. In this study, we carried out three experiments to determine the impact of sea water salinities on K_s and DOC release of (degraded) fen peat. We hypothesized that (1) a higher salinity increases the K_s also for fen peat, (2) salinity changes have less

impact on K_s of higher decomposed peat and (3) a salinity-induced change of K_s is associated with a change of DOC release.

2.2 Material and methods

2.2.1 Site properties and sampling

The principal sampling site was a peatland in northeastern Germany (Pölchow, 54° 00′ 34.8″ N, 12° 06′ 89.9″ E), which is drained and currently used for hay production. Thirty-five undisturbed samples of fen peat (Peat F1, see Table 2.1) were taken randomly horizontally from a pit in a depth of 40 to 60 cm with soil sample rings (V = 250 cm³, $\varnothing$ = 7.2 cm, L = 6.1 cm) made of steel.

Table 2.1: Properties (average values) of studied peats (three fen peats (“F”) and one bog peat (“B”)). The soil organic matter content, the organic carbon content, and the particle density were determined per peat (n = 2 to 3). The bulk density was determined for every single sample (depending on peat, n = 35 (Peat F1), n = 10 (Peat B), or n = 5 (Peat F2 and F3)).

Peat nr.	Site	Peatland type	Coordinates	Depth (cm)	Number and size of samples	Peat type	Degree of decom-position (von Post)	Soil organic matter (%)	Soil organic carbon (%)	Particle density (g cm^{-3})	Bulk density (g cm^{-3})	Porosity (-)
F1	Pöl-chow	drained fen	54° 00′ 34.8″ N 12° 06′ 89.9″ E	40 - 60	35 x 250 cm³, 3 x 412 cm³	sedge and reed	H6	83.6	47.5	1.40	0.22	0.84
F2	Zarne-kow	drained fen	53° 52′ 06.1″ N 12° 52′ 01.8″ E	50 - 60	5 x 250 cm³	amor-phous with wood	H8	83.9	48.0	1.42	0.19	0.87
F3				80 - 90	5 x 250 cm³	sedge and reed	H7	83.5	47.8	1.40	0.16	0.89
B	Ras-tede	drained bog	53° 15′ 25.5″ N 08° 14′ 54.6″ E	20 - 30	10 x 250 cm³	cotton grass and sphag-num	H4	94.7	51.9	1.20	0.11	0.91

Three additional samples of Peat F1 for the DOC release test were taken in the same manner, but with bigger sampling rings (V = 452 cm³, $\varnothing$ = 8 cm, L = 9 cm) made of plastic. The reed-sedge peat is, like in most of the peatlands in central Europe, decomposed due to the drainage. The degree of decomposition according to von Post (1922) is H6. For a comparison further samples were taken on different sites (see Table 2.1). At the site Zarnekow (drained fen) in total ten samples in two different depths (Peat F2 and Peat F3) and at the site Rastede (drained bog) ten samples (Peat B) were taken. The samples were stored in a refrigerator until being used for the experiments. After the experiments the dry bulk density was determined for each sample by drying it at 105°C (DIN EN ISO 11272, 2014). Further basic soil parameters were determined according to German standard methods for two to three disturbed samples of each peat layer: soil organic matter content by loss on ignition at 550°C (DIN EN 15935, 2012), soil organic carbon content with a C/N analyzer (vario PYRO cube) and particle density with a pycnometer (Blume et al., 2011). The porosity was calculated from the bulk and particle density. As the samples were taken from presumably homogenous peat layers the variability of the parameters was low (standard deviation of bulk density ranged from 0.010 to 0.018 g cm^{-3}).

2.2.2 K_s measurement

Water with different salinities was prepared by adding specific amounts of NaCl to deionized water with low gas content (2.3 mg O_2 L^{-1}, pH = 9.05 (low CO_2 content)). The salinity was determined using a conductivity probe (EC in mS cm^{-1}, corrected to 25°C). For capillary saturation the samples were placed in a water bath with a water level of 1 cm until a glimmer on the top of the sample appeared (generally after 1-2 d). For the complete saturation a hood was placed on the sample and the water level was then raised 1 cm h^{-1} until reaching the top of the sample. The K_s tests were carried out with a modified constant-head upward-flow permeameter (Figure 2.1(a)). With the known constant hydraulic gradient of 0.8 (controlled by the distance of the tube (ΔH) and a constant water level in the reservoir) and the outflow volume in a certain time, K_s was determined according to Darcy's Law. All measurements were conducted at room temperature (~ 20°C). For comparability with other studies K_s was temperature and salinity corrected by calculating the intrinsic permeability of the peat ($k = K_s \times \mu_f/(\rho_f \times g)$), with μ_f and ρ_f as the dynamic

viscosity and density of the water and *g* as the acceleration of gravity) and recalculating K_s with μ_f and ρ_f for a temperature of 10°C and an *EC* of 0.7 mS cm^{-1}.

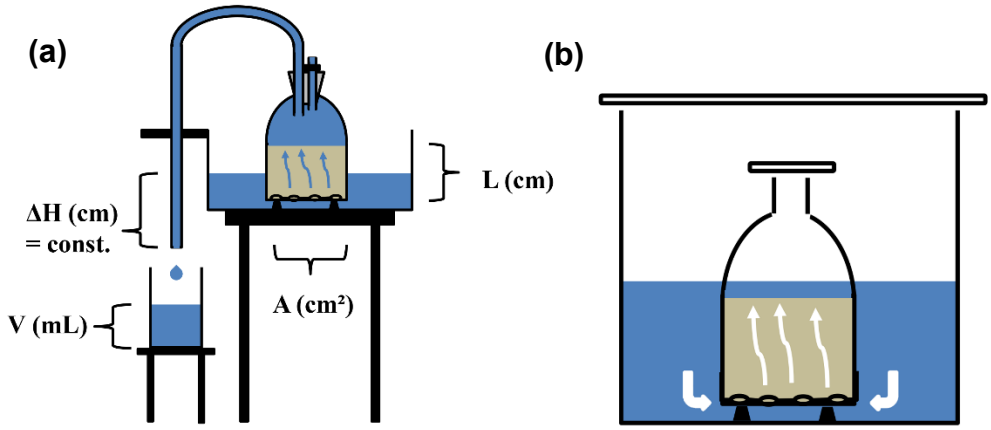

Figure 2.1: Set-up for the K_s tests. (a) Set-up for the measurement. The drip-off of the water causes an upward flow through the soil sample. The water level in the reservoir was kept constant manually during the measurement. Calculation of K_s according to Darcy's Law: $K_s = V \times L/(A \times t \times \Delta H)$. (b) Set-up for the salinization and desalinization of the samples within the interval K_s test. The salt in the saturating water enters the sample via diffusion from below (indication of arrows).

2.2.3 First experiment: Continuous K_s test with abrupt salinity change

The first experiment was designed to validate if K_s for fen peat increases directly after a rise in water salinity (Hypothesis 1) as it had been observed for bog peat by Ours et al. (1997). At first five samples from each considered peat type (F1, F2, F3, B, see Table 2.1) were saturated with water with an *EC* of 1 mS cm^{-1} (0.049 % NaCl) and K_s was measured for three hours. For this *EC* Kettridge & Binley (2010) had observed an increase of K_s. Afterwards and without stopping the experiment a water flow with increased *EC* of 21 mS cm^{-1} (1.2 % NaCl) was induced and K_s measured for another three hours. For comparison reasons also one undisturbed sample of a mineral soil (sandy loam) was measured, for which no salinity-induced increase of K_s was expected as the underlying process is related to peat-specific components.

2.2.4 Second experiment: Interval K_s test with long (de-)salinization periods

As the abundance of the process-relevant humic acids of higher molecular weight is likely to decrease with an advanced decomposition of the organic matter, the

impact of water salinity on K_s might be attenuated in more decomposed peat (Hypothesis 2). Because the pore dilation effect might be a long-lasting process (Kettridge and Binley, 2010), a second test series with longer (de-)salinization periods was carried out to detect a potentially less pronounced impact of the water salinity. Thirty samples of peat F1 were divided into six groups of five samples each and assigned to a salinity scenario (Table 2.2). Each scenario followed the same conceptual pattern: saturation of the peat samples with water with an initial electrical conductivity (*EC1*) and measurement of the initial saturated hydraulic conductivity (K_i), followed by a salinization or desalinization of the sample towards the second electrical conductivity (*EC2*) and a second K_s test, and finally a (de-)salinization of the sample towards the original salinity (*EC3* = *EC1*) and a third K_s test. The salinity values chosen were those that can actually occur in the natural environment in case of a saltwater inflow in a coastal peatland: 0.7 mS cm^{-1} (0.035 % NaCl, corresponding to fresh water), 21 mS cm^{-1} (1.2 % NaCl, corresponding to brackish water) and 55 mS cm^{-1} (3.5 % NaCl, corresponding to sea water from the oceans). As Edelstein et al. (2010) pointed out that for mineral soils not only the salinity itself but also the composition and kind of the salt have an impact on K_s, two scenarios were carried out with actual water from the Baltic Sea (19.6 mS cm^{-1}) and water from a ditch of the drained peatland (1.2 mS cm^{-1}). As the pore dilation has been observed so far only for bog peat, the experiment was also carried out for five samples of Peat B (Scenario 7) for comparison reasons.

Table 2.2: Salinity scenarios for the interval K_s test. In each scenario, three K_s tests with water with different electrical conductivity (*EC1, EC2, EC3*) were carried out. Scenarios 5 and 6 were carried out with natural water (Baltic Sea water and fen ditch water), whereas in all other scenarios, a sodium chloride solution was used.

Scenario	Number of samples	EC1 (mS cm^{-1})	EC2 (mS cm^{-1})	EC3 (mS cm^{-1})	Water salinity change
1	5 x F1	0.7	0.7	0.7	constantly fresh (blank)
2	5 x F1	0.7	55.0	0.7	fresh - ocean - fresh
3	5 x F1	0.7	21.0	0.7	fresh - brackish - fresh
4	5 x F1	21.0	0.7	21.0	brackish - fresh - brackish
5	5 x F1	1.2	19.6	1.2	fresh - brackish - fresh
6	5 x F1	19.6	1.2	19.6	brackish - fresh - brackish
7	5 x B	0.7	55.0	0.7	fresh - ocean - fresh

In the beginning the samples were saturated as described above with water with the first *EC* and subsequently kept with 1 cm of water ponding on top of the sample (Figure 2.1(b)). The samples were covered to reduce evaporation and an associated falsification of the *EC*. The experiment was carried out under darkened conditions to prevent algae growth. The *EC* in the water on top of the sample was monitored in intervals of several days by taking out 10 mL with a pipette. As the *pH* may also be relevant for the chemically induced process of pore dilation (Ardón et al., 2016), it was additionally measured in one of the five samples of each scenario. The removal of 10 mL corresponds to a decrease of water level of approximately 2 mm in the hood, causing only a very small and short-lasting hydraulic gradient. Besides this, salt transport within the sample took only place via diffusion. As this is a very slow process and the complete equilibration would take a long time, the (de)salinization was stopped, when all samples had reached at least 75% of the envisaged *EC* (increasing salinity) or 25 % of the previous *EC* (decreasing salinity). Therefore, the end values of the *EC* were not identical with the *EC* values used in the subsequent K_s tests. The duration of the (de)salinization depended on the magnitude of the *EC* change and was generally between 20 and 64 days (see an example in Figure 2). This time period should create the conditions for which the process can develop to its full extent.

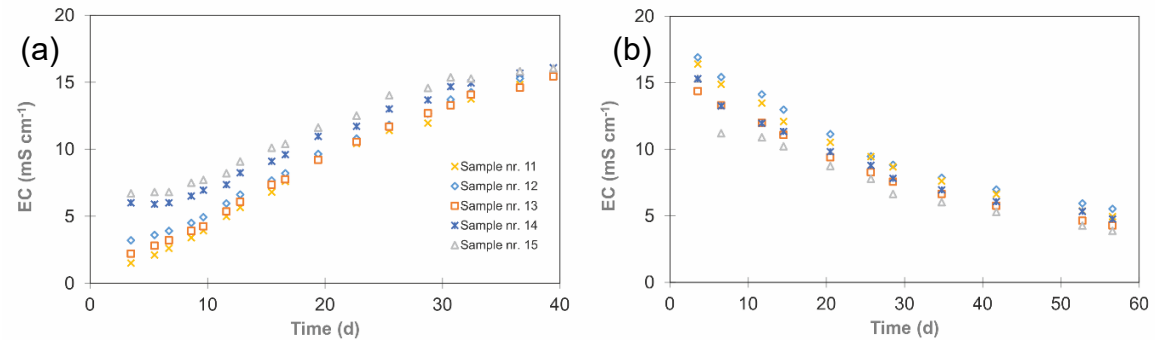

Figure 2.2: Salinization and desalinization of the peat samples for interval K_s test. (a) Salinization of the peat samples of Scenario 3 for the interval K_s tests (electrical conductivity of resaturating water (*EC2*): 21 mS cm^{-1}). (b) Desalinization of the peat samples of Scenario 3 for the interval K_s tests (*EC* of resaturating water (*EC3*): 0.7 mS cm^{-1}). The values of the *EC* at the beginning differ from the actual *EC* values used during the preceding K_s tests because of mixing of salt concentrations in the sample and the resaturating water.

The subsequent short K_s test (15 min discarding values, 15 min measurement) was carried out with water of the envisaged *EC*. Because processes like pore clogging due to fine particles or gas bubbles can reduce K_s during the measurements, it is generally recommended to measure K_s quickly (DIN 19683-9, 2012). Afterwards the samples were let drip off for one hour to empty the largest pores and resaturated with the following salinity level. The procedure was repeated for all the subsequent prescribed salinities. As chemical substances to eliminate microorganisms might interfere with the chemical-induced change of K_s, no such chemicals were added.

2.2.5 Third experiment: DOC release test

Additionally to the K_s tests a salt tracer test combined with a determination of the DOC content was carried out for three soil columns of Peat F1 (relating to Hypothesis 3). They were placed in a flow-through device connected to a peristaltic pump (an illustration of the set-up can be found in Liu et al. (2016)) and were saturated for one day with water with an *EC* of 0.7 mS cm^{-1}. Subsequently two pore volumes (PV) with the same *EC* were pumped through (0.7 mL min^{-1}). In Column 1 the *EC* was then kept constant at 0.7 mS cm^{-1} while in the other two soil columns the *EC* was changed to 21 (Column 2) and 55 (Column 3) mS cm^{-1}. The outflow was dosed in 28 mL samples, which were filtered through a 0.45 µm CME membrane and the DOC content was measured with a DIMATOC® 2000.

2.3 Results

2.3.1 Impact of salinity on K_s in the continuous test

The time curve during the continuous K_s test is shown in Figure 2.3 for each peat type and the mineral soil. The measured K_i (average of 5 samples) was highest for Peat F3 (570 cm d^{-1}) followed by the mineral soil (432 cm d^{-1}) and Peat F2 (216 cm d^{-1}). For Peat F1 (34 cm d^{-1}) and Peat B (4 cm d^{-1}) K_i was considerably lower. For the first measurement period of 3 hours with low *EC* K_s decreased continuously in all samples. The rate of decrease differed between peat types – the geometric mean and geometric standard deviation (in parentheses) after 3 hours were for Peat F1 83 % (1.08), Peat F2 46% (1.38), Peat F3 44% (1.15) and Peat B 40 % (1.67). After the *EC* raise the K_s of all fen peat samples continued to decrease and was reduced after 6 hours for Peat F1 to 69 % (1.25), Peat F2 to 29 % (1.73), Peat F3 to 25 % (1.46) and Peat B1 to 39 % (1.63). None

of the samples showed divergent behavior when the *EC* was increased. No increase of K_s like Ours et al. (1997) had observed could be found during this experiment. Instead, the time curves are similar to that of the mineral soil, for which K_s decreased constantly to 20 % after 6 hours.

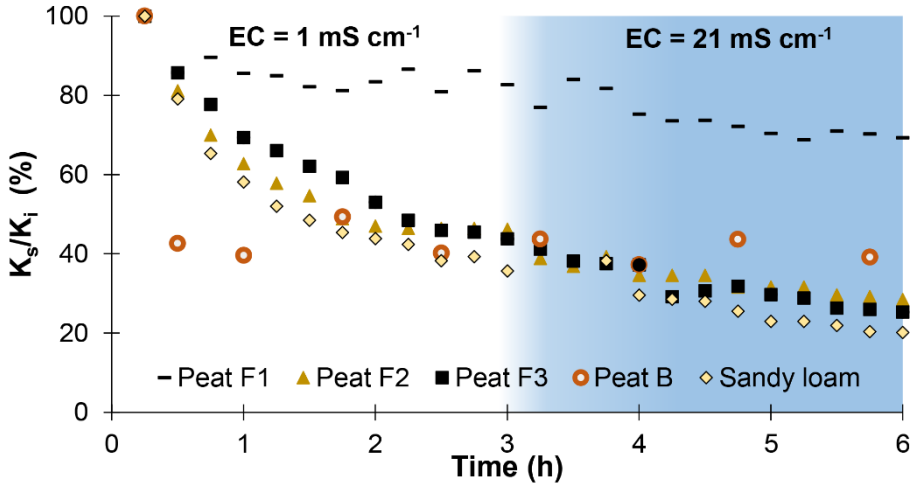

Figure 2.3: Time curve of the ratio of the saturated hydraulic conductivity K_s to the initially measured saturated hydraulic conductivity K_i within the continuous K_s test (geometric mean of five samples per peat). The values for K_i were 34 (Peat F1), 216 (Peat F2), 570 (Peat F3), and 4 cm d^{-1} (Peat B). After 3 hours of measurement the electrical conductivity of the flowing water was increased from 1 to 21 mS cm^{-1}.

2.3.2 Impact of salinity on K_s in the interval test

Figure 2.4 shows the percentage change of K_s after the first change of *EC* during the interval K_s test (data for second change of *EC* not shown). Because positive as well as negative values occurred in the same scenario, the results for the individual samples instead of mean values are shown. To align the results with the hypothesis the expected change of K_s according to Comas and Slater (2004) ($K \alpha EC^{0.3}$) is added. In Scenario 1, in which the *EC* was kept constant at 0.7 mS cm^{-1}, all samples showed a decrease of K_s, ranging between -16% and -47%. The rate of decrease did not seem to depend on the order of magnitude of K_i. Classifying this as the “blank” scenario with no impact of salinity changes, we would expect a moderate decrease of K_s for all samples when no impact of salinity is interfering.

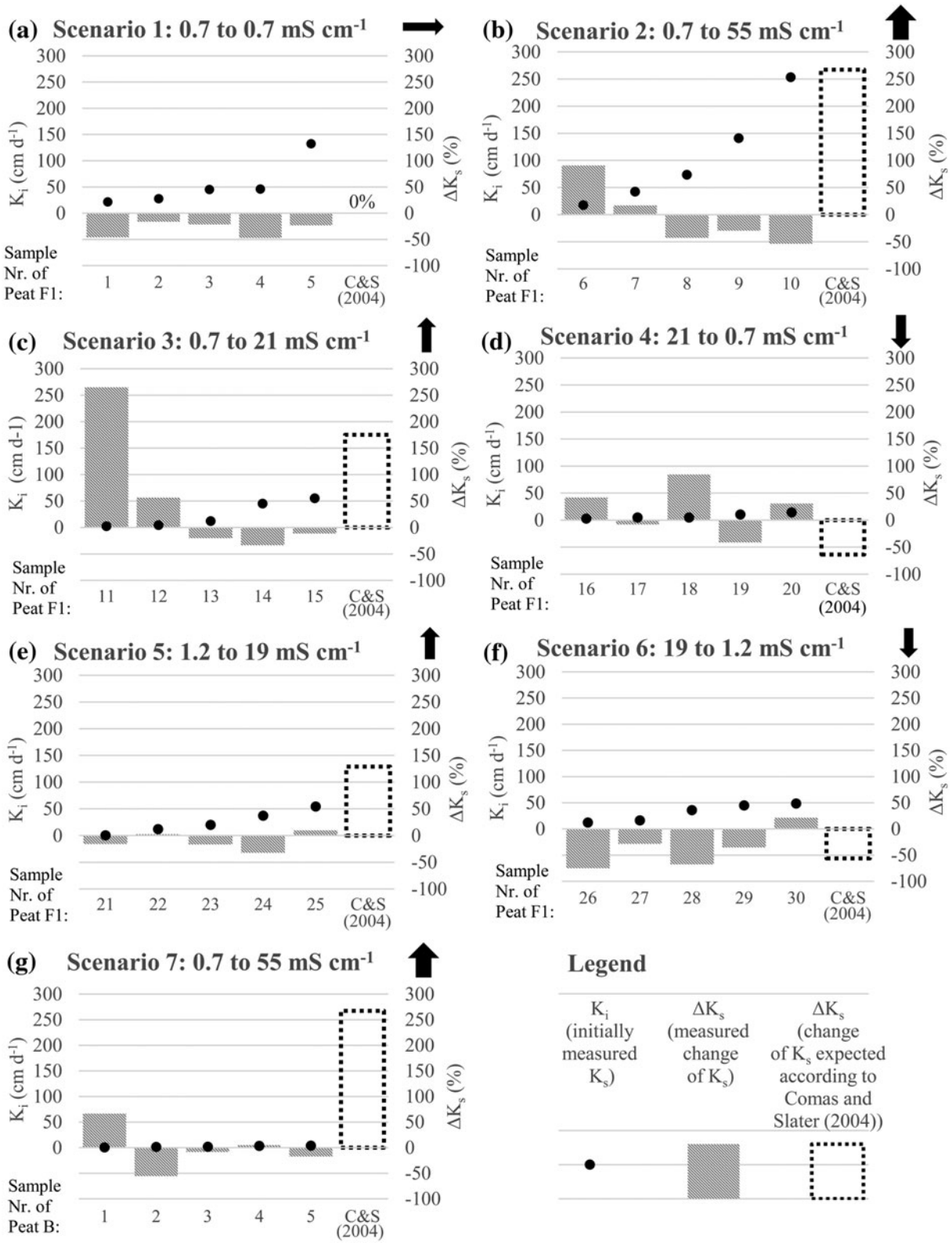

Figure 2.4: K_s measured in the interval K_s test for Peat F1 (Scenario 1–6) and Peat B (Scenario 7). Arrows indicate the direction of change of the electrical conductivity (*EC*) between K_s tests. The dots represent the K_s values measured for the first *EC* level, the bars the percentage change of K_s after the second *EC* level. The dotted bar corresponds to the theoretically expected change of K_s according to Comas and Slater (2004).

In Scenario 2 with the largest increase in *EC* the higher K_i values showed a decrease, which is in the same order of magnitude as Scenario 1, while for the two samples with lower K_i values an increase was observed. For Scenario 3 K_s was expected to move in the opposite direction of K_s in Scenario 4, as their respective *EC* change was carried out contrarily. However, in both scenarios increases and decreases of K_s were observed. The fundamental differences in K_s change between samples in the same scenario (for example samples 18 and 19 in scenario 4) were not correlated to (slight) bulk density differences. Regarding Scenario 5 and 6, the counterpart to Scenarios 3 and 4 with similar *EC* but natural sea/ditch water, the decrease of K_s in the second measurement was more pronounced in Scenario 6 than in Scenario 5. With two increases and three decreases, the results for the bog peat (Scenario 7) came out similar to the fen peat scenarios.

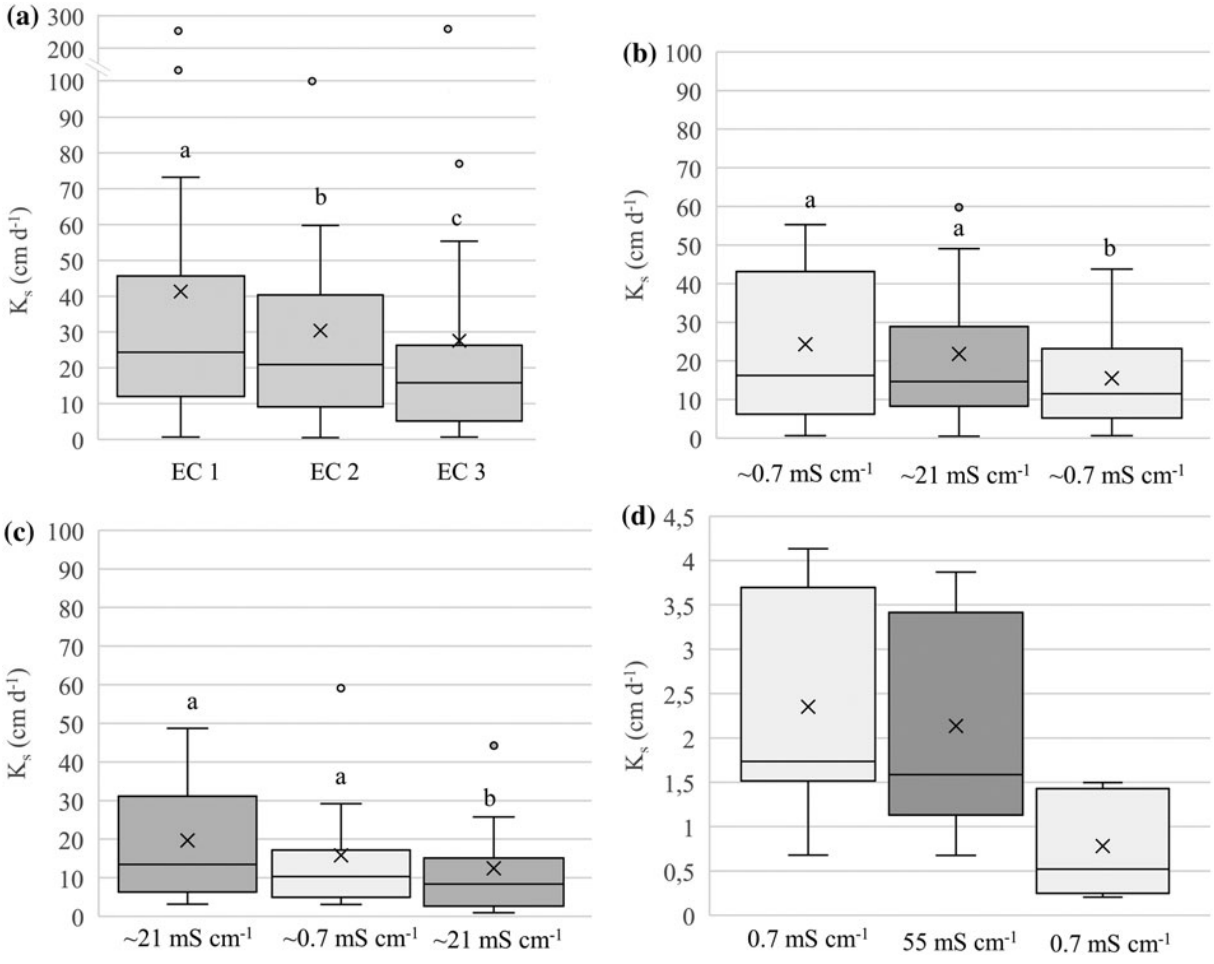

Figure 2.5: Box plot for interval K_s tests of (a) Scenarios 1–6, (b) Scenario 3 and 5, (c) Scenario 4 and 6, and (d) Scenario 7 (bog peat). Crosses mark the arithmetic mean. The letters indicate if the differences between the K_s tests are statistically significant (different letter) or not (same letter).

Regarding the complete sequence of all three K_s tests for fen peat (n = 30), there was a general tendency for K_s to decrease through test sequence in all scenarios (Figure 2.5 (a)). The differences between each of the three K_s tests were statistically significant according to the Wilcoxon signed-rank test with α = 0.05 (K_s data not normally distributed). In Scenarios 1-6 for 67 % (second K_s test with *EC2*) and 77 % (third K_s test with *EC3*) of the samples K_s was lower than in the previous measurement. The median decreased from 24 to 21 to 16 cm d^{-1} for *EC* 1 to 2 to 3. This is also true if only scenarios with corresponding salinities, but revised order are regarded (Scenarios 3 and 5 (Figure 2.5 (b)) or Scenario 4 and 6 (Figure 2.5 (c)), n =10), which shows that the sequence of salinities does not affect the temporal evolvement of K_s. However, the differences between the three K_s tests for the scenarios with corresponding salinity were statistically less significant than for all fen peat scenarios. The bog peat scenario (Figure 2.5 (d)) did not show a divergent characteristic. K_s decreased with time, although the statistical significance could not be tested due to the low number of samples (n = 5).

2.3.3 Impact of salinity on *pH* and DOC

The measured *pH* (data not shown) followed a similar pattern in all scenarios of the interval K_s test. It generally decreased with increasing *EC* by approximately 0.5 to 1 units over 6-8 weeks and increased by the same amount with decreasing *EC*. For fen peat it ranged from 6.5 to 8.5, for bog peat from 3.4 to 4.3. With increasing duration of the experiment colored dissolved organic matter (CDOM) was visually observed in the water samples. The darkest colors (corresponding to up to 900 mg DOC L^{-1}) occurred in Scenario 2 after the *EC* change from 55 to 0.7 mS cm^{-1}. In Scenarios 3 to 6 less CDOM and in Scenario 1 the least CDOM was visible in the water samples. This implies an influence of the salinity on CDOM: the higher the salinity the more pronounced the dissolution of organic matter. Although being exposed to a very high salinity, the bog peat samples (Scenario 7) released comparatively little CDOM.

The three soil columns of the DOC release experiment showed the same decrease in DOC concentration in the outflow of the sample during percolation with low-*EC* water (Figure 2.6). Absolute values for initial DOC export were 43, 32 and 20 mg L^{-1} for column 1-3 respectively. In the second step, the DOC concentration in the outflow of the column with a constant *EC* (Column 1) stabilized, while the DOC concentration increased after the *EC* increase for the

two other columns. The percentage increase was highest for Column 3 with the highest *EC*.

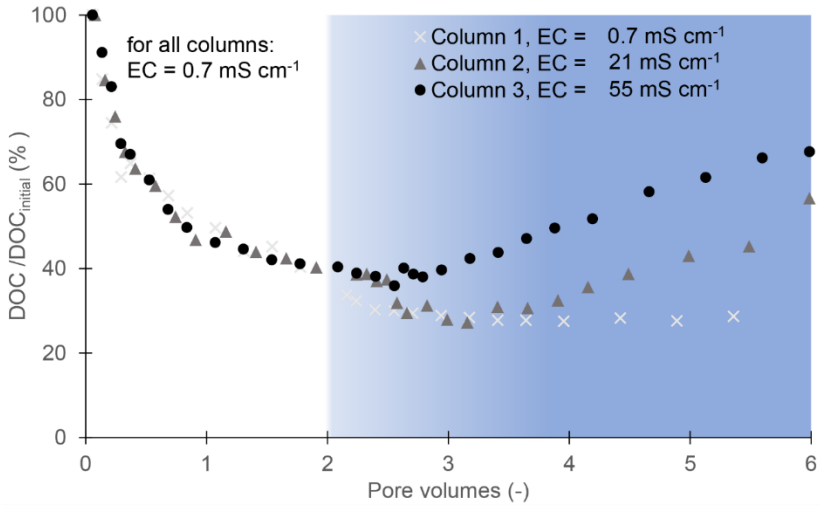

Figure 2.6: Dissolved organic carbon (DOC) in effluent of soil columns. Absolute values for initial DOC export were 43, 32, and 20 mg L^{-1} for columns 1-3, respectively. After 2 pore volumes, the electrical conductivity (EC) of the flowing water was increased for Columns 2 and 3, but was kept constant for Column 1.

2.4 Discussion

2.4.1 Impact of water salinity on K_s

The increase of K_s with increasing water salinity as it was described for peat samples in earlier studies was not observed in this study. The decreasing trend behavior of K_s with time (continuous K_s test) was not changed by an increase of the *EC*. Only during the interval K_s test an increase of K_s was observed for a few samples, which were predominantly (70%) samples with low K_s values (< 20 cm d^{-1}), leading to comparatively small absolute differences in terms of measured K_s. A different behavior of samples with a lower K_s would go along with theoretical assumptions of Kettridge & Binley (2010). By applying Poiseuille's Law they derived that the percentage K_s change due to pore dilation or constriction should be higher for lower K_s values than for higher K_s values. However, in this study this effect could not be attributed to the salinity change since it occurred in scenarios with reversed *EC* change (Scenarios 3 and 4). Striking differences between the salinity change levels or between artificial and natural salt solutions were either not observed. Merely the higher decrease of K_s in Scenario 5

compared to the lower decrease of K_s in Scenario 6 could indicate a diminution of the decrease of K_s with an increased natural salt content.

2.4.2 K_s decrease with time

The decrease of K_s with measurement time, as it occurred during the continuous K_s test for fen peat, has been observed in previous studies in both mineral soils (Dikinya et al., 2008), and bog peat (Kettridge and Binley, 2010). Since a salinity change did not affect this decrease with time in our study and also the mineral soil sample showed a strong decrease (Figure 2.3) it can be assumed that the decrease in the fen peat cannot be traced to the (salinity-dependent) pore constriction effect. It is therefore likely that other processes like the formation of gas bubbles (Baird & Waldron, 2003; Kettridge et al., 2013) or the dispersion and re-deposition of fine particles (Dikinya et al., 2008) were responsible for the reduction of K_s and that the characteristic of these processes depends on the peat type. The general decrease of K_s during the continuous K_s test is consistent with the results of the interval K_s test. However, the decrease of average K_s values for Peat F1 within the continuous K_s test (30 min: 33.83 cm d^{-1}, 60 min: 32.86 cm d^{-1}, 90 min: 31.03 cm d^{-1}) is lower than the one within the interval K_s test (3 times measured for 2x15 min: 30 min: 41.28 cm d^{-1}, 60 min: 30.41 cm d^{-1}, 90 min: 27.57 cm d^{-1}). This indicates that besides the K_s-decreasing processes that take place during the K_s measurement also further processes that decrease K_s over time take place. Therefore the decrease during the interval K_s test might be to time-dependent processes like bio-clogging due to microbial activities (Kleimeier et al., 2014) or gas bubble formation (Kettridge et al., 2013). However, only a weak correlation (r = -0.3) could be found between the duration of (de-)salinization (which is the same for all samples in the same scenario) and the change of K_s (median of each scenario). It can be assumed that the decrease depends on several factors – time being only one of them.

2.4.3 Impact of water salinity change on *pH* and DOC release

The change of *pH* and CDOM/DOC during the experiments indicate the occurrence of further chemical processes. As NaCl is generally considered a neutral salt, the *pH* change (*EC* increase leads to *pH* decrease and vice-versa) could be due to cation bridging and ion exchange (Tiemeyer et al., 2017b) or the carbonate buffer (equilibrium constant changes with increased ionic strength). The

decrease of the DOC concentration with time (Figure 2.6) corresponds to the frequently observed pattern of DOC leaching (Tiemeyer et al., 2017b), for which the concentration stabilizes after an initial flushing period. In this study the changed salinity did have an impact on the turnover of DOC, which might influence – maybe only in the long term – the pore structure of the peat. The fact that an increased *EC* increased the DOC export is in contrast to previous studies where high ionic strength caused a reduction of the solubility of DOC due to reduction of charge density (Münch et al., 2002; Tiemeyer et al., 2017).

2.4.4 Possible reasons for the non-occurrence of the chemical pore dilation effect

The absence of the pore dilation effect and the different behavior of DOC export in this study suggests that the process-relevant humic acids or functional groups might not be present in the studied peat samples. The assumption that the salinity dependence observed in previous studies might be related to *Sphagnum*-specific components in the peat (such as hyaline cells) was not supported when the bog peat did not show any increase of K_s with a high *EC*. However, as the bog peat in this study is not a pure *Sphagnum* peat, its chemical composition might differ considerably from bog peat samples of earlier studies. In any case, as humic substances are formed in soils their composition is highly related to the specific site conditions. It is well known from classical fractionation methods that humic acids react differently to salt solutions (Senesi and Loffredo, 1999). Recent studies have shown that the abundance of the different compound classes in peat DOM changes with a change in water salinity. Depending on the peat type, some compound classes are more abundant (for example carbohydrates) and some less abundant (for example lignin dimers) in saline water than in deionized water (R. Strehse, University of Rostock, personal communication). A predominance of the former would therefore rather lead to a dissolution of the humic acids than to a coagulation and an associated pore dilation. This could also explain the observed increased DOC concentrations during the DOC release test.

However, as the chemistry of humic acids is complex, multiple processes are possible to change the macromolecular structure and composition of functional groups of humic acids in a way, which is unfavourable for the occurrence of pore dilation. As Ours et al. (1997) attributed the pore dilation to the higher molecular weight humic acids, these humic acids might have been decomposed in a more

decomposed peat soil like Peat F1, F2 or F3. During the decomposition, the composition of the compound classes in the peat changes and the amount of higher molecular weight humic acids might decrease. This could cause a less pronounced pore dilation effect, which is potentially overlapped by other K_s-decreasing processes. However, no detailed information was given about the degree of decomposition in the previous studies which could be used for a comparison. Furthermore, the leaching of the relevant substances, as assumed by Ours et al. (1997) as reason for the fact that no more increase of K_s could be observed after a tracer test with sodium bicarbonate ($NaHCO_3$), is possible. However, also in this case the question arises why the bog peat did not show any salinity-dependent behavior. As no chemical comparison with the previously studied peat samples is possible, it remains unclear why the pore dilation effect could not be confirmed in this study.

2.5 Conclusions

In this study, no impact of water salinity on the saturated hydraulic conductivity of fen peat was detected. The saturated hydraulic conductivity generally showed a decrease with time regardless of the salt concentration, peat type and degree of decomposition. Potential underlying processes are the dispersion and re-deposition of fine particles and the formation of gas bubbles. For a few samples the saturated hydraulic conductivity increased with a slow, diffusion-based (de-)salinization, but without any salinity-dependent pattern. On the contrary, an increased water salinity did increase the concentration of dissolved organic carbon. A chemical comparison study would be necessary to find the cause for the absence of the pore dilation effect in this study. Before setting in context the saturated hydraulic conductivity and the electrical conductivity, we highly recommend a test run to validate whether the used peat type shows salinity-dependent hydraulic behavior. We assume that a potential impact of water salinity on the water and solute exchange between coastal peatlands and the adjacent sea is closely related to the chemistry of the present peat body. In coastal fens salt water intrusion might not change the hydraulic behavior of the peat.

3 SULFATE MOBILITY IN FEN PEAT AND ITS IMPACT ON THE RELEASE OF SOLUTES

Lennart Gosch[1], Heather Townsend[2], Matthias Kreuzburg[3], Manon Janssen[1], Fereidoun Rezanezhad[4] and Bernd Lennartz[1]

[1]Faculty of Agricultural and Environmental Sciences, University of Rostock, Rostock, Germany
[2]Ecohydrology Research Group, Department of Earth and Environmental Sciences, University of Waterloo, Waterloo, ON, Canada
[3]Leibniz Institute for Baltic Sea Research (LG), Warnemünde, Germany
[4]Ecohydrology Research Group, Water Institute and Department of Earth and Environmental Sciences, University of Waterloo, Waterloo, ON, Canada

Frontiers in Environmental Science (2019) 7: 1-13

Abstract

Sea-level rise coupled with land subsidence from wetland drainage exposes increasingly large areas of coastal peatlands to seawater intrusion. Seawater contains high concentrations of sulfate (SO_4^{2-}), which can alter the decomposition of organic matter thereby releasing organic and inorganic solutes from peat. In this study, a flow-through reactor system was used in order to examine the transport of SO_4^{2-} through peat as well as its effect on solute release. Moderately-decomposed fen peat samples received input solutions with SO_4^{2-} concentrations of 0, 100, 700 and 2700 mg L^{-1}; sample effluent was analyzed for a variety of geochemical parameters including dissolved organic carbon (DOC), dissolved inorganic carbon (DIC) and total dissolved nitrogen (TDN) as well as the concentrations of major cations and anions. The input solution remained anoxic throughout the experiment; however, no signs of a pronounced SO_4^{2-} reduction were detected in the effluent. SO_4^{2-} transport in the fen peat resembled non-reactive bromide (Br^-) transport, indicating that in the absence of SO_4^{2-} reduction the anion may be considered a conservative tracer. However, slightly elevated concentrations of DOC and TDN, associated with raised SO_4^{2-} levels, suggest the minor desorption of organic acids through anion exchange. An increased solute release due to stimulated decomposition processes, including SO_4^{2-} reduction, was observed for samples with acetate as an additional marine carbon source included in their input solution. The solute release of peats with different degrees of decomposition differed greatly under SO_4^{2-}-enriched conditions where strongly-decomposed fen peat samples released the highest concentrations of DOC, DIC and TDN.

3.1 Introduction

Over the millennia, large quantities of partly-decomposed organic matter have accumulated in waterlogged peatlands. The hydrological and biogeochemical conditions in a peatland determine whether it may serve as a sink or a source for carbon- and nitrogen-containing compounds. It is well known that the drainage of peatlands for agricultural purposes initiates the aerobic decomposition of organic matter in the top layer, resulting in the enhanced emission of greenhouse gases, including carbon dioxide (CO_2) and nitrous oxide (N_2O) (Kasimir-Klemedtsson et al., 1997) as well as a mobilization of dissolved organic matter (generally measured as dissolved organic carbon, DOC) and other nutrients such as ammonium (NH_4^+) (Zak and Gelbrecht, 2007). Hence, the drainage of peatlands has ramifications in the exacerbation of global warming, land subsidence and nutrient loads for adjacent aquatic ecosystems.

Under anoxic conditions, the decomposition of organic matter is controlled by the presence of electron acceptors such as sulfate (SO_4^{2-}), an inorganic and highly mobile form of sulfur, which is used in the metabolism of sulfate-reducing bacteria (SRB). While SO_4^{2-} concentrations in terrestrial ecosystems are generally low, marine ecosystems are SO_4^{2-}-enriched as seawater contains approximately 2700 mg L^{-1} (~29 mM, Algeo et al., 2015). Infiltration of seawater into peatlands can therefore drastically increase SO_4^{2-} concentrations, altering the biogeochemistry of the peat thereby implicating the mineralization of organic matter. Due to climate change and predicted sea level rise, sea water intrusion and the impact on the quality of groundwater resources will be relevant for larger areas of peatlands in the future (Sherif and Singh, 1999; Ardón et al., 2016).

However, when formerly drained peatlands are rewetted (i.e. the water level in the peatland is raised), increased SO_4^{2-} concentrations may aid climate protection by reducing emissions of the greenhouse gas methane (CH_4). The rewetting often results in water levels higher than in the initial state, as the land has subsided, which may result in an emission of a large quantity of CH_4 (Wen et al., 2018). When SO_4^{2-} is present, the SRB, although tending to be low-abundant even under favorable redox conditions, generally outcompete the methanogens in the peat and therefore impede the formation of CH_4 (Hausmann et al., 2016). Coastal peatlands are therefore considered well suited for rewetting projects associated with dyke removal (Koebsch et al., 2019), although under certain circumstances (e.g. abundance of suitable electron donors, Weston et al., 2011) methanogenesis

and SO_4^{2-} reduction can occur at the same time (Oremland et al., 1982; Hahn et al., 2015).

While the impact of water salinity and SO_4^{2-} on greenhouse gas emissions in peatlands has aroused scientific interest, there are hardly any studies focusing on the mechanistic understanding of SO_4^{2-} mobility in peat and its impact on the release of solutes from peat. Solute release from peat is known to be affected by a wide range of environmental variables, with water table fluctuations and the associated change of redox conditions being the most prominent one (Borch et al., 2010). In particular, factors prompting the DOC release from peatlands have been studied previously, since DOC concentrations in surface water in Europe have increased in the last decades (Roulet and Moore, 2006), which is for example problematic for drinking water treatment (Ritson et al., 2014). Factors influencing DOC release from peat include ionic strength (and its proxy, electrical conductivity (*EC*)) and *pH* of the pore water. When *EC* increases and *pH* decreases, amounts of DOC released typically decline as a result of decreased charge density, limiting the solubility of the DOC (Münch et al., 2002; Clark et al., 2011; Ardón et al., 2016; Tiemeyer et al., 2017). Increases in *EC* have also been observed to impact other geochemical processes in peat, including the desorption of NH_4^+ by salt ions (Ardón et al., 2013), an increase of hydraulic conductivity due to a pore dilation (Ours et al., 1997) and a decrease in plant uptake of nutrients as a result of salt stress (Hanin et al., 2016). The explicit impact of changing SO_4^{2-} concentrations on solute release has been studied mostly for moderately increased concentrations simulating atmospheric deposits (Blodau et al., 2007; up to 10 mg L^{-1}), discharge of river water to a wetland (Lamers et al., 1998; up to 400 mg L^{-1}) or intrusion of highly diluted seawater into a wetland (Ardón et al., 2016; up to 300 mg L^{-1}). In an extensive mesocosm experiment, Lamers et al. (1998) observed an increase in alkalinity due to the consumption of hydrogen ions during SO_4^{2-} reduction, a reduced uptake of nutrients, such as potassium (K^+), due to the toxicity of sulfide (HS^-) and an increased release of NH_4^+ due to the increase of organic matter decomposition. They also observed that increased SO_4^{2-} concentrations can turn peat into a source for phosphate, similar as observed for other aquatic sediments (Caraco et al., 1989). The underlying process is the formation of iron sulfide, which reduces the availability of iron (Fe) as binding partner for P both in the reduced form of vivianite or as oxidized Fe(III)-P binding forms (Zak et al., 2010). However, the sulfur cycle in peatlands is complex as sulfur can occur in various organic and

inorganic forms and can be recycled multiple times (i.e. reduced and reoxidized) as stated for bogs (Wieder and Lang, 1988; Blodau et al., 2007), forested wetlands (Mandernack et al., 2000) and salt marshes (Gardner, 1990). To the author's knowledge, there has been no comprehensive study on SO_4^{2-} dynamics and mobility within fen peat with respect to release of solutes from peat induced by SO_4^{2-}-related processes. The main objective of this study was to gain an improved understanding of the processes determining the mobility of SO_4^{2-} of varying concentrations in fen peat samples and their short-term impact on the solute release from the peat.

3.2 Material and Methods

3.2.1 Field sampling and peat properties

Fifteen undisturbed core samples of moderately-decomposed reed-sedge fen peat (referred to as "MD-Peat") were collected in May 2018 horizontally at a depth of 50 cm below surface from a drained fen in northwestern Germany ("Pölchow", 54°00'20.3"N, 12°06'58.8"E). The acrylic glass sampling tubes (Ø = 4.2 cm, L = 10 cm, V = 139 cm³) were incorporated into a sharpened shuttle corer which was pushed manually into the peat. The groundwater level was 75 cm below surface so that the taken peat samples were wet but not completely water-saturated. The peatland has not been affected by Baltic seawater intrusion (SO_4^{2-} concentrations in the groundwater accumulated in the profile pit were low (3.7 mg L^{-1})). For comparison reasons additional samples (n = 3) of two fen peats with a different degree of decomposition were collected: firstly a degraded highly-decomposed peat (referred to as "HD-Peat") taken horizontally from the dried top soil in Pölchow in a depth of 20 cm, secondly a SO_4^{2-}-affected and water-saturated slightly-decomposed peat (referred to as "SD-Peat") taken vertically in a depth of 10 cm in the shallow water of the Baltic Sea adjacent to the coastal fen *Hütelmoor* (54°13'19.38"N, 12°10'7.02"E). The coastline on the latter site has transformed over time to constantly expose parts of the peat layer to seawater (Kreuzburg et al., 2018). Additional disturbed samples of each peat were collected to determine the organic matter content as well as the solid-phase total carbon, nitrogen and sulfur (C/N/S) contents. After collection, all peat samples were refrigerated and transported to the Ecohydrology Research Group at the University of Waterloo (Canada) for the laboratory experiments. The basic physicochemical properties of the peat material used in this study are shown in Table 3.1. The C/N/S contents

were measured for homogenized and freeze-dried samples on a CHNS Carbo Erba analyzer (method detection limit: 0.1 % dwt) without any pre-treatment of the freeze-dried samples. The Fe content was determined by Inductively-Coupled Plasma Optical Emission Spectrometry (ICP-OES) after an aqua regia digestion according to HFA (2014). The bulk density (ρ_b) was determined gravimetrically based on the sample volume and the oven-dried (3 days at 80°C) sample mass. Subsequently, the peat samples were ignited at 550 °C to determine the loss on ignition (*LOI*) as a proxy for the organic matter content (DIN EN 15935, 2012), which was used to calculate the particle density (ρ_s) of the peat samples with standard values for organic (1.4 g cm^{-3}) and mineral (2.65 g cm^{-3}) components (ρ_s = (1.4 × *LOI* + 2.65 × (100 – *LOI*)) / 100). The total porosity was then calculated from bulk and particle densities ($\Phi = 1 - \rho_b / \rho_s$).

Table 3.1: Basic properties of peat material. Bulk density (ρ_b) and porosity (Φ) of the samples were determined for each of the undisturbed peat samples after the experiment, all other parameters were determined on the basis of untreated, disturbed peat material. In case of average values, the number of replicates (*n*) is indicated in parentheses.

Parameter	**SD-Peat**	**MD-Peat**	**HD-Peat**
Sampling location	Beach of the Baltic Sea in front of the *Hütelmoor*	Grassland in *Pölchow*	Grassland in *Pölchow*
Sampling depth (cm bsf)	10	50	20
Number of samples	3	15	3
Peat type	Sea-exposed, slightly-decom-posed reed-sedge fen peat	Moderately-decomposed reed-sedge fen peat	Degraded, highly-decomposed fen peat
Degree of decomposition (von Post)	H4-5	H6	H9
Organic matter content (% dwt)	83.7 (*n* = 2)	83.3 (*n* = 2)	39.8 (*n* = 2)
C_{org} (% dwt)	41.6	39.9	22.0
C_{inorg} (% dwt)	0.05	0.45	0.11
N (% dwt)	1.6	3.1	2.0
S (% dwt)	3.4	0.5	0.3
Fe (mg kg^{-1})	1173	22730	61600
ρ_b (g cm^{-3})	0.17 (*n* = 3)	0.19 (*n* = 15)	0.49 (*n* = 3)
Φ (-)	0.90 (*n* = 3)	0.89 (*n* = 15)	0.78 (*n* = 3)

3.2.2 Flow-through reactor experiment

A one-month SO_4^{2-} displacement experiment was carried out using a flow-through reactor (FTR) set-up (Figure 3.1). These reactors are designed to measure biogeochemical reaction rates on undisturbed soils or sediments and yield kinetic parameters and information on reaction pathways that can be extrapolated to natural conditions (Pallud et al., 2007). They have been used to study solute transport in peat (Kleimeier et al., 2017) as well as SO_4^{2-} and NO_3^- reduction in sediments (Pallud and Van Cappellen, 2006; Stam et al., 2010; Laverman et al., 2012). In addition to information on SO_4^{2-} transport, the one-month monitoring of this experiment also provided insight into the short-term effects of increased SO_4^{2-} concentrations on the release of solutes.

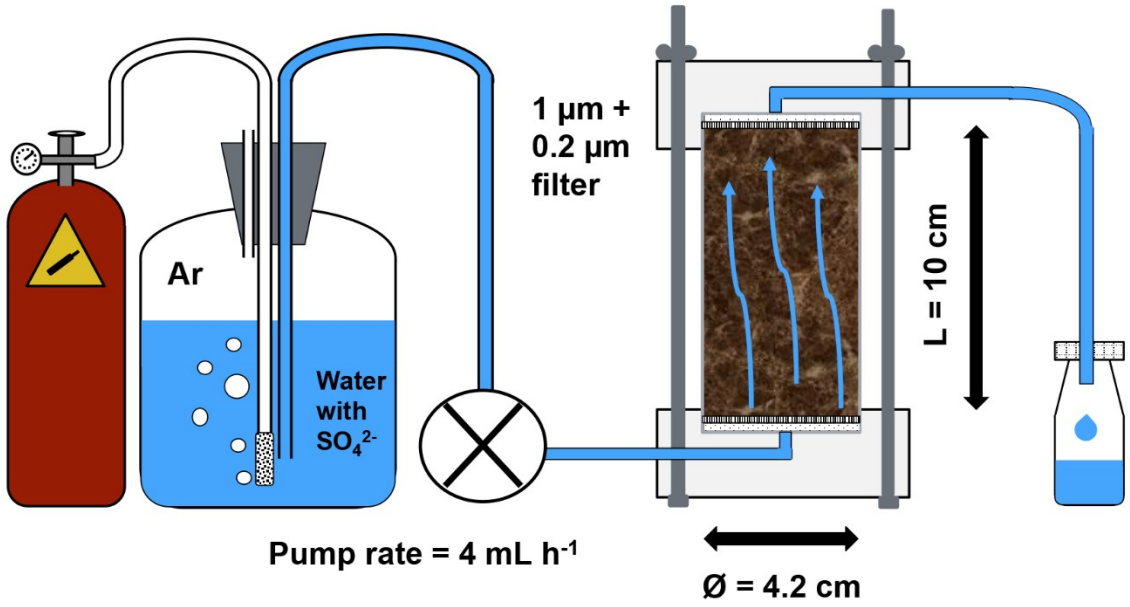

Figure 3.1: Schematic diagram of the experimental flow-through set-up. The reactors were placed in an environmental chamber at constant temperature of 15°C. The sulfate-enriched water was depleted in oxygen via sparging with argon (Ar), flowed with a pump rate of 4 mL h^{-1} through the peat samples and was subsequently collected and sampled.

The FTRs (21 reactors in total) consisted of the peat core contained within an acrylic glass tube attached to two PVC plate end-caps with an opening for tubing connection. Between each plate end-cap and the soil column an O-ring, a glass fiber filter (pore size 1 µm) and a hydrophilic polypropylene membrane filter (pore size 0.2 µm) were inserted to avoid leakage, uniformize inflow and reduce the filtration effort for the effluent sampling. The bottom end-cap of the FTRs was connected to a peristaltic pump (Gilson MINIPULSE® 3) and served as an inflow

channel while the top end-cap connected to the outflow channel allowed the effluent to collect in polyethylene sampling bottles (125 mL). Inflow and outflow channel consisted of viton tubing (ID = 1.59 mm). During the entire experiment duration of one month, the pump rate (PR) was set to 4 mL h^{-1} (corresponding to a Darcy flux of 7 cm d^{-1}) with slight differences between the pump channels (range of 3.4 to 4.5 mL h^{-1}). Triplicates of MD-peat samples were assigned to different SO_4^{2-} treatments corresponding to SO_4^{2-} milieus in terrestrial (0 and 100 mg L^{-1}), brackish (700 mg L^{-1}) and marine (2700 mg L^{-1}) ecosystems (see Table 3.2). The latter treatment was also applied to the SD-peat and HD-peat samples. Furthermore, another treatment of the MD-peat containing 2700 mg SO_4^{2-} L^{-1} and 590 mg acetate (CH_3COO^-) L^{-1} (concentration inspired by Schmaljohann, 1996) simulating a potential input of marine dissolved organic matter (DOM) was added to guarantee an excess of electron donors, as the peat consists of rather persistent plant residues. Acetate is generally considered as the most relevant electron donor for anaerobic decomposition of organic matter by SRB in the marine environment (Boschker et al., 2001). In the following, the different treatments are referred to with the labels shown in Table 3.2 (e.g. SULF0), the addition of acetate to a treatment is indicated within the label with a "+A".

Table 3.2: Overview of the different applied SO_4^{2-} concentrations and associated number of peat samples. The number in the label of the treatments refers to the SO_4^{2-} concentration (mg L^{-1}) and "+A" indicates the additional addition of acetate (CH_3COO^-) in form of sodium acetate.

Label of treatment	**Simulated SO_4^{2-} milieu**	**SO_4^{2-} (mg L^{-1}) and *(mmol L^{-1})***	**CH_3COO^- (mg L^{-1}) and *(mmol L^{-1})***	**EC (mS cm^{-1})**	**Number of samples of**		
					SD-Peat	**MD-Peat**	**HD-Peat**
SULF0	Control	0 *0.0*	0 *0.0*	2.5		3	
SULF100	Fresh water	100 *1.0*	0 *0.0*	2.6		3	
SULF700	Brackish water	700 *7.3*	0 *0.0*	3.6		3	
SULF2700	Ocean water	2700 *28.1*	0 *0.0*	6.3	3	3	3
SULF2700+A	Ocean water with marine DOM in form of acetate (A)	2700 *28.1*	590 *10.0*	6.6		3	

The artificial brackish input solution was prepared by diluting the quantitatively most important seawater salts according to Kester et al. (1967) (NaCl, KCl, $MgCl_2 \cdot 6H_2O$, $CaCl_2 \cdot 2H_2O$, $NaHCO_3$) in 20-fold dilution in ultra-pure water (Milli-Q) and then adding Na_2SO_4 to adjust the different SO_4^{2-} treatments and $NaCH_3COO$ for the treatment SULF2700+A. The *EC* of the five different input solutions was between 2.5 and 6.6 mS cm^{-1} (measured with a Horiba LAQUA B-213 Twin EC meter*)*, representing seawater diluted by freshwater in the mixing zone (observed in the *Hütelmoor* field site, but see also e.g. Jørgensen et al., 2008). To induce the development of anoxic conditions the input solutions to the FTRs were continuously sparged with argon gas reducing oxygen concentrations to levels between 0.2 and 0.9 mg L^{-1} (measured with a Thermo Scientific Orion 5 Star multifunction meter). The continuous sparging with argon also led to an increase in the *pH* of the input solution (up to 8.8, measured with a Horiba LAQUA B-213 Twin pH meter) due to degassing of carbon dioxide, which was adjusted to values between 7 and 7.5 through addition of minor amount of hydrochlorid acid. However, as the *pH* of seawater (~ 8.1) is generally higher than freshwater, variations of *pH* may also occur under natural field conditions. As the SO_4^{2-} reduction rate is sensitive to the temperature (Stam et al., 2010), the FTR experiment was conducted in an environmental chamber (Percival Scientific CTH-118) at a constant temperature of 15°C representing common summer temperatures in peatland groundwater at the *Hütelmoor* field site (M. Ibenthal, University of Rostock, personal communication). The placement of the experimental set-up in the chamber also ensured dark conditions to prevent algae growth in the acrylic glass tubes.

Prior to the SO_4^{2-} treatments, a control solution (SULF0) containing 0 mg SO_4^{2-} L^{-1} was pumped (4 mL h^{-1}) into the FTRs for three days to purge the cores of gas bubbles that may block water flow as well as to flush out the pre-existing SO_4^{2-} and equilibrate the peat cores with the salt solution. Only for the marine SD-peat a solution with 700 mg SO_4^{2-} L^{-1} was used to maintain the natural SO_4^{2-} milieu in those three samples. The outflow of the first and the last 50 mL of the flushing phase was analyzed to determine the initial and stabilized chemical concentrations. During the SO_4^{2-} treatment phase (one month), the outflow samples were collected every 24 hours for the first three days and afterwards every 48 to 72 hours. During the first five days of the SO_4^{2-} treatment, an additional bromide (Br^-) concentration of 100 mg Br^- L^{-1} was added into the input solutions in

form of 149 mg KBr L^{-1} as a step input to obtain a non-reactive tracer breakthrough curve (BTC). During the Br^- injection outflow water samples were collected every two hours on the first day, every four hours on the second day, every eight hours on the third day, every twelve hours on the fourth day and every 24 hours on the fifth day and the samples were analyzed for Br^- concentration with ion chromatography (see below).

3.2.3 Pore water geochemistry analyses

During the SO_4^{2-} treatments, water samples were collected from the outflow of the FTRs and were sub-sampled into separate vials. 1 ml of pore water was refiltered (to protect the measurement device) through a 0.2 µm membrane filter (Thermo Scientific Polysulfone filter) for analysis of major anions including Cl^-, NO_3^- and SO_4^{2-} using ion chromatography (IC, Dionex ICS-5000 with a capillary IonPac® AS18 column). A volume of 7 ml of pore water sample was acidified with 3 drops of 1M HCl and was analyzed for DOC and total dissolved nitrogen (TDN) using the non-purgeable organic carbon method on a total organic carbon analyzer (Shimadzu TOC-LCPH/CPN). Another volume of 7 mL pore water sample was subsampled for concentrations of dissolved inorganic carbon (DIC) that was measured using the same TOC analyzer. For the SULF2700+A treatment, an additional 1 mL sample was treated with 20 µL of a 500 ppm CrO_4^{2-} solution and analyzed for organic acids using IC to assess acetate concentrations (method detection limit: 0.017 mg L^{-1}) and subtract them from the measured DOC concentrations to get the “acetate-free” DOC release, accepting inaccuracies due to a potential acetogenesis in the peat. For one FTR per treatment, 10 mL of the water samples were filtered through a 0.45 µm membrane filter (Thermo Scientific Polysulfone filter) and were acidified with 2 % ultrapure HNO_3 for analysis of major cations and trace metals including Fe and manganese (Mn) using Inductively-Coupled Plasma Optical Emission Spectrometry (Thermo iCAP 6200 Duo ICP-OES). Once or twice a week a volume of 1.5 mL was collected into vials containing 50 µL of a 5 % zinc acetate solution and the concentration of HS^- was measured colorimetrically according to Cline (1969) and using an UV-Visible spectrophotometer (Thermo Scientific Evolution 260 Bio) measuring the absorbance at 670 nm.

3.2.4 Modeling of breakthrough curves

For the evaluation of the BTCs the software “STANMOD” (available for download from www.pc-progress.com) with the incorporated model CTXFIT (Toride et al., 1999) was used to determine solute transport parameters by fitting a modelled BTC to the measured data with a least-square fitting procedure. As previous studies have shown that peat acts as a dual porosity medium (e.g. Rezanezhad et al., 2012, 2016), a physical non-equilibrium model was used. The mobile-immobile model (MIM) solves the advection-dispersion equation for a mobile pore region, which exchanges solutes via diffusion with an immobile pore region. The dispersion coefficient D (cm^2 h^{-1}) and the two dimensionless parameters β (equivalent to the mobile water content for non-sorbing solutes) and ω (mass transfer coefficient) served as calibration parameters. The retardation factor R was set to 1 (meaning no adsorption occurs), as a pronounced anion adsorption to organic compounds is generally only expected under acidic conditions (Ottow, 2011) and high organic matter contents adversely affect SO_4^{2-} adsorption (Johnson and Todd, 1983). The average pore water velocity v (cm h^{-1}) was also set to a fixed calculated value (v = PR / (sample cross section × Φ)).

3.3 Results and Discussion

3.3.1 Sulfate transport

The SO_4^{2-} BTCs for the different treatments showed slightly different shapes and reached a similar relative concentration (C/C_0) after approximately three pore volumes, as shown in Figure 3.2 (a). However, the differences in their shape are not due to differences in the SO_4^{2-} input concentration, they are instead a result of differences in the soil pore distribution for the individual peat samples. This effect is verified by non-reactive Br^- BTCs (which were always performed for the same Br^- concentration) which show a very similar shape to the SO_4^{2-} BTCs, as exemplified in Figure 3.2 (b) for a breakthrough of 100 mg Br^- L^{-1} and 100 mg SO_4^{2-} L^{-1}. These results suggest that no SO_4^{2-} reduction occurred and SO_4^{2-} behaved as a conservative anion (such as Br^-) during solute transport in the studied fen peat samples. The Br^- and SO_4^{2-} BTCs for all tested peats showed an early breakthrough characterized by a $C/C_0 > 0.5$ at one pore volume (Rezanezhad et al., 2016). This is indicative of nonequilibrium flow, meaning that the MIM serves as an appropriate simulation model in this scenario. The obtained

solute transport parameters for the different peats contrasted for Br^- and SO_4^{2-} (Table 3.3) are similar and in the same range as in comparable studies on fen peat (Liu et al., 2017; Kleimeier et al., 2017; McCarter et al., 2018). Generally, the parameters *D*, *β* and *ω* are considered soil sample-specific and should not depend on the applied solute, which also was supported in this study with Wilcoxon signed-rank tests (α = 0.05), that did not reveal any significant differences between Br^- and SO_4^{2-} parameters. Yet, the variations between the parameters of the different peats were also minor suggesting that the effect of degree of decomposition and organic matter content on the shape of the BTC is less pronounced than what has been shown in previous studies (Liu et al., 2017).

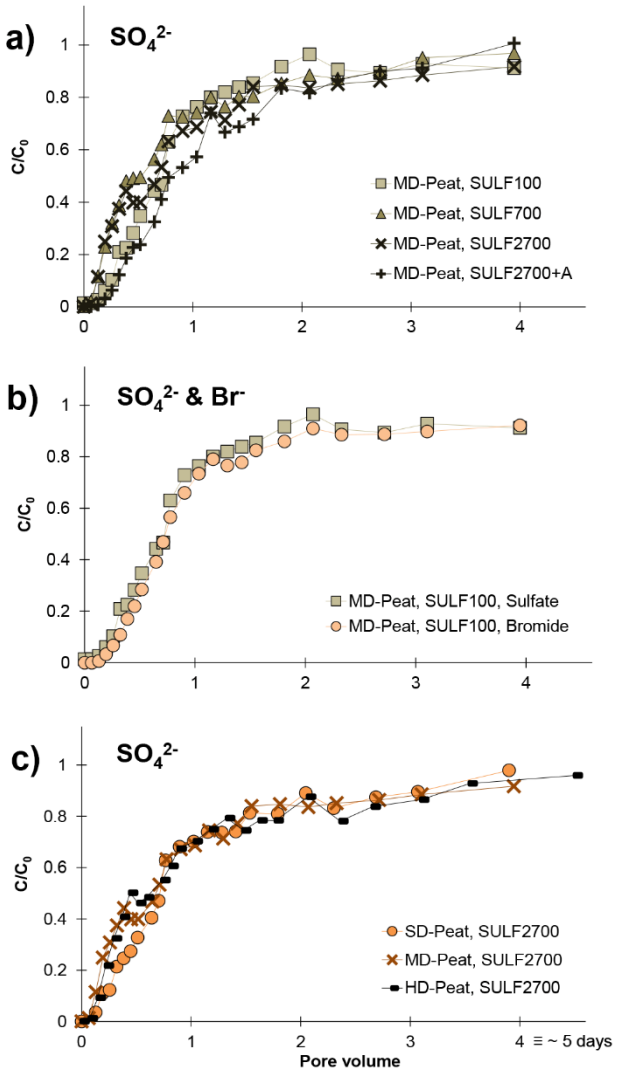

Figure 3.2: Average (*n* = 3) Br^- and SO_4^{2-} breakthrough curves a) all applied SO_4^{2-} concentrations for the moderately-decomposed peat, b) SO_4^{2-} and Br^- for the treatment SULF100 for the moderately-decomposed peat and c) SO_4^{2-} for the treatment SULF2700 for slightly, moderately and highly-decomposed peat.

Table 3.3: Average solute transport parameters (± standard deviation) (v = average pore water velocity, D = dispersion coefficient, β = fraction of the mobile water content, ω = exchange coefficient between mobile and immobile regions) determined with CTXFIT for the slightly, moderately and highly-decomposed peat for SO_4^{2-} and Br^- breakthrough. For a better comparability with other studies the parameters λ = dispersivity, θ_{mo} = mobile water content and α = exchange rate coefficient were calculated from the fitted parameters [$\lambda = D / v$; $\theta_{mo} = \beta \times \Phi$; $\alpha = \omega \times q / L$ with q as the Darcy flux (cm h^{-1})].

	Parameter	SD-Peat	MD-Peat	HD-Peat
Br^-	v (cm h^{-1}) (fixed)	0.32	0.32	0.37
	D (cm² h^{-1})	1.17 ± 1.72	0.66 ± 0.43	1.32 ± 0.46
	λ (cm)	3.66 ± 5.36	2.06 ± 1.35	3.56 ± 1.25
	β (-)	0.65 ± 0.14	0.57 ± 0.22	0.62 ± 0.22
	Θ_{mo} (cm³ cm^{-3})	0.58 ± 0.12	0.51 ± 0.20	0.49 ± 0.17
	ω (-)	0.99 ± 0.61	1.41 ± 2.22	0.38 ± 0.45
	α (d^{-1})	0.69 ± 0.42	0.98 ± 1.54	0.26 ± 0.31
SO_4^{2-}	v (cm h^{-1}) (fixed)	0.32	0.32	0.37
	D (cm² h^{-1})	0.99 ± 1.32	0.93 ± 0.70	0.91 ± 1.01
	λ (cm)	3.10 ± 4.13	2.90 ± 2.20	2.45 ± 2.73
	β (-)	0.60 ± 0.10	0.54 ± 0.22	0.35 ± 0.09
	Θ_{mo} (cm³ cm^{-3})	0.54 ± 0.09	0.48 ± 0.19	0.27 ± 0.07
	ω (-)	0.70 ± 0.36	1.06 ± 1.09	0.89 ± 0.45
	α (d^{-1})	0.49 ± 0.25	0.74 ± 0.75	0.62 ± 0.31

SO_4^{2-} and sodium (Na^+) concentrations in the outflow of the peat samples reached the input concentration after five days for SO_4^{2-} and ten days for Na^+ and remained stable throughout the experiment. Only during the final phase of the experiment a slight difference in SO_4^{2-} concentration was observed between the input and output concentrations of the SULF2700+A treatment implying that SO_4^{2-} reduction occurred only in the latter case. This is consistent with the results of the measurement of HS^-, which was only detected in higher concentrations (up to 2.4 mg L^{-1}, other treatments of MD-peat: 0.03 to 0.13 mg L^{-1}) for the SULF2700+A treatment in the later phase of the experiment – although a non-detection of HS^- can also be related to reactions of HS^- with other compounds such as ferrous iron (Fe^{2+}) (see effect of acetate). The SD- and HD-peat samples produced HS^- concentrations between 0.06 and 0.2 mg L^{-1} with only a slight increase in effluent concentration occurring over time, indicating a very weak background SO_4^{2-} reduction. Results from all treatments imply that more SO_4^{2-} reduction could have

been detected if the experiment was run for a longer duration. For the Fe-rich peat samples, MD-peat and HD-peat, the delayed stimulation of SO_4^{2-} reduction can be attributed to an initial period of Fe(III) reduction. The predominance of Fe(III) reduction over SO_4^{2-} reduction has been observed by Küsel et al. (2008), who found that in an upper peat horizon in a lowland fen with a similar Fe content (33 g kg^{-1}), the Fe(III) reduction made up 72 % of the anaerobic organic carbon mineralization. Conversely, for the SO_4^{2-}-affected SD-peat with lower Fe content, it can be postulated that the microbially available carbon pool was depleted due to previous pronounced SO_4^{2-} reduction occurring under field conditions.

3.3.2 Solute release

Initial flushing

Containing 40 % organic carbon and 3 % nitrogen (Table 3.1), the MD-peat represents a potential source for nutrients. During the equilibration period with SO_4^{2-}-free water (3 days ≡ 2.3 PV), the substances which had accumulated in the pore water in the peat were flushed and the concentrations of DOC, DIC and TDN decreased, on average, from 9 to 4 mg DOC L^{-1}, from 16 to 3 mg DIC L^{-1} and from 0.7 to 0.4 mg TDN L^{-1}. The initial values measured for DOC are lower than in previous studies using flow-through experiments with peat (32 mg DOC L^{-1} in Gosch et al. (2018), 11 mg DOC L^{-1} in Tiemeyer et al. (2017)), which can be explained by a larger sample volume of 50 mL in this study causing a dilution of the peak concentration as well as a sample filtration using 0.2 µm filters rather than the commonly used 0.45 µm filters. However, in the cases of this experiment as well as the aforementioned previous studies, the DOC concentrations stabilized in a range of 30 to 40 % of the initial concentration. Field concentrations of DOC and TDN from the sampling site were measured to be 16 mg DOC L^{-1} and 3.6 mg TDN L^{-1}. The apparent discrepancy between the field values and laboratory column experiments has already been observed in other studies (Stutter et al., 2007; Tiemeyer et al., 2017), and is generally explained by longer residence times and limited dilution in the field. The initial values for the HD-peat were higher than for the MD-peat with a decrease from 13 to 6 mg DOC L^{-1}, 17 to 6 DIC mg L^{-1} and 6.6 to 0.5 mg TDN L^{-1}. Formerly drained and degraded peat is known to release more solutes than less decomposed peat, due to the formation of more mobile compounds through aerobic mineralization (Zak et al., 2010). Therefore for rewetting purposes the degraded top soil of formerly drained peatlands is

sometimes removed to reduce the leaching of nutrients and emission of greenhouse gases (Zak et al., 2018). In this study, the initial release of 22 mg NO_3 L^{-1} from the HD-peat was 440 times higher than that of 0.05 mg NO_3 L^{-1} release occurring from the underlying MD-peat. For the marine SD-peat, which was initially flushed with a 700 mg L^{-1} SO_4^{2-} solution, the concentrations changed from 28 to 25 mg DOC L^{-1}, 12 to 1 mg DIC L^{-1} and 3 to 1 mg TDN L^{-1}, and no NO_3^- was detected in the effluent. The relatively lower decrease in DOC concentrations observed for the MD-peat sample group might be related to the effects of changes in *EC* wherein the antecedent *EC* from the marine field conditions was closer to the artificial seawater than in the terrestrial peat.

Effect of sulfate concentration

During the SO_4^{2-} application in the FTRs, the solute release evolved differently for the various SO_4^{2-} treatments of the MD-peat (Figure 3.3 a-c). For most of the samples DOC and TDN concentrations decreased continuously. However, the higher the SO_4^{2-} concentration in the input solution the lower the average slope of the linear trend for DOC and the higher the average DOC concentration at which the values seemed to stabilize (for SULF0 and SULF100 ~ 2 mg L^{-1}, for SULF700 ~ 3 mg L^{-1} and for SULF2700 ~ 5 mg L^{-1}). These results imply a positive correlation between *EC* and DOC and do not confirm observations by previous studies on DOC fluctuations, who observed a negative correlation between *EC* and DOC release (Münch et al., 2002; Clark et al., 2011; Tiemeyer et al., 2017). For example, in Tiemeyer et al. (2017) an increase in *EC* from ~ 100 to 1000 µS cm^{-1} caused a decrease of DOC from ~ 10 to 1 mg DOC L^{-1}. However, the results in this study are consistent with a previous study by Gosch et al. (2018), who observed a positive relation between *EC* and DOC for peat material from the same field site from which samples were collected for this study. The non-validity of the negative correlation between *EC* and DOC relation for the MD-peat might be attributed to the peat (pore water) chemistry (see effect of peat decomposition degree). The existence of interfering impact factors is also indicated by contradicting effects comparing laboratory and field data (Tiemeyer et al., 2017b) or surface water and pore water geochemistry (Knorr, 2013).

This result also does not confirm previous findings by Ardón et al. (2016), who observed a decreasing DOC release with higher SO_4^{2-} concentrations (range of 100 to 300 mg SO_4^{2-} L^{-1}). Ardón et al. (2016) concluded that the consumption of

DOC via SO_4^{2-} reduction was responsible for this decline. However, peat samples undergoing the SULF0, SULF100, SULF700 and SULF2700 treatment exhibited no pronounced SO_4^{2-} reduction, hence Ardón et al. (2016) conclusion cannot be considered as the cause for the observed differences in DOC/DIC/TDN between the treatments. Instead, minor differences observed in DOC release from the different SO_4^{2-} treatments may be attributed to anion exchange of DOM anions by SO_4^{2-} (Brouns et al., 2014). An increased dispersion of organic matter caused by a replacement of calcium (Ca^{2+}) by Na^{+} (e.g. Edelstein et al., 2010) is considered unlikely as increased Ca^{2+} concentrations were observed in effluent immediately after the start of the SO_4^{2-} treatments (see segment about cation-related processes below). In contrast, DOC release in the different treatments differed more towards the end of the experiment.

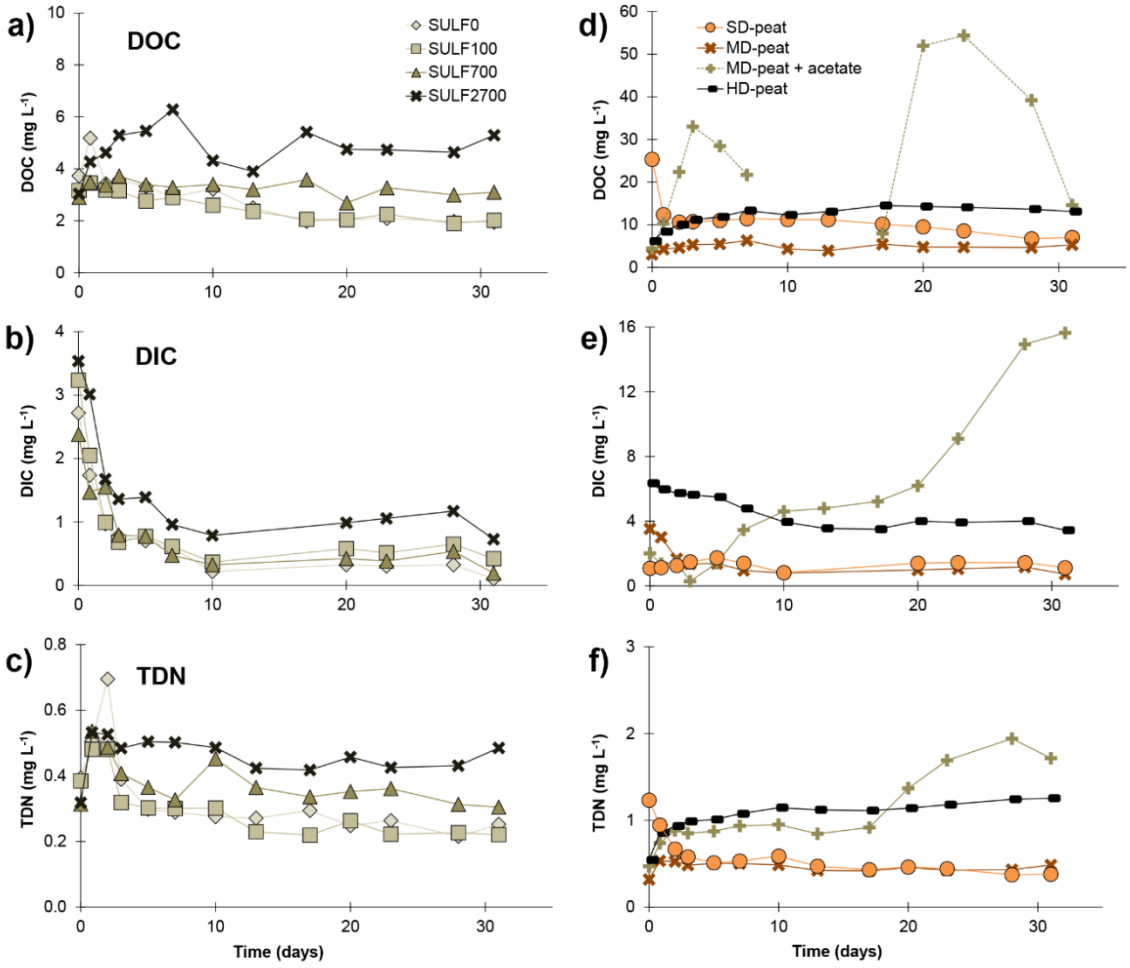

Figure 3.3: Average concentrations (n = 3) for DOC, DIC and TDN in the effluent of the FTRs during the SO_4^{2-} applications (a, b, c) for the different SO_4^{2-} treatments and (d, e, f) for the different degrees of decomposition for the SULF2700 treatment and for the MD-peat for the SULF2700+A treatment. Note the scaling differences.

The release of TDN over time resembled the release of DOC, which is reflected by a correlation coefficient calculated between 0.5 and 0.9, indicating a strong relationship between these two parameters. This result suggests that the majority of the nitrogen released derived from DOM rather than from NH_4^+. This is consistent with observations made in a shrub-dominated peatland by Wang et al. (2016) who found that 68 % of nitrogen compounds released from peat monoliths were dissolved organic nitrogen (DON), while NH_4^+ and NO_3^-/ NO_2^- made up only 8 % and 24 %, respectively. In this study, NO_3^- (method detection limit: 0.05 mg L^{-1}) was detected only irregularly and in a low concentration between 0 to 0.13 mg L^{-1} in the effluent of MD-peat samples.

The release of DIC as an indicator for decomposition of organic matter showed less treatment-dependent tendencies than DOC and TDN. The SULF0, SULF100 and SULF700 treatments caused similar releases of DIC. Only peat samples treated with SULF2700 led to slightly higher DIC concentrations. However, DIC concentrations in the effluent of all samples first decreased before stabilizing at values between 0 and 1 mg L^{-1}. This supports the assumption that none of the SO_4^{2-} concentrations led to a pronounced SO_4^{2-} reduction in the time frame of this experiment. As the decrease also occurred for the SULF0 treatment, it can be assumed that the decrease is the continuation of the initial leaching of DIC.

Increased Na^+ concentrations from the input solution resulted in cation exchange leading to variable increases in different cation concentrations throughout the experiment (data not shown). For the MD-peat, the concentrations of Ca^{2+} and K^+ increased shortly after the treatment commenced with the highest Ca^{2+}/K^+ peak occurring in samples treated with the greatest Na^+ concentrations (SULF2700 and SULF2700+A) and subsequently decreased towards the value of the input solution. It stands to reason that Ca^{2+} and K^+ were exchanged by Na^+, although Ca^{2+} is generally bound more strongly to the peat than Na^+ as a result of its bivalence (Succow and Joosten, 2001). Magnesium (Mg^{2+}) concentrations increased very slowly over time and had not reached the input concentration value after 31 days, indicating that the displacement of other cations by Mg^{2+} took longer than the experimental duration. Total dissolved manganese (TDMn) (showing a peak right after the start of the treatment and then stabilizing at a value between 0.12 and 0.28 mg L^{-1}) and total dissolved aluminum (TDAl) (stable value, but graduated from SULF0 with 0.01 mg L^{-1} to SULF2700+A with 0.05 mg L^{-1}) concentrations were lowest for the SULF0 treatment and highest for the

SULF2700+A treatment suggesting that, for the corresponding ions (Mn^{2+}, Al^{3+}), the Na^{+} concentrations determined the release of these solutes. However, the evaluation is less clear for Fe and Mn as they may potentially be involved in the anaerobic decomposition processes and are present in different oxidation states that ICP measurements cannot distinguish. Increased concentrations of total dissolved iron (TDFe) were observed in all treatments compared to SULF0. Although, the order of magnitude of the measured peaks varied greatly (between 0.8 and 17 mg L^{-1}) and did not correlate with the SO_4^{2-} treatments.

Effect of acetate

In contrast to the SO_4^{2-}-only treatments, a pronounced increase of DIC release accompanied by an increase in HS^{-} was observed for the acetate-enriched SULF2700+A treatment (Figure 3.4), providing evidence for SO_4^{2-} reduction (with hydrogen carbonate and sulfide as end-products). The duration of the experiment covered only the initial phase of SO_4^{2-} reduction as the concentrations of HS^{-} and DIC were still increasing after 31 days. A pronounced SO_4^{2-} reduction appeared to begin after ~ 17 days (≡ ~ 15 pore volumes). This time period represents a lag time during which redox conditions favorable for SO_4^{2-} reduction established in the samples. The SRB are generally outcompeted by microorganisms active at higher redox potentials that get energy via aerobic respiration, denitrification or Fe(III) and Mn(IV) reduction. As major HS^{-} concentrations and DIC increase were only observed in acetate addition treatment (SULF2700+A), it can be assumed that the peat in this study did not represent a suitable carbon source for the SRB under the prevailing laboratory conditions, to which also the non-increase of SO_4^{2-} reduction rate for SO_4^{2-}-treated bog peat has been attributed (Vile et al., 2003). These findings confirm recent results of isotopic measurement of DIC in the pore water of sea-exposed fen peat of the *Hütelmoor* field site, which indicate that the detected DIC concentrations do not originate from the submerged peat itself, but from easily degradable marine DOM (J. Westphal, Leibniz Institute for Baltic Sea Research Warnemünde, personal communication). The measured HS^{-} concentrations were considerably lower than the measured DIC concentrations (comparison in molar concentrations see Figure 5). This means that either not all HS^{-} was detected due to its chemical reactivity or other processes than SO_4^{2-} reduction co-drove the DIC production. It is possible that a part of the released HS^{-} was bound to the DOM (Heitmann and Blodau, 2006) or precipitated as iron sulfide (van der Welle et al.,

2007) and was, therefore, not detected with the applied method in this study. Other mineralization processes such as Fe(III) reduction could have driven the DIC production as an increase of DOC and TDN in the SULF2700+A treatment was observed indicating a general stimulation of decomposition processes. Concentrations of TDFe were highly elevated in the SULF2700+A treatment (peak concentration of 28 mg L^{-1}) compared to the acetate-free SULF2700 treatment (peak concentration of 2 mg L^{-1}). These results imply that Fe(III) reduction had occurred, during which Fe^{2+} is released; yet, the time curve of HS^- indicates that DIC production was mainly controlled by SO_4^{2-} reduction (Figure 3.4 (a)). This also applies to other parameters – overall, the release of DOC, DIC, TDN and total dissolved phosphorus (TDP) was stimulated by SO_4^{2-} reduction. Conversely, the release of TDMn in the SULF2700+A treatment resembled its counterpart (SULF2700) and experienced only a slightly lower peak concentration. This suggests that TDMn-release was mainly affected by cation exchange and not Mn(IV) reduction, which is consistent with the gradations in TDMn-concentrations for the acetate-free treatments following Na^+ input concentrations (see effect of sulfate concentration).

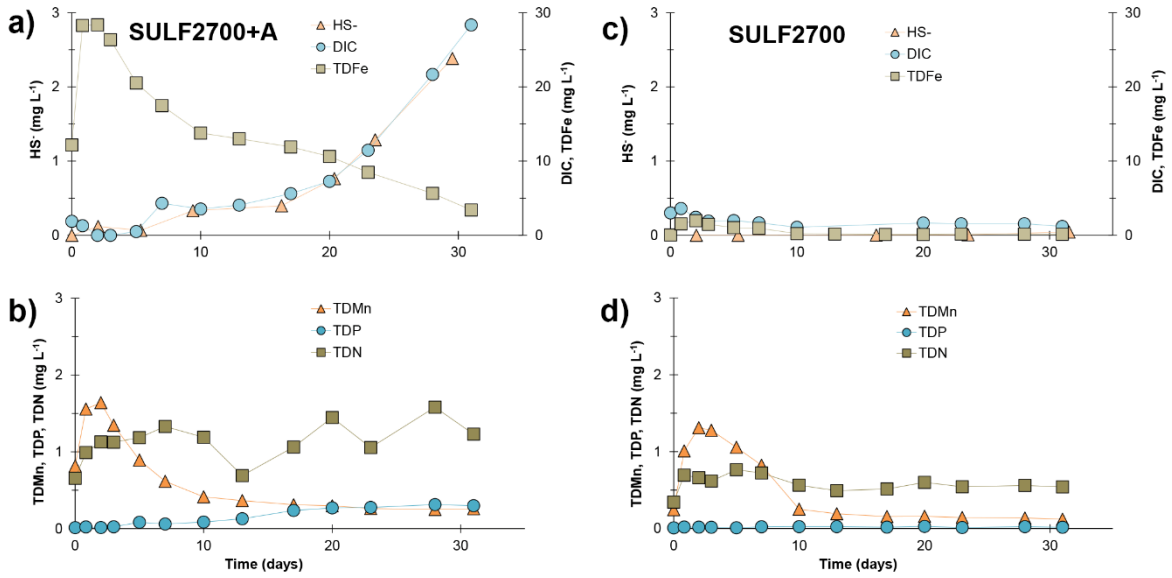

Figure 3.4: Release of HS^-, DIC and TDFe as well as TDMn, TDP and TDN measured in the effluent of the FTR from an individual peat sample during a,b) SULF2700+A and c,d) SULF2700 treatment.

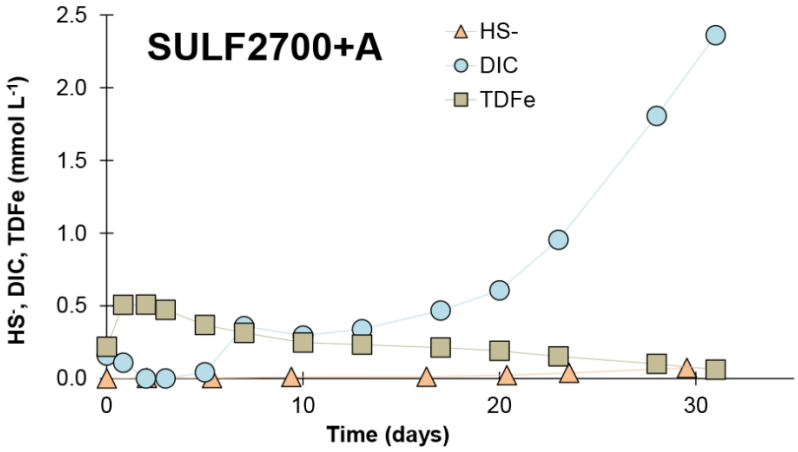

Figure 3.5: Release of end products of SO_4^{2-} reduction (HS-, DIC) and of TDFe as interfering substance in molar concentration measured in the effluent of the FTR from an individual peat sample during SULF2700+A treatment.

Effect of peat decomposition degree

The observed differences of solute release between the peats of varying degrees of decomposition were more pronounced and clearer than between the different SO_4^{2-} concentrations applied to one peat material (Figure 3.3 for DOC/DIC/TDN, Figure 3.6 for TDFe). The substance release of the SD-peat matched the expectations that the DOC would decrease abruptly after an *EC* increase (see effect of sulfate concentration). Following an increase in *EC* from 3.6 mS cm^{-1} (SULF700) to 6.3 mS cm^{-1} (SULF2700), DOC and TDN concentrations decreased on average by 51 % and 22 %, respectively. In contrast, DOC and TDN concentrations varied only slightly for the MD-peat and responded immediately with an increase to the SULF2700 treatment for the HD-peat (Figure 3.3 (d)). The observed differences in the time curve of DOC and TDN between the three peats could be related to the large differences in Fe content (Table 3.1), where the HD-peat contains 50 times more Fe than the SD-peat. As previously discussed (see initial flushing), the long-term drained and degraded peat generally has a different composition than less decomposed peat. While the percentage of organic carbon decreases with decomposition, the percentage of phosphorus (P), Fe and Al increases (Zeitz and Velty, 2002; Litaor et al., 2004). Knorr (2013) observed that DOC and TDFe concentrations had a clear positive correlation in pore and surface water while the impact of water salinity was not consistent for the two types of water. Iron salts such as ferric sulfate are well known to induce flocculation of fine organic and inorganic particles from the production of cationic hydrolysis products

and are generally used to clean drinking water from DOM (Sharp et al., 2006). However, during Fe(III) reduction Fe^{2+} is released thereby co-mobilizing the previously flocculated DOM with other formerly bound solutes like phosphate. The correlation coefficient R^2 between TDFe and DOC concentrations in the effluent of this study ranged between 0.36 (SULF2700) and 0.95 (SULF100) for the pure SO_4^{2-} treatments of the MD-peat. The Fe-rich HD-peat samples have a calculated R^2 value of 0.58, demonstrating Fe-related interference is an important impact factor for DOC.

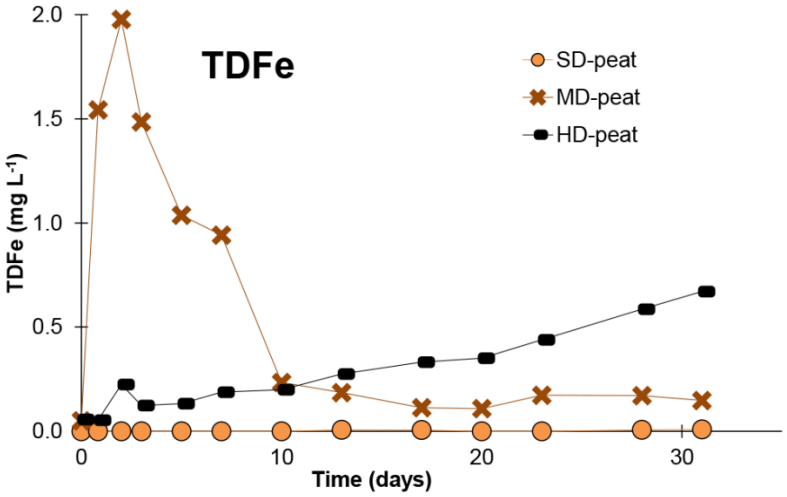

Figure 3.6: Release of TDFe from SD-, MD- and HD-peat measured in the effluent of the FTRs.

The observed differences between the SD-, MD- and HD-peat in solute release could also be related to their pore-related parameters, such as porosity and proportion of the immobile pore regions detected via BTC analysis. Immobile zones provide an opposing effect on DOC concentrations where stagnant pore water zones may serve as hot spots for DOM production, as they represent the preferred habitat for microorganisms (Nunes et al., 2015; Rezanezhad et al., 2016). Immobile pore regions also increase the average pore water velocity and preferential flow thereby reducing the residence time of the water in the mobile pore regions and the potential for solute exchange between liquid and solid phase (Tiemeyer et al., 2017b). However, as the release of DOC/TDN from SD-peat and MD-peat reached comparable values during the experiment, physical differences – whose effect should be long-lasting – may only be relevant to the HD-peat. Generally, the greater the degree of decomposition in peat the more pronounced the preferential flow occurs (Liu et al., 2017) and the immobile pore region fraction

increases. In case of the HD-peat the greater proportion of immobile pore water might have contributed to the higher constant release of DOC/TDN.

3.4 Conclusions

In this flow-through experiment peat samples treated with sulfate (SO_4^{2-})-enriched water did not produce pronounced SO_4^{2-} reduction within one month's time. SO_4^{2-} and bromide (Br^-) breakthrough curves were similar indicating that SO_4^{2-} behaved as a conservative tracer within the experiment and that the SO_4^{2-} penetration was dependent on the physical properties of the peat samples. The addition of acetate, a major electron donor in marine sediments, initiated SO_4^{2-} reduction after ~ 17 days and led to a strong increase of release of solutes such as dissolved organic carbon (DOC) and inorganic carbon (DIC). This suggests that under these experimental conditions the composition and decomposability of the organic matter was more important to enabling decomposing processes than the presence of terminal electron acceptors. This was also demonstrated by the increased solute concentrations for peat with a higher degree of decomposition. However, increased SO_4^{2-} concentrations did result in slightly elevated levels of DOC and total dissolved nitrogen (TDN). These results are attributed to the potential desorption of negatively charged organic molecules via anion exchange with SO_4^{2-}. For the different tested peats, the short-term release of DOC was presumably affected not only by the ionic strength of the inflowing water but also by the iron (Fe) content of the peat, as DOC bound to Fe compounds can get mobilized during Fe(III) reduction. Overall, the main short-term effects of SO_4^{2-}-rich seawater inflow in peatlands seem to be desorption processes, whose characteristics are controlled by the ionic composition and strength of the seawater, and peat chemistry, particularly Fe content and degree of decomposition. Decomposition-related solute release may develop in the long-term, when anoxic, stagnant conditions prevail. This may be accelerated if marine, easily degradable organic matter is flushed in the peatland during seawater flooding even though concentrations of bioavailable DOC might be lower than the applied acetate concentrations in this study. The onset of SO_4^{2-} reduction may reduce the gaseous emissions of carbon-containing methane (CH_4) from the peatland, but may also increase the load of dissolved carbon compounds in the peatland's outflow.

4 CARBON RELEASE AND TRANSFORMATION FROM COASTAL PEAT DEPOSITS CONTROLLED BY SUBMARINE GROUNDWATER DISCHARGE: A COLUMN EXPERIMENT STUDY

Matthias Kreuzburg[1], Fereidoun Rezanezhad[2], Tatjana Milojevic[2], Maren Voss[1], Lennart Gosch[3], Susanne Liebner[4], Philippe Van Cappellen[2] and Gregor Rehder[1]

[1]Leibniz Institute for Baltic Sea Research, Warnemünde, Germany
[2]Ecohydrology Research Group and Water Institute, Department of Earth and Environmental Sciences, University of Waterloo, Waterloo, Ontario, Canada
[3]Faculty of Agricultural and Environmental Sciences, University of Rostock, Rostock, Germany
[4]GFZ German Research Centre for Geosciences, Section 3.7: Geomicrobiology, Potsdam, University of Potsdam, Institute of Biogeochemistry and Biology, Potsdam, Germany

Limnology and Oceanography (2020) 65: 1116–1135

Abstract

Although the majority of coastal sediments consist of sandy material, in some areas marine ingression caused the submergence of terrestrial carbon-rich peat soils. This affects the coastal carbon balance, as peat represents a potential carbon source. We performed a column experiment to better understand the coupled flow and biogeochemical processes governing carbon transformations in submerged peat under coastal fresh groundwater (GW) discharge and brackish water intrusion. The columns contained naturally layered sediments with and without peat (organic carbon content in peat 39 ± 14 dwt%), alternately supplied with oxygen-rich brackish water from above and oxygen-poor, low-saline GW from below. The low-saline GW discharge through the peat significantly increased the release and ascent of dissolved organic carbon (DOC) from the peat ($\delta^{13}C_{DOC}$ − 26.9‰ to − 27.7‰), which was accompanied by the production of dissolved inorganic carbon (DIC) and emission of carbon dioxide (CO_2), implying DOC mineralization. Oxygen respiration, sulfate (SO_4^{2-}) reduction, and methane (CH_4) formation were differently pronounced in the sediments and were accompanied with higher microbial abundances in peat compared to sand with SO_4^{2-}-reducing bacteria clearly dominating methanogens. With decreasing salinity and SO_4^{2-}-concentrations, CH_4 emission rates increased from 16.5 to 77.3 μmol m^{-2} d^{-1} during a 14-day, low-saline GW discharge phase. In contrast, oxygenated brackish water intrusion resulted in lower DOC and DIC pore water concentrations and significantly lower CH_4 and CO_2 emissions. Our study illustrates the strong dependence of carbon cycling in shallow coastal areas with submerged peat deposits on the flow and mixing dynamics within the subterranean estuary.

4.1 Introduction

Sea-level rise is considered to be one of the main impacts of climate change, with significant implications for mineralization processes within coastal wetlands (Nicholls and Cazenave, 2010; Neubauer, 2013; Plag and Jules-Plag, 2013; Hahn et al., 2015; Wang et al., 2016). In particular, coastline retreat may cause submergence of terrestrial, organic carbon-rich peat sediments. The extent of submarine peat and the process-based impacts on carbon transformation processes and exchange of trace gases in shallow coastal areas have been poorly addressed. Sediment column experiments are powerful tools to investigate subprocesses and simulate changes of environmental and hydrological conditions. These changes are accelerated by land subsidence of peatland caused by their large-scale drainage for agricultural use. Land subsidence alters the hydrologic exchange processes across the land-sea interface (Nieuwenhuis and Schokking, 1997; Hooijer et al., 2012) including changes in surficial runoff, subsurface mixing, and submarine groundwater discharge (SGD).

SGD is comprised of all flow of water from the seabed into the coastal ocean, predominantly recirculated seawater (SW), driven by wave action, density gradients, and sea-level dynamics (Robinson et al., 2007; Moore, 2009; Cyberski, 2011; Santos et al., 2012). SW-derived solutes, such as dissolved oxygen (O_2) and SO_4^{2-}, affect the mineralization of organic matter in the seabed (Mulholland, 2003; Weston et al., 2011; Chambers et al., 2014; Rezanezhad et al., 2016). The minor fraction of freshwater SGD, typically in the order of 4–10% (Li et al., 1999; Burnett et al., 2006; Moore, 2009), is mainly controlled by the hydraulic gradients and is often O_2 depleted and enriched in methane (CH_4) and free hydrogen (H_2) (Andersen et al., 2005; Bugna et al., 1996; Slomp and Van Cappellen, 2004). Because coastal peatlands mostly exhibit low topographic relief, their hydraulic gradients and freshwater discharge into coastal areas tend to be relatively low (Barlow and Reichard, 2010). Nonetheless, even in coastal regions of low elevation, SGD can reach values of up to 200 cm d^{-1} (Rapaglia, 2005) and can, therefore, result in high fluxes of chemical compounds to the coastal environment. For instance, SGD-borne nitrogen fluxes can be of the same order of magnitude as those delivered by rivers (Knee et al., 2010; Knee and Paytan, 2011; Seitzinger and Harrison, 2008). This may be one factor, driving coastal productivity toward phosphorus limitation (Slomp and Van Cappellen, 2004). In addition, SGD has

been identified as a carbon source to nearshore marine environments (Bugna et al., 1996; Bussmann and Suess, 1998; Porubsky et al., 2014; Schlüter et al., 2004).

Peatlands cover only 3% of the earth's surface, but they store about 20–25% of the global soil organic carbon (C_{org}) (Gorham, 1995; Limpens et al., 2008; Strack, 2008). Uptake and release of C_{org} are strongly controlled by the prevailing hydrological conditions (Moore and Dalva, 1993; Roulet et al., 1992; Sirin and Laine, 2008; Wang et al., 2016; Zauft et al., 2010). When drained, peatlands can switch from being a carbon sink to a source, emitting greenhouse gases such as carbon dioxide (CO_2) (Strack, 2008). In contrast, flooded peatlands usually represent a source of atmospheric CH_4 (Gatland et al., 2014; Hahn et al., 2015), which has the second largest radiative forcing after CO_2 (Ramaswamy, 2001). On a global scale, the atmospheric CH_4 concentration has increased by more than 250 % since 1750, contributing ~ 32% of the anthropogenic radiative forcing (IPCC, 2013). Global methane emissions from wetlands, coastal zones, and estuaries into the atmosphere have recently been assessed at 117.2 ± 49.7, 13, and 7 Tg CH_4 yr^{-1}, respectively (Borges et al., 2016; Zhang et al., 2017), but coastal estimates of CH_4 emissions remain highly uncertain due to a small number of studies and may indicate strong variations (Weber et al., 2019). Together, coastal zones were estimated to generate approximately 75% of the total marine CH_4 emissions to the atmosphere (Bange et al., 1994). In-field studies, CH_4 emissions of 126–134 μmol m^{-2} d^{-1} were associated with gassy sediments containing high organic carbon (Borges et al., 2016). The most abundant process of marine CH_4 production is microbial methanogenesis (Cicerone and Oremland, 1988), a form of anaerobic respiration using, for example, CO_2 instead of O_2 as an electron acceptor (e.g., $CO_2 + 4H_2 \rightarrow CH_4 + 2H_2O$) to degrade dissolved organic carbon (DOC). Other pathways of methane production results from acetate degradation (e.g., $CH_3COOH \rightarrow CO_2 + CH_4$) (Deppenmeier, 2002). The production of CH_4, however, is closely related to SO_4^{2-} reduction, which is the dominating metabolic process of DOC mineralization in anoxic marine sediments (Gosch et al., 2019; Zehnder and Mitchell, 1978). Sulfate-reducing bacteria (SRB) are generally able to successfully outcompete methanogens during organic matter degradation (Whiticar et al., 1986). High SO_4^{2-} concentrations also sustain anaerobic CH_4 oxidation, which provides an effective barrier, limiting the amount of sedimentary CH_4 that reaches the water column (Dale et al., 2008; Iversen and

Blackburn, 1981; Jørgensen et al., 2001; Reeburgh and Alperin, 1988). Nevertheless, in near-coastal shallow regions, sediment-derived CH_4 may still represent a significant source of dissolved CH_4 in the water column. In 2010–2011, Borges et al. (2016) recorded an average CH_4 concentration in Belgian coastal surface water (< 15 km offshore) of 139 nmol L^{-1}, with values as high as 1128 nmol L^{-1}, presumably caused by outgassing from Pleistocene peat-containing sediments.

Peatlands along the coastal margins are also a major source of DOC to coastal and shelf areas (Freeman et al., 2001; Mulholland, 2003). Currently, the majority of experimental studies considering carbon transformation processes from wetland soil focus on onshore processes (Chambers et al., 2011; Kalbitz et al., 2000; Säurich et al., 2019; Wen et al., 2019). A number of experimental approaches have identified the ionic strength of the advective pore water as an important factor controlling DOC concentrations and mobilization, where increasing ionic strength results in decreasing DOC release from organic soils and vice versa (Limpens et al., 2008; Tiemeyer et al., 2017b; Tipping and Hurley, 1988). Furthermore, Tiemeyer et al. (2017b) reported that the production of DOC is dependent on the residence time of the pore water, showing a negative correlation between the DOC concentration and the pump rate-controlled advective pore water velocity. Previously observed positive correlations between the release of DOC from subsedimentary sources (e.g., buried peat) and CH_4 concentrations in the water column suggested a common carbon source (Aravena and Wassenaar, 1993; Liu et al., 2011). Submerged organic-rich peat sediments can be found in shallow coastal waters offshore of adjoining peatlands (DeLaune et al., 1994; Kreuzburg et al., 2018; Taffs et al., 2012), where marine microbial communities can be supplied by peat-derived DOC and SW-derived electron acceptors (e.g., O_2, SO_4^{2-}, NO_3^-). How these submerged peat deposits in the offshore areas contribute to coastal carbon cycling, however, is currently not well constrained.

In this study, we investigate the mobilization of peat-derived DOC and biogeochemical processes that control carbon transformations using a novel flow-through column experiment with natural sediments. During the experiment, we imposed alternating cycles of upward flowing oxygen-depleted groundwater (GW) and downward flowing oxygen-rich brackish water. The main goal of the study was to monitor the biogeochemical processes governing carbon transformations in submerged coastal peat in the mixing zone of low-saline GW

and brackish water. To the best of our knowledge, this is the first experimental study investigating DOC mobilization and mineralization processes in submerged coastal peat soil, in conjunction with the production of climate relevant trace gases, under dynamic (bidirectional) flow conditions mimicking freshwater–SW mixing in the so-termed “subterranean estuary” (Moore, 1999).

4.2 Study site

The coastal peatland and nature reserve “Heiligensee and Hütelmoor” (Figure 4.1) northeast of Rostock-Warnemünde (extending roughly 1.6 km in the north-south direction and 1.4 km in the east-west direction) experienced large anthropogenic disturbances. The site was drained for agricultural purposes until the 1970s (Dahms, 1991; Voigtländer et al., 1996), and subsequently rewetted by freshwater for restoration of the biodiversity in the 1990s (Hahn et al., 2015; Hübner, 2013; Miegel et al., 2016). Until today, the peatland drains through an extensive channel system towards the south. In the last decades, the onshore area has been subject to a wide range of investigations, including gas emissions and the investigations of landside biogeochemical processes, hydrology monitoring programs as well as geologic surveys (Jurasinski et al., 2018; Koch et al., 2014; Koebsch et al., 2015; Lasak et al., 2010; Miegel et al., 2016; Strehse et al., 2018; Voigtländer et al., 1996; Wen et al., 2018).

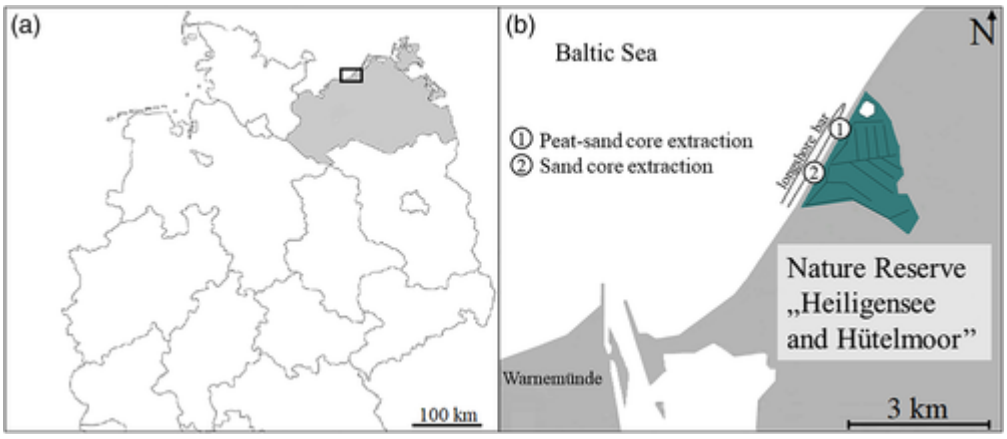

Figure 4.1: Location of the study site showing (**a**) Germany with the state of Mecklenburg-Vorpommern shaded gray; the black rectangle indicates the close-up of the right side, and (**b**) location of the coastal area near Rostock-Warnemünde where sediment cores were collected in front of the nature reserve “Heiligensee and Hütelmoor” and a rough position and shape of a coast parallel longshore bar.

The beach area has been subject to beach nourishments, wooden groynes were installed to retain the sand and a dyke was constructed after several wash-over events (Kolp, 1957; Voigtländer et al., 1996). The shoreline is covered by permeable heterogeneous sediments except for areas with peat deposits (Hübner, 2013; Kreuzburg et al., 2018), which are only low-permeable substratum (Gosch et al., 2019). In a recent geological assessment of the development of the seabed (Kreuzburg et al., 2018), Holocene peat deposits with C_{org} contents of 37–53 % and C/N ratios of 21.3–36.4 were found more than 90 m (areal extent: 0.16-0.2 km^2) in front of the coastline (Figure 4.1). The isotopic signature of the lowermost offshore peat seems to be purely terrestrial ($\delta^{13}C$ –28.9‰) and thus no fractionation processes or contamination with marine organic carbon were detected. The outer boundary of the peat deposits roughly coincides with the offshore limit of a dynamic coast-parallel longshore bar (Kreuzburg et al., 2018). The location of shallower outcropping peat deposits in the northern coastal area coincides with temperature, salinity and bottom water CH_4 anomalies most likely originating from SGD (Jurasinski et al., 2018).

4.3 Materials and methods

4.3.1 Sediment sampling

Sediment cores were collected, in ~ 20 cm water depth, off the coastal nature reserve “Heiligensee and Hütelmoor” on 25 August 2017 using PVC liners measuring 60 cm in length and 7.5 cm in width. The sampling site of the cores P1, P2, and P3 (54.222139°N, 12.168361°E) was characterized by submarine outcropping peat layers and was covered with ~ 20 cm of marine sand. The degree of decomposition of the peat, which according to von Post (1922) is defined by the color of the extracted pore water, was H 3–4.

The sand cores S1, S2, and S3 were collected in the south of the study site (54.2108°N, 12.1582°E), where the coastline was covered with permeable marine sediments and peat deposits were absent along the coastline. Details of the geology have been presented in Figure 2 in Kreuzburg et al. (2018). One core from each site was kept as a reference to compare geochemical parameters of initial and altered conditions. In order to ensure similarity of the four replicates, cores were taken within an area of < 0.25 m^2. Immediately after sampling, the cores were sealed at the top and bottom with gastight and watertight endcaps and transported to the laboratory, where they were stored at 4°C with supernatant

water. Within 9 d of extraction the cores where drained, packed in a cryobox and transported via airfreight to the University of Waterloo, Canada. Visual inspection showed that the sediment sequence of the cores remained intact, but slight changes in sediment deposition could not be excluded. In the laboratory at the University of Waterloo, Canada, the sediment cores were unsealed to prevent complete anoxia and stored at 4°C for additional 16 d until the cores were installed in the experimental setup. Modifications in microbial communities and abundances, as well as redox conditions, likely occurred after transportation and storage. However, the initial microbial and redox conditions were not recorded; therefore comparison to natural conditions is limited.

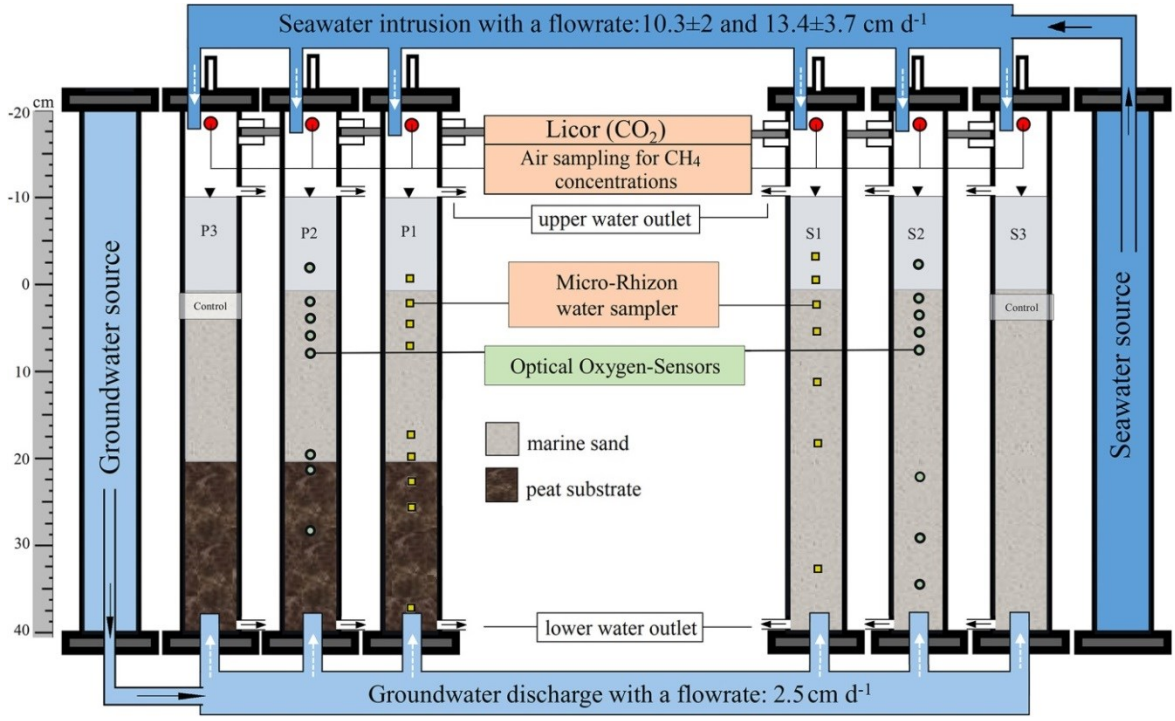

Figure 4.2: Schematic diagram of the controlled flow regime column system. The six sediment columns were simultaneously and alternatingly exposed to advective flow with artificial SW from the top (outflow at the bottom) and artificial GW from the bottom (outflow near the top). Intrusive measuring devices were installed for pore water sampling (P1/S1) and optical oxygen monitoring (P2/S2).

4.3.2 Column experiment setup and instrumentation

The experiment setup included eight columns (six for sediment cores and two for water storage) made of transparent acrylic glass and matching the sediment core size. The water flow velocity through all cores was controlled by a computer-controlled pump (CAT-Multichannel-Pump Tower II, Figure 4.2). A

mostly similar column system was formerly described by Rezanezhad et al. (2014), but has been specifically refined for the variable water flow regimes in this study. In contrast to Rezanezhad et al. (2014), water of different salinities (GW, SW) was pumped through the marine sediment cores in two directions (alternating upward and downward) and discharged at the opposing end. Furthermore, the water level was kept constant and sediments were fully water saturated. The water level above all sediment columns was ~ 10 cm to approximate shallow water conditions. The lower half of three of the six 40-cm long columns was filled with naturally layered submerged peat sediments, which were overlain by marine sand. The other three cores only contained marine sand. For both sediment types, one column (P1/S1) was used to sample pore water for solute analysis, one column (P2/S2) was used for monitoring of the vertical aqueous oxygen distribution, and one column was used as a control for additional measurements of the gas fluxes and to compare pore water solute concentrations (P3/S3). The emissions of CH_4 and CO_2 were measured in all six cores.

The columns were filled from the bottom by a custom-made lifting jack and wrapped in tinfoil to prevent subsedimentary photosynthetic activity. Three of the columns were filled with 40 cm peat–sand cores containing ~ 20 cm of sand at the top. The other three columns were filled with 40-cm sand cores. The top and bottom of the columns were closed with acrylic endcaps that had O-rings lining the inner rims to form tight seals. A filter membrane (Soil Measurement Systems, LLC, bubbling pressure: 600 mbar) closed off the bottom of the column and a nylon mesh (Soil Measurement Systems, LLC, bubbling pressure: 32 mbar) was placed on top of the filter membrane. For each column, three steel rods connected the acrylic top and bottom endcaps and were secured with bolts. The sediment columns were connected to the water storage columns with chemically resistant polyurethane tubing. In order to completely replace the air-filled pore space with water, the initial filling was conducted from the bottom with artificially produced GW (*see* "Chlorinity and conductivity" section) for 3 d at a rate of 0.3 mL min^{-1}. The total headspaces above the sediment surface were partly filled with water in the amount of ~ 888 cm^3 in Columns P1, P2, and P3 and ~ 1002 cm^3 in Columns S1, S2 and S3, respectively. All columns contained an air-filled headspace volume of ~ 478 ± 57 cm^3 (mean ± SD) above the water.

The storage columns were filled with artificial SW and fresh GW, which were continuously sparged with air and argon gas, respectively, with the latter intended

to ensure oxygen-depleted conditions (details of the GW and SW compositions are given in “Chlorinity and conductivity” section). The columns were incubated at 24 ± 2°C during the entire course of the experiment. Each sediment column had 18 lateral ports (1/8″ NPT compression fittings) equally spaced every 3 cm for pore water sampling. The ports were airtight and fitted with Teflon tape. In the following text, all depths are referenced with respect to the depth below the sediment surface. The ports of four columns (P1, P3, S1, S3) were equipped with ceramic samplers, 5 cm in length and 0.25 cm in diameter, with a filter pore size of 0.15 μm (CSS5 MicroRhizon™ samplers, #19.21.23F) (Seeberg-Elverfeldt et al., 2005). The samplers were introduced horizontally into the sediment matrix, below the sediment surface, to extract pore water samples for pore water chemical and dissolved gas analyses (Figure 4.2). A vacuum pump (Soil Measurement Systems, LLC, #CL-042) set at − 100 mbar was used to extract pore water through the samplers. The headspace above the stable water surface in the columns was periodically closed in order to measure sediment-derived trace gas accumulation.

Water flow regime

The upward flowing GW and downward flowing SW were set to simulate discharge and recirculation regimes through permeable coastal sediment impacted by submerged peat. The pore water flow velocities were adapted from the column experiment conducted by Tiemeyer et al. (2017b), who identified a relation between DOC solution properties from organic soils, pore water velocity and composition. The height of the water table in the sediment columns was imposed using a computer-controlled, multichannel pump connected to the water storage reservoirs. The total volume of the storage columns was ~ 3.3 Liters, but the quantity of water contained varied according to flow conditions and was refilled for continuous flow. The constant ponding of the water above sediment surfaces ensured complete water saturation in the sediments and resulted from the equilibrium between the programmed pump rate and the water outflow, whereby the water in the sediment column was continuously exchanged. The GW upward flow was pump controlled at rates of 2.5 cm d^{-1} and the water-level height was limited by the water outlet ~ 10 cm above the sediment surface. The SW downward flow was controlled by the valve settings and rates were measured at 10.3 ± 2 cm d^{-1} through peat–sand cores and 13.4 ± 3.7 cm d^{-1} through sand cores. The flow ratio and flow rate were chosen to produce visible effects and

changes in dissolved concentrations and volumes of the sediment column with the 50-day experiment. The ratio of GW to SW in natural shallow water conditions is typically > 1 : 10 (Burnett et al., 2006; Li et al., 1999). During the different flow regimes, the water was discharged on the opposite side of the inflow. Flow direction and water type were adjusted using valves settings. The level of the water table in the soil columns fluctuated between 7.5 and 10 cm above the soil surface, respectively.

Coastal aquifers can be strongly depleted in oxygen (Andersen et al., 2005; Bugna et al., 1996), while shallow water along the shoreline is saturated with oxygen due to constant mixing with the atmosphere. To imitate similar conditions, argon gas was used to deoxygenate the GW and air from the laboratory was used to saturate the SW with oxygen. The artificial GW salinity was set at $S \approx 1.6$, which is slightly lower than measured values in the field ($S \approx 3$), but chosen in order to achieve a better differentiation of the end-member concentrations. The salinity of artificial SW is based on highest salinity measured ($S \approx 18$) along the shoreline of the study site (all observations from 2017). The salinity-based chloride (Cl^-) concentrations were 882 ± 66 mg L^{-1} (range: 806–1015) for GW and 8666 ± 407.1 mg L^{-1} (range: 7987–9577) for SW. Chloride was used as a conservative tracer to describe physical transport behavior and as a measure of salinity with $S = 0.00180665 \times Cl^-$ mg L^{-1} (Lyman, 1969). The ratio of the other elements to chloride was based on SGD surveys in Kiel Bay, Baltic Sea in 2015 (unpublished data). Although the salinity of the Baltic Sea is largely described, there are lack of stoichiometric data on shallow shorelines and coastal aquifers. For ionic composition, *see* Table 4.1. All six columns were fed with SW and GW, from identical water reservoirs for the 50 d-period of the experiment.

Table 4.1: Composition of artificial seawater (SW) and artificial groundwater (GW) used in the experiment.

	Na^+	K^+	Ca^{2+}	Mg^{2+}	NH_4^+	Cl^-	SO_4^{2-}	HCO_3^-	NO_3^-	PO_4^{3-}	SiO_2	Salinity
	----------(mmol L^{-1})----------											
SW	223	4.6	5.2	25	0.002	259	13.2	2.5	0.004	0.0005	0.009	17.8
GW	17.4	0.37	4.2	1.6	0.0002	29	0.2	0.37	0.007	0.02	0.07	1.6

4.3.3 Analytical methods

CH_4 and CO_2 flux at the water–headspace interface

The water/headspace gas flux, F_{gas}, of each column was obtained by measuring the change in gas concentration over time in the headspace after closure from the laboratory atmosphere, according to the following equation:

$$F_{gas} = \frac{dC_{gas}}{dt}\frac{V_h}{A}\frac{p}{R_{gas}T} \quad (6)$$

where dC_{gas}/dt describes the changing gas concentration (ppm) over time, V_h (m^3) is the volume of the headspace, and A (m^2) is the exposed water surface area. p is the atmospheric pressure (Pa), R_{gas} is the gas constant (8.314 Pa m^3 K^{-1} mol^{-1}), and T is the absolute temperature (°K). To avoid uncontrolled gas accumulation and to minimize evaporative losses from the sediments over time, the air-filled headspaces of the sediment columns were continuously flushed with water-saturated air by passing the air through a water-filled vial. In order to determine the gas emissions from the aqueous phase into the headspace, the air ventilation was stopped. Fluctuations of the headspace volumes were taken into account in every gas flux measurement.

The fluxes of CH_4 (μmol m^{-2} d^{-1}) were monitored two to three times a week from all six cores. The concentrations were determined at the beginning (t_0) and end (t_N) of incubation (24 ± 6 h) by sampling 10 mL of headspace gas using glass syringes and were measured by gas chromatography (GC; Shimadzu Gas Chromatograph, Model GC-2014), equipped with an advanced flame ionization detector technology and helium used as an inert carrier gas. To ensure equipment accuracy, calibration standards were measured before measurement of the samples. The concentrations of the samples were within the range of calibration. For standards, a three-point calibration was used with the following certified standard gases: Level 3 = “Praxair Canada” Certified Standard, carbon dioxide 900 ppm, ± 2%, methane 95 ppm, ± 2%; Level 2 = “Praxair Canada,” carbon dioxide 100 ppm, ± 2%, methane 9.8 ppm, ± 2%; and Level 1 = Air Liquide America Specialty Gases LLC (formerly Scott Specialty Gases)—Scotty analyzed gas, analysis by moles, ± 5%, carbon dioxide 600 ppm, methane 5 ppm. For CH_4 measurements with a standard deviation < 1% were conducted following a linear calibration through zero. In total, 6 mL of gaseous sample was injected into the gas chromatograph, 5 mL of which were used for flushing the system and the 1-mL sample loop.

The pore water samples for dissolved CH_4 were extracted in peat–sand columns from the sediment at depths of -1 (i.e., above the sediment), 2, 5, 8, 17, 20, 23, 26, 38 cm and from the sand column at sediment depths of -4.5, -1.5, 1.5, 10.5 19.5, and 34.5 cm. Before sampling, 0.5 mL of water was extracted for flushing and eliminate the air-filled void in the syringe. Pore water samples of 1 mL were collected with 10-mL watertight, pretreated (HgCl = 25 μL) glass syringes (MICRO-Mate®) by connecting to the MicroRhizon water samplers. The sample volume of the pore water was determined by the weight (scale precision: 0.1 mg). Eight milliliters of helium was then added to form a headspace for gas equalization. After 2 h of equilibration time, by carefully shaking the syringe, which has been shown to strip at least 95% of CH_4 from the solution (Dillon et al., 1999) into the headspace, all samples were analyzed by GC on the same day of collection.

The water-headspace CO_2 fluxes were sampled daily by an automated multiplexer CO_2 flux measurement system (LI-8100, LI-COR Biosciences) via two lateral ports (Figure 4.2). Air from the headspace above the water surface was then circulated through the infrared gas analyzer of the LI-8100 and back to the column. The CO_2 fluxes were calculated according to Equation 11, whereas the rate (dC_{CO2}/dt) was estimated from six consecutive 180-s observation windows spanning a 15-min time interval. Volume (m^3) is a combination of the headspace volume, tubing, and the sampling loop through which the headspace gas circulates. This method has been previously described by Rezanezhad et al. (2014). The CO_2 concentrations of LI-COR and GC were tested for comparability before the experiment (data not shown).

Pore water geochemistry

Pore water samples (8 mL per depth; peat–sand n = 134, sand n = 97 in total) were extracted from cores P1 and S1 with MicroRhizon™ samplers (Cabrera, 1998; Knight et al., 1998; Seeberg-Elverfeldt et al., 2005) and were subsampled into separate vials. One milliliter of each water sample was filtered through a 0.2-µm membrane filter (polysulfone filter, Thermo Scientific) for the analysis of Cl^-, SO_4^{2-}, NO_3^-, and acetate ($C_2H_3O_2^-$) by ion chromatography (Dionex ICS-5000 with a capillary IonPac® AS18 column). To measure DIC and DOC concentrations by using the nonpurgeable organic carbon method on a total organic carbon analyzer (Shimadzu TOC-LCPH/CPN, method detection limit (MDL) = 0.011 mM),

1 mL each was used. The DIC analyses were run on 7 mL samples by diluting the 1 mL samples and accounting the dilution factor in the final DIC results. DIC was sampled using open test tubes made of glass and were immediately sealed with parafilm and cooled until analyzation. This was the same for DOC analysis. The samples for DOC analyses were acidified with 20 µL of 1 M HCl. The range of reproducibility of the measurements for DIC and DOC were ± 5 and ± 12 µmol L^{-1}, respectively. Filtered pore water (< 1 mL) was analyzed for electrical conductivity (*EC*) using a WTW EC Meter (three-point calibration at 99.1, 999, 9976 µS cm^{-1}). The *EC* analyses were run on 15 mL samples by diluting 0.75 mL of pore water samples and accounting the dilution factor in the final results. Carbon isotopes of DOC were investigated at Day 50 in the pore water of the peat–sand core (P1). For the analyses of $\delta^{13}C_{Doc}$, a portion of sample equivalent to 0.2 mg carbonate was removed from the sample aliquot and was injected in a 12-mL flat bottom Exetainer vial (Labco #739 W), where it was treated with orthophosphoric acid and potassium persulfate. The phosphoric acid addition converts inorganic carbonates present in the sample to CO_2 which is removed by bubbling with a helium gas stream for about 10 min (EPA, 2002; IsoPrime, 2014). The sample was then sealed in the vial and microwaved. During heating, the persulfate oxidizes any DOC in the sample to CO_2. The CO_2 in the headspace of the sample vial was analyzed. Standards ranged from − 12‰ (EIL-36—cane sugar) to − 26.5‰ (EIL-35—beet sugar). Delta values obtained by dual inlet mass spectrometry (MS) calibrated with International Atomic Energy Agency (IAEA) carbonate standards and verified by Elemental Analyzer/Isotope Ratio Mass Spectrometry (EA-IRMS) analysis normalized with IAEA-CH3 (cellulose) + IAEA-CH6 (sugar), USGS-40, and USGS-41 (L -glutamic acid) (St-Jean, 2003; Stainton et al., 1977). The results of the samples and all standard runs were statistically evaluated and were within the specification of ≤0.2‰.

Dissolved oxygen concentration monitoring

The sediment cores P2 and S2 were fitted with multifiber optode (MuFO) oxygen sensors to measure the dissolved O_2 concentration at regular depth intervals. The sensing ends were installed into the sediment columns. Eight were installed in the peat–sand column at 2, 5, 8, 14, 17, 20, 38 cm and above the sediment (− 1 cm), and eight were installed in the sand column, at 1.5, 4.5, 7.5, 10.5, 16.5, 31.5 cm and above the sediment (− 4.5, − 1.5 cm). The MuFO is a luminescence-based

optode technique that uses optical sensors made of fiber optic cables, where each cable has one sensing tip and one imaging tip (Larsen et al., 2011). The sensor was built in-house using a sensing solution containing Pt(II) mesoTetra (pentaflourophenyl)–porphine as the lumniophore (Badocco et al., 2012). The uncoated ends were placed in front of a DSLR camera and blue LED light (447.5 nm wavelength) in a similar setup as described by Larsen et al. (2011). The emitted light was photographed every 2 h for the duration of the experiment and, following image processing using ImageJ software (Rasband, 2015), the light intensity was related to the O_2 concentration through the Stern–Volmer relationship. The sensors were calibrated in water of the same composition as used in the experiment, in order to obtain the correct relation between light intensity and O_2 concentration. To evaluate optode light intensity responses as a function of salinity, calibrations for each sensor were conducted at a range of different salinities prior to the experiment.

Statistical analysis and data visualization

Statistical data analysis was performed to identify significant levels among the water flow regime under changing salinities and DOC and DIC production. Moreover, the relationship between salinity and O_2 as well as between SO_4^{2-} concentrations and CH_4 and CO_2 fluxes were statistically analyzed. Significant differences were accepted when the p value was smaller than significance level $\alpha = 0.05$. Gridding of pore water concentrations was performed in R-3.4.0 (R Foundation for Statistical Computing) within RStudio-1.0.143.

Quantification of methanogenic archaea and SRB

Genomic DNA was extracted from 0.2 to 0.3 g of duplicates of sediment or peat sample retrieved from Column P2 at the end of the experiment using a EURx GeneMatrix Soil DNA Purification Kit (Roboklon, #E3570). DNA concentrations were quantified with a Nanophotometer P360 (Implen GmbH) and Qubit 2.0 Fluorometer (Thermo Fisher Scientific). Quantitative polymerase chain reaction (qPCR) for the determination of functional gene copy numbers of methanogenic archaea and SRB was performed via SybrGreen assays on a Bio-Rad CFX instrument (Bio-Rad) as described elsewhere (Vuillemin et al., 2018; Wen et al., 2018) with slight modifications. In detail, the methyl coenzyme M reductase alpha subunit (mcrA) as the functional methanogenic gene was amplified with the primer combination mlas-F/mcra-R (ggT gTM ggD TTC ACM CAR TA /CgT TCA TBg

CgT AgT TVg gRT AgT) with primer annealing at 60°C. The dissimilatory sulfite reductase beta subunit (dsrB) as a functional gene for SRB was quantified with the primers dsrB2060-F/dsrB4-R (CAA CAT CgT YCA YAC CCA ggg /gTg Tag CAG TTA CCg CA) with annealing at 62°C. Different DNA template dilutions (1 : 10, 1 : 50, 1 : 100) were tested prior to the qPCR runs to determine optimal template concentration without inhibitions through co-extracts. The 25 µL reactions contained 12.5 µL of KAPA SYBR® FAST mastermix (Life Technologies, San Francisco, CA), 0.25 µM concentrations of the primers, and 5 µL of DNA template. Data acquisition was done at 80°C to avoid quantification of primer dimers. The specificity of each run was verified through melt-curve analysis and gel electrophoresis. Only runs with efficiencies between 80% and 105% were used for further analysis. Measurements were performed in triplicate. Equimolar DNA mixtures of Methanosarcina barkeri, Methanobacterium lacus, and Methanosarcina soligelidi SMA21 were used for plasmid standards of mcrA and of Desulfovibrio vulgaris for dsrB.

Solid-phase geochemistry

At the end of the experimental period, all peat–sand and sand cores were drained overnight, extruded and sliced every 3 cm. The sediment slices from each depth were homogenized and separate aliquots were taken for geochemical characterization. For the latter, the samples were freeze-dried and stored at room temperature. Organic carbon contents (C_{org}) were measured after removal of carbonates with 10% HCl. The stable isotopic ratio of solid organic carbon ($\delta^{13}C$) were determined on the initial (kept as a reference) and postexperimental sediment cores. The samples were ground in an agate motor mill. Splits of 10–20 mg powdered, homogenized sample were weighed in tin and silver containers (Nieuwenhuize et al., 1994). Stable isotope analyses on $\delta^{13}C$ were performed using an IRMS (Thermo Fisher Scientific), connected to an elemental analyzer via an open split interface (Multi EA 2000 CS). The reference gas was ultrapure CO_2 from a bottle calibrated against international standards (IAEA-C3, IAEA-C6, NBS 22) at the Leibniz-Institute for Baltic Sea Research (IOW). Calibration for carbon quantities was done with acetanilide reagent. The lab internal standard was peptone (Merck) with a standard deviation of < 0.2‰. Considering the 3-cm slice thickness, the depth data were interpreted and compared with the initial cores.

4.4 Results

4.4.1 Solid-phase geochemistry

Results from C, N, and $\delta^{13}C$ isotope analyses (Figure 4.3) identified strong variations in elemental concentrations with depth within both the experimental cores (end) and the initial (init.) core. The experimental cores were exposed to the 50-day flow-through treatments, whereas the initial cores were kept as a reference until geochemical analysis at the end of the experiment. The stable isotope values ($\delta^{13}C$) in the peat layers were in the range of −27.9‰ to −26.8‰, with mean values of −27.3‰ ± 0.3‰, and exhibited higher values in the upper 20-cm sand layer (in the range of −25.3‰ to −22.6‰, with a mean value of −24.6‰ ± 1.5‰). In peat–sand columns, the mean concentration of C_{org} in the peat layers (depth below 30 cm sediment depth) was 44.2% ± 5.3% compared to 15.9% ± 20.2% in the transition layer between the peat and sand (sediment depth of 30–21 cm) and 0.04% ± 0.02% in the upper sand layer (Figure 4.3).

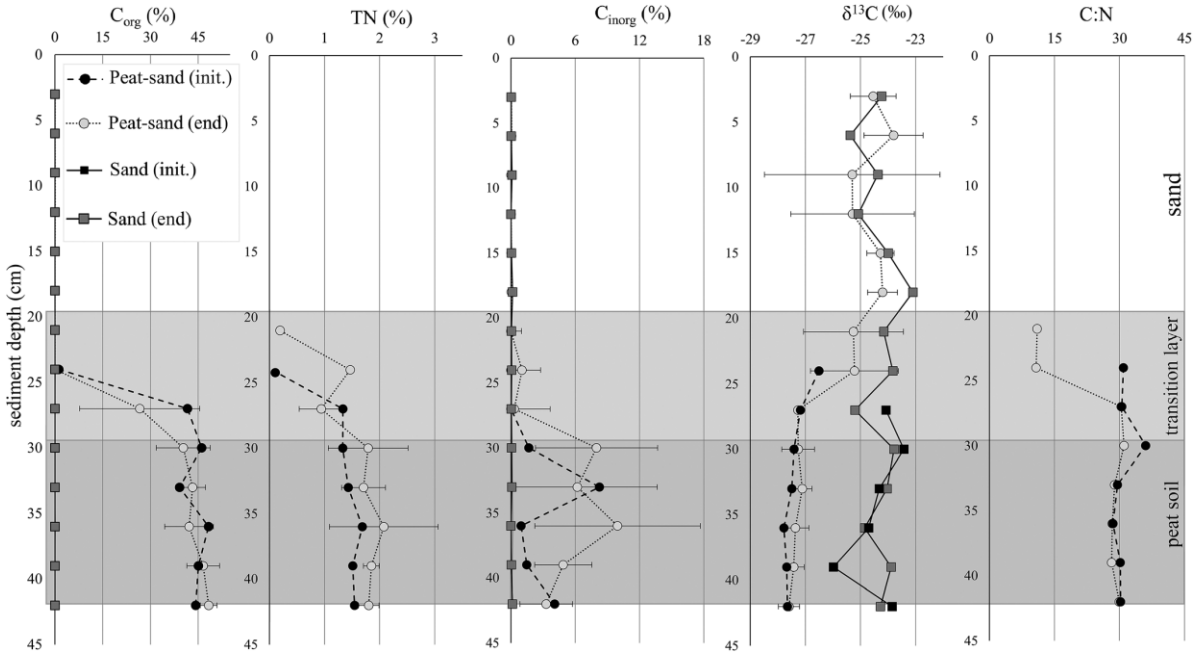

Figure 4.3: Depth distribution of organic carbon contents (C_{org} %), total nitrogen (TN %), inorganic carbon (C_{inorg} %), stable isotopic signature of organic carbon (δ13C‰) and carbon/nitrogen ratios (C : N) in the peat-sand and sand columns from the cores after the 50 d treatment (end) and from cores in their initial state (init). Shown are mean values and standard deviation of cores of the same sediment type and represent a sediment slice of 3 cm thickness. The gray box shading indicates peat layers for the peat-sand columns. All measurements were made after the end of the experiment.

Total nitrogen was only detectable in the peat layers (a mean value of 1.5% ± 0.6%) and followed the depth distribution of C_{org} (r^2 = 0.85, p = 0.007). Here C : N ratios decreased from 29.5 ± 1.7 in the peat layer to 10.9 ± 0.2 in the transition layer (20–30 cm). In contrast, in the sand columns, the mean concentrations of C_{org}, C_{inorg}, and TN were very low or not detectable and a greater variance was observed for $\delta^{13}C$ (Figure 4.3). The concentration of C_{inorg} in the peat layer and the sand on top in the peat–sand core (end.) was 6.5% ± 5.3% and 0.04% ± 0.03%, respectively, with significant differences to the peat–sand core (init.).

4.4.2 Aqueous-phase geochemistry

Chlorinity and conductivity

A high correlation for the salinity calculated with Cl^- and the salinity resulting from the EC was observed for peat–sand columns (r^2 = 0.79, p < 0.001, n = 134) and sand cores (r^2 = 0.90, p < 0.001, n = 97). Because Cl^- is known not to be affected by sorption processes, it was chosen as a measure of salinity (S). The highest salinities (S > 12) were measured during the three SW cycles in the entire depths of the peat–sand and sand columns. During the GW cycles, the salinity along the column depth decreased to 6.7–9.5, and the lowest salinity (S < 5) was measured at the bottom of the peat–sand column during the upward GW flow after 14 d at the end of the experiment (Figure 4.4).

Pore water chemistry

The dissolved oxygen (O_2) concentration in both peat–sand and sand columns varied following the SW and GW flow regimes and increased with SW intrusion phases (Figure 4.4). In the peat–sand column, sediment depths > 15 cm showed oxygen concentrations of 42 ± 10.9 μmol L^{-1}, but were 70 ± 50 μmol L^{-1} in sediments above and 121 ± 29 μmol L^{-1} at the uppermost sensor in the water column. In comparison, the sand columns were entirely penetrated with oxygen. The highest O_2 concentrations (240.5 ± 67 μmol L^{-1}; range: 103–374 μmol L^{-1}) were observed at Day 7 in the upper part of the sand columns during SW downward flow regime (Figure 4.4).

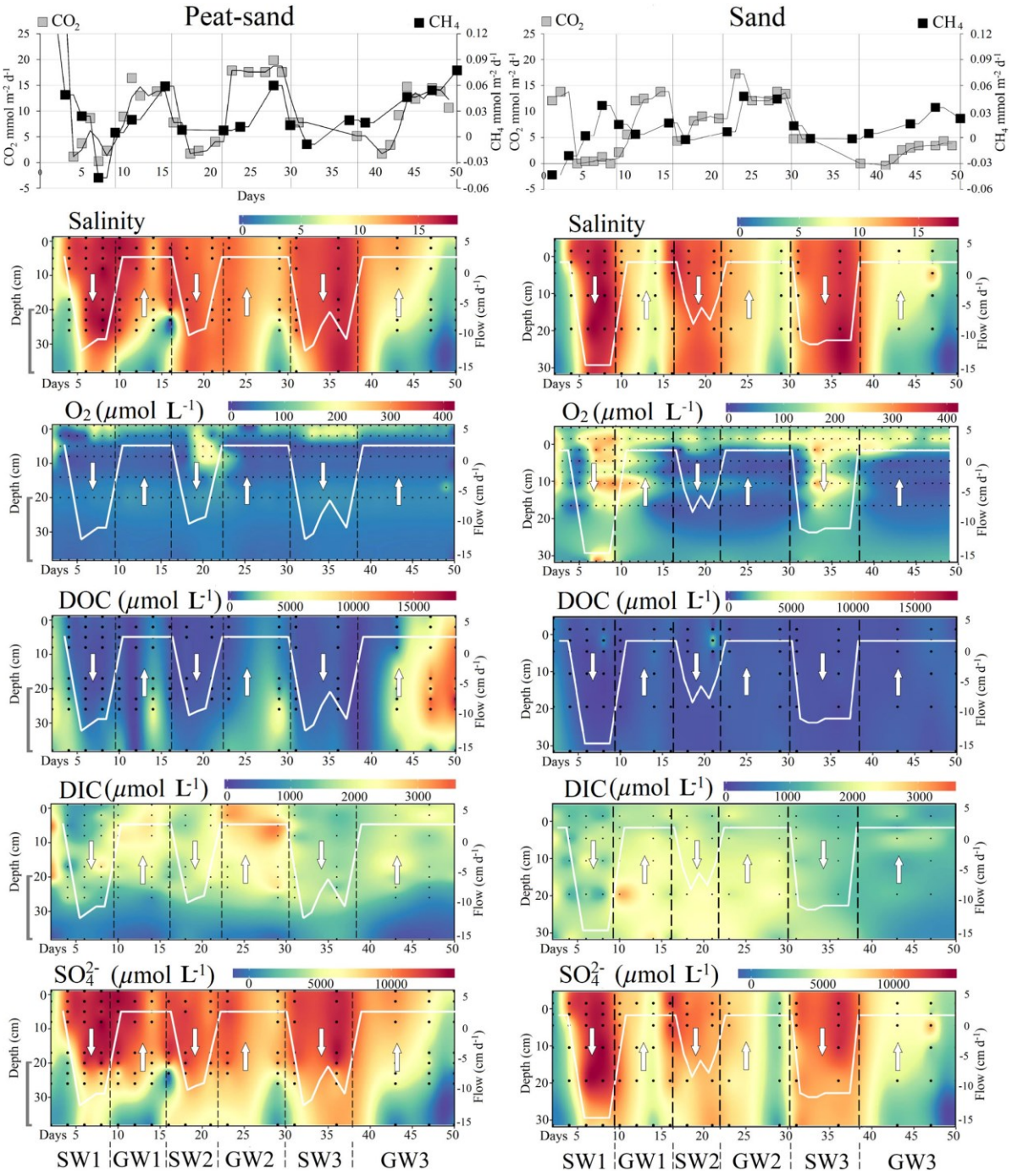

Figure 4.4: The fluxes of CO_2 and CH_4 (upper graphs) derived from concentration change rates in the headspace of all columns for peat-sand (left) and sand (right). Depth distributions of aqueous concentrations of salinity, O_2, DOC, DIC and SO_4^{2-} are presented for each column set, over the 50 d of the experiment period and under GW and SW flow regimes. The white arrows show the flow direction, the white lines indicate the advective flow rates with negative values indicating downward SW flow and positive values show upward GW flow. The black dots represent the pore water sampling depths and time of sampling. The gray bracket left of the peat-sand data indicates the peat layer in the lower section (20–40 cm) of the core.

In both the peat–sand and the sand columns, the aqueous concentration of SO_4^{2-} showed a positive correlation with the SW downward flow events (peat–sand: $r^2 = 0.85$; sand: $r^2 = 0.92$), identifying the SW as the source of SO_4^{2-}, but showed increasing deviation with depth (Figure 4.4). During the GW upward flow a significant increase in concentrations of DOC ($r^2 = 0.81$, $p < 0.001$) was detected with decreasing salinities in the peat–sand column. Furthermore, the increased production of DOC with advective GW upflow resulted in ascent and enrichment of DOC in the sand sediment above the peat layer (Figure 4.4) and revealed acetate concentrations of 6 ± 1.2 mg L^{-1} (GW1), 8.4 ± 1.4 mg L^{-1} (GW2), and 4.6 ± 1.3 mg L^{-1} (GW3) (data not shown). With increasing salinities during SW downward flow, a significant decrease of DOC concentration in the pore water was observed. During the downward flowing SW2 phase (Day 18, Figure 4.4), the O_2 concentrations strongly increased in the surface sediments. The following GW2 upward flow showed highest pore water DIC concentrations and occurred together with highest CO_2 emissions (Figure 4.4) in the peat–sand cores. The final GW3 upward flow event lasted for 14 d, and strongly lowered the salinity and substantially increased the concentrations of DOC (~ 18 mmol L^{-1}) over the entire sediment core length (Figure 4.4).

Stable isotopic composition of DOC

The isotopic signatures of $\delta^{13}C_{DOC}$ in P1 were 26.7‰ ± 4.5‰ with lowest values of − 26.9‰ to − 27.7‰ at salinities of $S \leq 5$. Slightly heavier $\delta^{13}C_{DOC}$ − 26.7‰ to −25.6‰ were detected at salinities $S > 5$. A linear multiple regression between $\delta^{13}C_{DOC}$, DOC, and salinity indicate a moderate adjusted determination coefficient ($r^2 = 0.72$) with lighter values found with higher DOC concentration and decreasing salinities.

4.4.3 CO_2 and CH_4 fluxes

During GW upward flow regimes, average CO_2 fluxes were significantly higher in peat–sand (11.4 ± 5.8 mmol m^{-2} d^{-1}) and sand (6.9 ± 5.7 mmol m^{-2} d^{-1}) compared to SW downward flow regimes with 4.6 ± 3.4 mmol m^{-2} d^{-1} (peat–sand) and 3.7 ± 3.4 mmol m^{-2} d^{-1} (sand) (Figure 4.4). The lowest average CO_2 fluxes of 0.5 mmol m^{-2} d^{-1} were observed in the sand cores during the SW1 down flow regime. In both sediment cores, the highest fluxes occurred during GW2 (15.7 ± 1.2 mmol m^{-2} d^{-1} in peat–sand and 12.9 ± 0.9 mmol m^{-2} d^{-1} in sand). Likewise, CH_4 fluxes reacted to the flow dynamics showing significantly higher

average CH_4 fluxes during GW upward flow regimes with 35.7 ± 26.3 μmol m^{-2} d^{-1} in the peat–sand cores and 21.2 ± 16 μmol m^{-2} d^{-1} in the sand cores, compared to the SW downward flow regimes with average CH_4 fluxes of 1.5 ± 26.6 μmol m^{-2} d^{-1} peat–sand and 8 ± 15.4 μmol m^{-2} d^{-1} in the sand cores. The highest average CH_4 fluxes (32.9 ± 16.8 μmol m^{-2} d^{-1}) in the sand core were measured during GW2 and in the peat–sand cores during GW3 (48.5 ± 25.1 μmol m^{-2} d^{-1}). The longer the GW flow condition persisted, the more CH_4 was emitted (from 16.5 to 77.3 μmol m^{-2} d^{-1} during GW3) in the peat–sand cores (Figure 4.4). During several SW intrusion regimes (SW1 and SW3), a reduction of the CH_4 concentrations indicate negative fluxes.

4.4.4 Abundances of methanogenic archaea and SRB

The results of the qPCR in the peat–sand column reveal significantly lower abundances of methanogens (*mcrA*) and sulfate reducers (*dsrB*) in the upper 20 cm of sand sediment (*mcrA* : $1.2 \times 10^3 \pm 1 \times 10^3$ copies g^{-1}; *dsrB* : $1.4 \times 10^4 \pm 1.2 \times 10^4$ copies g^{-1}) compared to the lower peat section (*mcrA* : $5.6 \times 10^5 \pm 2.1 \times 10^5$ copies g^{-1}; *dsrB* : 6.7 copies g^{-1}) (Figure 4.5).

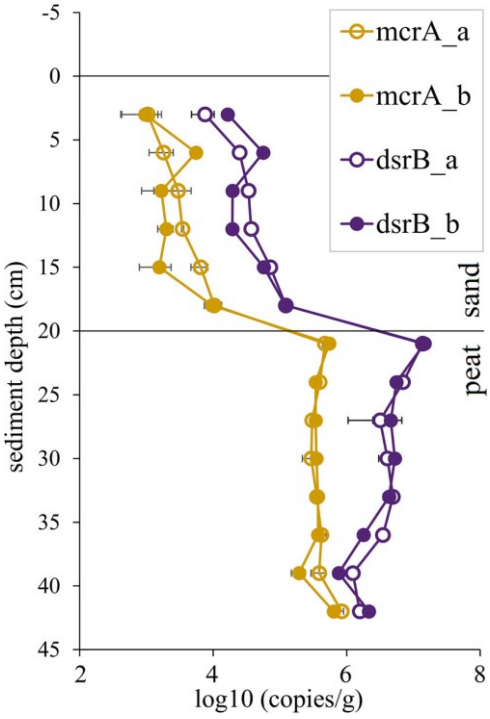

Figure 4.5: Microbial abundances of methanogens and sulfate reducers. Replicates (**a**,**b**) of gene copy numbers (*mcrA*, *dsrB*) were measured in sediments of the peat-sand column (P2) after the experiment. The line indicates the peat–sand interface.

The highest copy numbers of *dsrB* (1.9×10^7 copies g^{-1}) are detected in the transition zone (*see* Figure 4.4) of highly degraded peat, whereas *mcrA* reveal highest abundances (1.02×10^6 copies g^{-1}) in the lowermost sample where peat is least decomposed. The abundances of *dsrB* are overall dominating those of the *mcrA* , while the abundance of *dsrB* declined toward the bottom section.

4.5 Discussion

4.5.1 Solid-phase geochemistry

A distinct shift from a terrestrial, freshwater environment (peat) to a marine saltwater environment (sand) is indicated by a sudden vertical change of the substrate at 20 cm sediment depth in the peat–sand cores (Figure 4.3). The peat layer is characterized by low C : N ratios of ~ 30 and light $\delta^{13}C$ values of approximately − 27‰. A typical enrichment in the isotopic signatures of the organic carbon toward the sand confirms a change into marine deposit conditions (Bickert, 2000) and is supported by lower C : N ratios of the organic carbon source (Meyers, 1997). Sediment cores without peat (S1, S2, S3) and the sandy part of the peat–sand cores have higher $\delta^{13}C$ values of − 24.3 (± 1)‰ typical for marine origin (Stein, 1991). The close proximity of marine sandy sediments with peat layers induces a high downcore gradient of organic carbon of different composition and origin. Moreover, the degree of decomposition of the peat, changed from being less decomposed (*H* 3–4) in depths > 30 cm to moderately decomposed (*H*7–8) toward the peat–sand interface (i.e., within the transition layer), coinciding with a C_{org} decrease of 99.9% (Figure 4.3). These findings indicate that peat soil covered with permeable sediments is subject to decomposition, progressing from the sand–peat interface. In contrast, coastal peat deposits in > 30 cm sediment depth remained largely unaffected by SW circulation-related decomposition. This can be assumed on the basis of the content (44.2% ± 5.3%; range: 31–50%) and the isotope signature (− 27.9‰ to − 26.8‰) of C_{org} and can be explained by the low permeability of the degraded peat surface. As a result of the high C_{org} and C_{inorg} concentrations detected in the lower peat layers (> 30 cm, Figure 4.3), an enhanced mineralization rate is assumed.

4.5.2 Advective flow regime and solute transport

Geochemical variables and fluxes in the peat–sand core and the homogenous sand core were very different. Although it was possible to generate comparable

flow regimes in the two types of sediment cores by gravity driven, valve-controlled downward flow and pump-controlled upward flow, the mixing of the two salinity end-members showed clear differences assumed to be caused by the different permeabilities between the peat–sand and the sand cores. The sand cores had less constrained internal mixing compared to the peat–sand cores (Figure 4.4, salinity). The mixing of GW and SW in the sand cores extended over the entire profile, resulting in a smooth vertical salinity gradient. The formation of low-saline pore water reservoirs in sediment depths > 20 cm was mostly inhibited and only formed during GW3 during Days 43–50 ($S \approx 1.6$, Figure 4.4). The higher density of saline SW compared to the low-saline GW underneath may have caused density-driven convection currents as described for permeable coastal sands (Robinson et al., 2007; Santos et al., 2012). In contrast, peat soils are highly complex porous media that include open and connected, dead-end, and isolated pores, where flow and convergence of GW and SW is restricted to the hydrologically active pore space (Rezanezhad et al., 2016). The solution capacity of DOC increases with decreasing conductivity (Kalbitz et al., 2000; Tipping and Hurley, 1988), which has also been shown to affect the hydraulic conductivity of peat substrate (Plaut et al., 2013). In the Baltic Sea, where peat deposits and the discharge of low-saline GW are frequently observed along the coastal zones (Kotwicki et al., 2014; Kreuzburg et al., 2018; Peltonen et al., 2002; Schlüter et al., 2004; Sergeev et al., 2015), these processes can have potential implications on the marine carbon balance. Coastal hydrodynamics in the Baltic Sea are predominantly controlled by wind conditions, and the water circulation in coastal sediments depends on the wave setup, water level, and GW recharge. Apart from a highly complex circulation pattern under in situ conditions, being, for example, not limited by vertical flow directions as in the experiment, the SW properties of the Baltic Sea (salinity, temperature, nutrient concentration) can be subject to large variations.

4.5.3 Carbon mineralization processes

Mobilization and transformation of DOC

Downcore concentration profiles of DIC, DOC, salinity, and SO_4^{2-} in the pore waters clearly show different slopes above and below the peat layer, indicating different processes in these substrates. Throughout the cores, salinity steadily decreases in the downcore direction (Figure 4.6), while the other substances

undergo production, consumption, and conversion processes. Within the organic-rich peat soil (> 30 cm), pore waters were depleted in SO_4^{2-}, which indicates SO_4^{2-} reduction in the sediments above and favors CH_4 production in deeper peat layers (Figures 4.6 and 4.7). The rate of DOC production from C_{org} appears to be primarily controlled by the conductivity of the pore water and indicates that the source of DOC is of low-saline water, resulting in an inverse relation between the concentrations of Cl^- and DOC. The impact of pore water flow velocities, different flow regimes, and temperature can be relevant for DOC production from organic carbon (Evans et al., 2012; Kalbitz et al., 2000; Koehler et al., 2009; Tiemeyer et al., 2017b; Tipping and Hurley, 1988). In contrast to most studies, Gosch et al. (2018) observed an increase of DOC release with increasing salinities, which was explained by the specific geochemical properties of the investigated peat substrate. However, in our study, elevated concentrations of DOC and a stronger conformity of $\delta^{13}C$ values between DOC and C_{org} were observed at salinities < 5, confirming peat as the carbon source for DOC in low-salinity conditions. Heavier $\delta^{13}C_{DOC}$ values were observed with increasing salinity conditions, likely a result of organic carbon degradation by SO_4^{2-} reduction (Anderson and Arthur, 1983; Boutton, 1991).

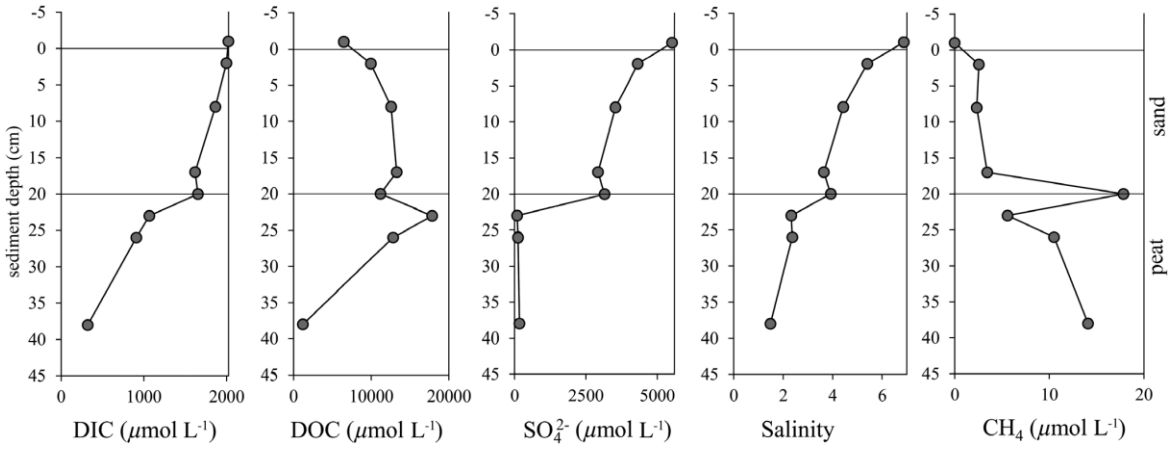

Figure 4.6: Concentrations of DIC, DOC, SO_4^{2-}, CH_4 in pore water profiles of peat–sand column (P1) at the last day of the experiment (Day 50). The black line at 20 cm sediment depth indicates the peat/sand interface.

The upward convection of DOC with advective fluxes is obvious during GW flow regimes and is mostly pronounced during GW3 showing high concentrations (DOC ≈ 6.5 mmol L^{-1}) even in discharging surface water (Figure 3 and 5) at Day 50, which is caused by leaching of solid C_{org}. According to other studies, the

effects of ionic strength on DOC release are not consistent and varies with substrate and physicochemical factors (Berry et al., 1990; Gosch et al., 2018; Tiemeyer et al., 2017b; Tipping and Hurley, 1988), but the mobilization of DOC from organic sediments is apparently reduced by increasing ionic strength due to flocculation processes (Kalbitz et al., 2000). SO_4^{2-} reduction and oxic respiration are responsible for the major share of DOC oxidation in marine endobenthic environments (Bender and Heggie, 1984; Henrichs and Reeburgh, 1987) and we assume that this is also true for the peat-derived DOC in our experiment. Highly decomposed peat has only small quantities of organic carbon that can still be turned into decomposable DOC (Strehse et al., 2018). The peat in deeper layers exhibits significantly lower degrees of decomposition and higher C_{org} contents, thus we assume this peat may still contain significant amounts of decomposable DOC. The fate of this DOC in pore or surface waters containing mineralization-relevant substances (e.g., electron acceptors such as SO_4^{2-}, O_2) leads to the oxidation of DOC and transformation into DIC. Our results from the pore water analysis indicate the occurrence of these processes, in particular at the end of the experiment, where an increase in DIC at the peat–sand interface coincides with a decrease in DOC and a deviation between SO_4^{2-} and salinity (Figure 4.6).

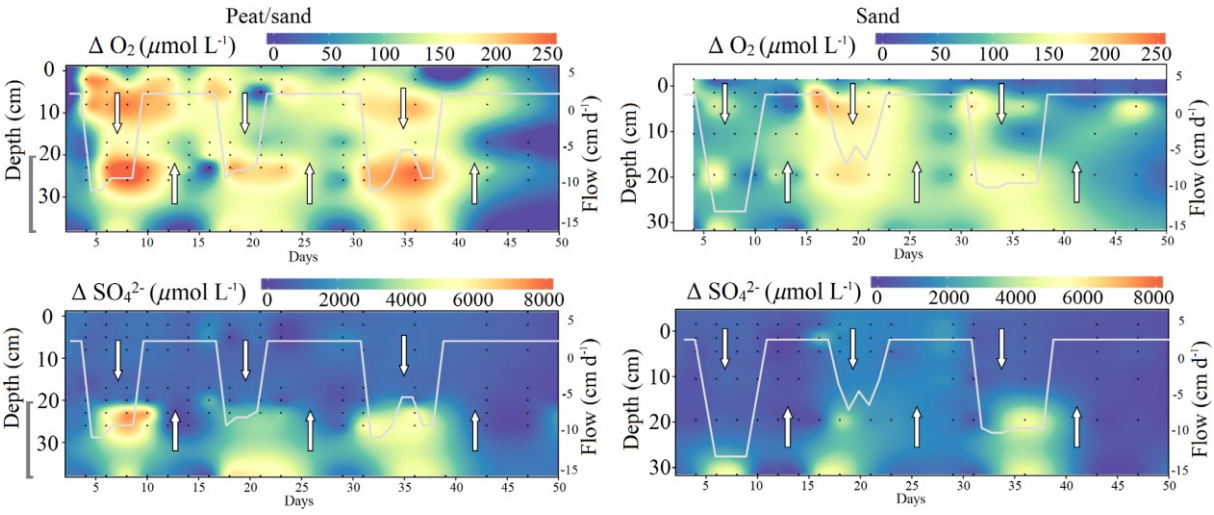

Figure 4.7: Depth distribution of O_2 and SO_4^{2-} deviating from the initial end-member concentration, ΔO_2 and ΔSO_4^{2-}, presented for each column set (column P1 and S1), over 50 d of the experiment period. The gray bracket left of the peat–sand data indicates the peat layer in the lower section (20–40 cm) of the core.

Previous studies have shown that with salinities $S > 10$, SO_4^{2-}-derived DOC mineralization is the preferred metabolic process, causing increased CO_2 production due to DOC mineralization (Chambers et al., 2014; Weston et al., 2011). In contrast to O_2, which is depleted in the surface sediments in our experiment (< 10 cm, Figure 4.4 and 4.7), there is a moderate correlation between Cl^- and SO_4^{2-} (*see* "Solid-phase geochemistry" section). Without any metabolic processes, the concentration of the main electron acceptors, O_2 and SO_4^{2-} in our experiment is predefined by the mixture of the two end members (SW and GW, for composition, *see* Table 4.1). Under the assumption that the concentration within the GW end member is negligible, used electron acceptors (ΔEA) can be directly derived from the salinity content:

$$\left(\frac{EA_{max}}{Sal_{max}} Sal_{sample}\right) - EA_{sample} = \Delta\mathrm{EA} \qquad (7)$$

This allows calculating the loss of electron acceptors (ΔEA) by calculating the difference between this "preformed" available electron acceptors (AE_{SW-GW}) and the observed AE_{Sample} at any point of the experiment for O_2 and SO_4^{2-} (Figure 4.7). The data clearly indicate the higher use of electron acceptors in the peat–sand cores in comparison with the sand cores, indicating SO_4^{2-}-fueled oxidation driven by penetration of SO_4^{2-} into the decomposable peat layer. The upward advection of DOC and DIC during the GW stages leads to the increase of both parameters in the peat-overlying sands, where further oxic DOC decomposition might be partially responsible for oxygen demand and DIC increase. During phases of SW intrusion, SO_4^{2-} entering the decomposable DOC pool apparently enhances anaerobic DOC oxidation in the sediments at depth > 20 cm. Terminal electron acceptors (O_2, SO_4^{2-}) have been constantly added during SW phases of the experiment, while the solution was free of iron (Fe^{3+}) or manganese (Mn^{4+}). However, these terminal electron acceptors can be present in peat soils and fuel mineralization processes (Burdige, 2012; Küsel et al., 2008). A major depletion of the terminal electron acceptors in organic-rich sediments can facilitate methanogenesis.

Depth profiling of microbial abundances (Figure 4.5) supports the suggested electron acceptor utilization along the sediment column. The ratio of gene copy numbers of *dsrB* and *mcrA* increases in the peat in an upward direction, indicating SRB to be more abundant in the transition zone in which SO_4^{2-} and DOC are easily available (Figure 4.5). Although gene copy numbers of *dsrB* dominate

overall, the copy numbers of *mcrA* are stable across the whole peat section, suggesting their abundance does not depend on the peat characteristics nor on the increasing abundance of the sulfate reducers in an upward direction. Instead, this could be evidence that the high availability of peat-generated dissolved DOC enables the coexistence of both methanogenic and sulfate-reducing microbial communities and that their activity is subject to the changing environmental conditions. However, it cannot be excluded that the detected overlap of both groups was at least to some degree triggered by advective fluxes in the peat–sand core. The molecular data are mostly dependent on the choice of primers. Although the primers used in this study are well evaluated and have been applied for estimating the abundance of methanogens (Wen et al., 2018) and sulfate reducers (Vuillemin et al., 2018), the primers used are covering only a small diversity of microorganisms involved in the complex biogeochemical processes. However, the total abundance of microorganisms across the sediment columns has identified the peat as the favorable habitat.

Gas formation, transport, and emissions

The upward flowing GW regularly decreases the pore water salinity and thus displaces required oxidants (SO_4^{2-}) for SRB. This likely promotes anoxic DOC mineralization by methanogensis and CH_4 formation, which can be the result of fermentation of acetate (Stadtman and Barker, 1949; Whiticar et al., 1986). It is further notable that in the peat–sand cores CO_2 emissions during GW1, GW2, and GW3 reached similar and constant flux rates. This may indicate a limit of mineralization activity controlled by the amount and composition of solutes present and additional, the result of anaerobic CH_4 oxidation (Reeburgh, 1980).

Most pathways of microbial organic carbon oxidation, except for SO_4^{2-} reduction, are less active with increased Cl^- or HS^- concentrations (Chambers et al., 2011; Joye and Hollibaugh, 1995; Luo et al., 2019). However, microbial DOC oxidation by SRB and methanogens can also coexist (Figure 4.5) and may depend on availability and quality of the substrate (Dar et al., 2008; Holmer and Kristensen, 1994; Sela-Adler et al., 2017) and species-dependent metabolic traits (Ozuolmez et al., 2015). The emissions of CH_4 have been described as the residual of CH_4 production (e.g., methanogenesis) and CH_4 oxidation (e.g., aerobic and anaerobic CH_4 oxidation), and the magnitudes of CH_4 emissions can be controlled by advective transport processes (Heyer and Berger, 2000). Assuming that CH_4

formation increases with DOC concentration in the absence of O_2 and SO_4^{2-}, this process is likely more relevant in peat-containing coastal sediments, where DOC production is not limited due to the solid organic carbon source. The transfer and extrapolation of CH_4 emissions observed during the experiment to the coastal area of peat-containing sediments have to be treated with caution, as coastal processes are difficult to assess and the microbial and physicochemical properties change during sampling, transport, and construction of the column setup. Although the main driver of air–water CH_4 transfer in experimental approaches is often assumed to be driven by molecular diffusion (Moore and Dalva, 1993; van Winden et al., 2012), the emissions of CH_4 in shallow water can also be the result from ebullition (Ostrovsky, 2003) and can be enhanced by wind and wave action interacting with coastal sediments as well as temperature and may display large spatial and temporal variabilities (Aben et al., 2017; Bange, 2006; Upstill-Goddard, 2006). In the case of our experiment, the advective transport of dissolved methane, forced by alternating phases of advective inflow and outflow, has a strong control on the gas flux into the water column (Figure 4.4). Our mean experimental CH_4 fluxes during GW discharge (35.7 ± 26.3 μmol m^{-2} d^{-1} peat–sand core; 21.2 ± 16 μmol m^{-2} d^{-1} sand core) were in the range of the field-based study reported by Bange et al. (1994), where they estimated an average CH_4 flux of 22–37 μmol m^{-2} d^{-1} from the continental shelves of the Baltic Sea and the North Sea with total emissions ranging from 0.35 to 0.75 Tg C yr^{-1} (Bange, 2006; Upstill-Goddard, 2006). However, a direct comparison to the literature is only possible with more information about the experimental and in situ conditions (e.g., hydrodynamics, gas transfer velocity). Strongly increasing CH_4 fluxes were detected during the last GW phase, GW3 (from 16.5 to 77.3 μmol m^{-2} d^{-1}) indicating an unreached maximum of the CH_4 fluxes. On a global scale, enhanced hydrodynamic exchange with organic-rich sediments, such as those found in coastal wetlands and thawing coastal and subsea permafrost (especially in the northern hemisphere), might thus modulate coastal carbon dynamics in the framework of climate change and sea-level rise scenarios. Coastal erosion caused by sea-level rise can cause not only the loss of ecosystems, but also a shift in the carbon reservoir balance.

4.6 Conclusions and limitation

Coastal wetlands and carbon-rich deposits are found along a majority of the German Baltic Sea coast (Sterr, 2008) and are abundant on every continent (Strack, 2008). Thus, submerging of peatlands due to sea-level rise, subsidence as well as rewetting of drained coastal peatlands has potential to reshape the nearshore coastal fluxes of various environmentally important compounds in the future, creating a pressing need to understand the biogeochemical processes in these settings.

Specific to this study, we aimed to better understand the effect of salt water intrusion in the near-coast peat environments. We ran a controlled column experiment, which, although the method may have limited transferability to natural conditions, it is to date the most appropriate technique for the purposes of this research and reliable and field-comparable results can still be obtained. The experimental setup simulated coastal circulation conditions and represented a fragment of the complex in situ conditions along the study site. The 3-km-long coastline of the adjacent wetland of the study site is exposed to changing conditions leading to large variations in sediments and physicochemical conditions. However, the sediment cores investigated represent a larger area of the sedimentary conditions along the coastline (Kreuzburg et al., 2018).

The aims of the column experiment have been summarized in Figure 4.8. The implications of our results for coastal zones illustrate: (1) the intrusion of SO_4^{2-}-containing SW through C_{org}-rich sediments of terrestrial origin (peat deposits), results in SO_4^{2-} reduction, with DIC as the end product. (2) The discharge of O_2-depleted GW triggered enhanced DOC release from the sediments and facilitated methanogenesis. The resulting release of CO_2 and CH_4 may represent a so far unnoticed source of coastal greenhouse gas emissions.

Our results provide clear evidence of bioavailable DOC being produced from solid-phase C_{org} (of that peat) that had already been submerged for considerable lengths of time. The results also show that substrate, transport processes, redox conditions and salinity control peat degradation, DOC mobilization, and CO_2 and CH_4 release. Regarding the distribution of microbial, key players, we found that the abundance of the methanogens increased with increasing depth in the peat sediments and was not dependent on the abundance of the SRB. Thus, we

conclude that the microbial activity is closely coupled with biodegradable organic carbon.

The experimental findings (particularly with the high spatial and temporal resolution of measurements) improve the understanding of biogeochemical processes of peat-derived carbon cycling and transformation. Sediments containing peat deposits can be hot spots of increased release of and mineralization of DOC and may play an important role in the release of climate relevant gases (CH_4, CO_2) in coastal zones. Ongoing coastal erosion and suspension of peat deposits and wetland loss due to sea-level rise and the frequency of storm events might promote the processes that have been investigated in this study. However, more detailed information about the hydrological cycles, geochemical properties, and solute concentrations is fundamental for process balancing and to justify comparisons with the field.

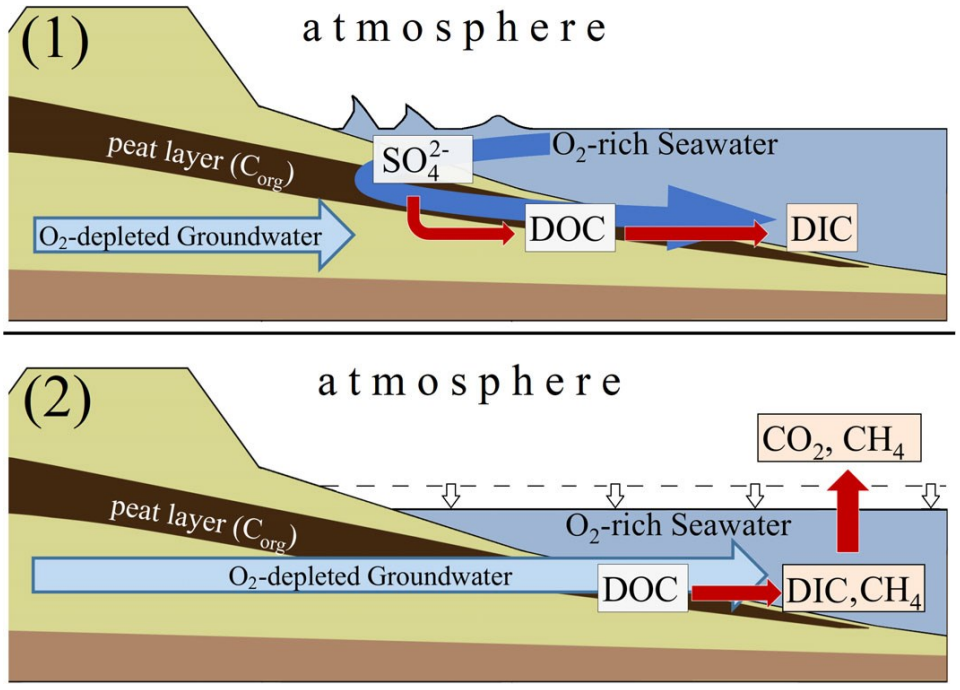

Figure 4.8: Conceptual extraction of the carbon exchange processes in the submarine, peat-containing estuary along the shoreline of the study site with (1) elevated sea-level situation and wave setup. The blue arrow visualizes the intrusion of SW into carbon-rich sediments, the red arrows showing the mineralization pathway. The process includes DOC mineralization via SO_4^{2-} reduction resulting in a discharge of DIC. (2) Low sea-level situation and calm surface water conditions. The discharge of GW displaces methane oxidants (O_2, SO_4^{2-}), increases DOC release and facilitates CH_4 production and emission.

5 SYNTHESIS

In terms of water flow and solute mobility, the reaction of the different peats studied in this thesis to an increased seawater impact simulated in laboratory experiments varied markedly. The results for the peat, which was sampled at the drained fen *Pölchow* and which was used for the majority of column experiments in Gosch et al. (2018) and Gosch et al. (2019), did not show the expected sensitivity towards a rising water salinity. This is surprising against the background of previous studies, which showed a very clear positive correlation between K_s of bog peat and water salinity (Comas and Slater, 2004; Kettridge and Binley, 2010; Ours et al., 1997) and were confirmed in a recent study for tropical peat in the Everglades (Sirianni and Comas, 2020), and a very clear negative correlation between DOC release from peat and water salinity (Liu and Lennartz, 2019b; Tiemeyer et al., 2017b). The results of this thesis indicate that a pronounced peat-specific reaction to seawater inflow needs to be ruled out before transferring generally observed results to less well-studied peatlands. As indicated by biogeochemical studies on peat (Emsens et al., 2016; Portnoy and Giblin, 1997), a strong impact of land-use history, i.e. drainage and rewetting, renders seawater effects on peat soil functions more diverse than proclaimed previously, at least in the short-term.

5.1 Short-term seawater effects on peat soil processes

The duration of the laboratory experiments carried out in the framework of this thesis was restricted to several weeks. Hence, the findings of this thesis apply to short-term seawater effects, e.g. caused by temporary seawater flooding of the peatland. In the following, the consequences of seawater inflow on water flow, solute transport and solute release are discussed bearing in mind that, due to scale effects and the controlled environmental conditions, the transferability of laboratory results to the field is always subject to uncertainties. Each section contains a statement as to whether the associated hypothesis (see Section 1.3) was confirmed or rejected (marked in bold).

5.1.1 Water flow

In Gosch et al. (2018) the saturated hydraulic conductivity K_s as the key parameter for water flow in a soil did not show any dependency on water salinity for the studied fen peats and the bog peat. This finding was unexpected, as the

experiment actually had been designed to quantify the impact of water salinity on K_s for fen peat and not to validate its (non-)occurrence. The lack of bridging polyvalent cations such as Ca^{2+} for inducing flocculation due to the use of a pure NaCl solution does not seem to be a reason since also no effect was observed in case of using natural seawater (Figure 2.4, Scenarios 5 and 6) and previous studies like Ours et al. (1997) also used NaCl solutions without polyvalent cations. Therefore, the reason must be sought in the peat substrate itself. The bog peat used as reference material in Gosch et al. (2018) may not represent peat material of previous studies (Kettridge and Binley, 2010; Ours et al., 1997; van Dijk et al., 2017) since it was sampled in a bog, which was drained and fertilized (Huth et al., 2019), and had a very low K_s.

Hypothesis (i), i.e. the increase of K_s with rising water salinity, is rejected for the tested peat samples. However, since in the majority of cases in previous studies the positive correlation between K_s and *EC* was confirmed, the results of this thesis might represent an exception to the rule.

5.1.2 Solute transport

For all tested peat samples in the framework of this thesis, the BTC data revealed non-equilibrium behavior indicating that the peat acted as dual-porosity medium for solute transport also under salt-enriched conditions. This implies that a proportion of solutes in inflowing seawater, including labile substances like SO_4^{2-}, penetrates the peat matrix with a higher velocity than what would be expected from the low K_s values. However, this may not result in an immediate SO_4^{2-} reduction in deeper peat horizons since reactivity of SO_4^{2-} was strongly reduced without an additional labile carbon source. Seemingly, SO_4^{2-} reduction was limited by energy substrate as it has been shown by Howarth and Teal (1979) in salt marsh peat, where SO_4^{2-} reduction occurred primarily in the (anoxic) root zone, i.e. with a sufficient supply in labile carbon due to dead roots and root exudates. SO_4^{2-} reduction in Gosch et al. (2019) also showed a pronounced lag time even under anoxic conditions. In Kreuzburg et al. (2020) SO_4^{2-} showed a lower reactivity than O_2, which was depleted in the first few centimeters of the sandy sediment, but concentrations within the peat were reduced (Figure 4.4), which matches to the higher total abundance of SRB in the peat than in the sand (Figure 4.5). The DOC release during the O_2-depleted fresh water inflow has likely supplied the SRB with an easily-degradable carbon source. Arguably, the absence of increased DIC

concentrations despite SO_4^{2-} reduction might be attributed to DIC consumption by the methanogenic microbes (M. Kreuzburg, Leibniz Institute for Baltic Sea Research Warnemünde, personal communication).

Hypothesis (ii), i.e. the nonconservative transport of SO_4^{2-} characterized by physical non-equilibrium flow, is partly rejected. In case of a reduced availability of a labile carbon source, SO_4^{2-} moved through most fen peat samples just like Br^-, showing non-equilibrium flow, also for poorly-decomposed peat. The occurrence of SO_4^{2-} reduction depended on factors such as time, the concentration of DOC and the presence of other electron acceptors.

5.1.3 Solute release

The laboratory flow-through experiments in Gosch et al. (2018) and Gosch et al. (2019) showed a leaching of DOC and other solutes at the beginning of the water flow, which indicates that a sudden inflow of water in a drained peatland can cause a flushing of dissolved substances in the direction of water flow. Especially the highly decomposed peat showed a high leaching of solutes and was the only peat, which released significant amounts of NO_3^-. In drained peat soils NH_4^+ as a product of decomposition is oxidized to NO_3^- and can then be easily leached from the peat. Furthermore, peat soils under agricultural use can have an enhanced N-pool due to fertilization just like mineral soils (Beetz et al., 2013). Although NH_4^+ was not measured, the expected cation exchange processes following saltwater incursion were detected in Gosch et al. (2019) by rising concentrations of K^+ and Ca^{2+}, which were most pronounced for the highest applied Na^+ concentration.

SO_4^{2-} reduction, although only observed and confirmed by measurement of HS^- for three samples in Gosch et al. (2019), led to an increased release of solutes such as DIC, TDN and TDP. A statement about DOC release during SO_4^{2-} reduction was difficult to achieve as the added acetate complicated the DOC measurement. However, the data also suggest an increase of DOC release during SO_4^{2-} reduction (Figure 3.3 d). The fact that SO_4^{2-} reduction led to an increased release of dissolved nitrogen and phosphorus, although acetate does not contain these elements, could indicate a “priming effect”, i.e. a general stimulation of soil decomposition processes due to an addition of easily degradable OM (Kuzyakov et al., 2000).

The release of DOC with rising water salinity varied between the studies of this thesis: While the constantly seawater-exposed peat showed a decreasing DOC release (Gosch et al., 2019; Kreuzburg et al., 2020), which goes along with previous observations for peat, the drained peat from *Pölchow* released either more or a constant amount of DOC with increasing sodium chloride and/or sodium sulfate addition, which is uncommon, but not unprecedented (Weston et al., 2006). As the absolute differences in DOC concentrations between the salinity treatments in Gosch 2018 as well as in Gosch 2019 were rather small (< 5 mg L^{-1}), this might indicate a weak anion exchange, possibly on organometallic complexes, with Cl^- and SO_4^{2-} replacing organic anions, with which they compete for sorption sites (Martinez et al., 1998). This, however, would also imply that the assumption for the retardation factor R = 1 underestimated the actual R value for SO_4^{2-}, at least for the highest concentration (2700 mg SO_4^{2-} L^{-1}).

Hypothesis (iii), i.e. the reduced release of DOC during saltwater inflow, is partly confirmed, since the results are not consistent. Just like for hypothesis (i), the non-occurring decrease in DOC release in Gosch et al. (2018) during saltwater inflow might be a special case attributed to an uncommon peat composition. Slight increases in DOC concentrations with increasing water salinity were likely due to the desorption of organic anions.

5.1.4 Potential factors interfering with salinity effects

Water flow, solute transport and solute release were not affected by an increased water salinity as hypothesized. It is likely that the reason is rooted in the peat chemistry of the fen peat, which is strongly impacted by land management.

A factor that might have interfered with salinity effects is the presence of iron oxides in the drained fen peat. Iron can interact with OM by adsorption and coprecipitation leading to the formation of Fe-organic complexes (Chen et al., 2014). OM of higher molecular size is preferentially adsorbed to iron oxides (Gu et al., 1995), which might impair the coiling of the fibers, which are likely causing the pore dilation effect (Ours et al., 1997). Furthermore, the iron oxides seem to be located mostly at the edges of the larger pores (visually observed as reddish rust spots in the peat during sampling), where water content fluctuations enable O_2 intrusion. Besides an uncommon organic composition of the peat, this might be one explanatory approach to why the pore dilation effect was not observed in Gosch et al. (2018).

In a column experiment with peat with different iron contents from drained fens, Emsens et al. (2016) observed an increased release of Fe, DIC, DOC, NH_4^+ and P for the iron-enriched peats (≥ 3.0 % dwt) compared to the iron-poor peats (1.4 % dwt) after a simulated rewetting. They explained this fact by an enhanced decomposition of organic matter due to iron reduction. The release of DOC during iron reduction, which was previously bound to the oxidized iron compounds, can superimpose salinity-induced flocculation processes (Knorr, 2013). In the SO_4^{2-} displacement experiment (Gosch et al., 2019), iron reduction may also explain the lag time before SO_4^{2-} reduction occurred, since ferric iron (Fe^{3+}) serves as an energetically more favorable electron acceptor than SO_4^{2-}. An initial peak of iron reduction followed by a dominance of sulfate reduction was also observed in flow-through experiments during salt water treatment by Weston et al. (2006). However, no additional carbon source was added as in Gosch et al. (2019) and the occurrence of iron reduction was explained by an increase in available surface area of iron oxides with increasing *EC* and decreasing *pH*. Furthermore, the DOC release in Weston et al. (2006) was not affected by salinity, which also resembles the results in Gosch et al. (2019).

Peat in pristine peatlands is generally low in iron, but especially lowland fens, which receive water inflow from a mineral catchment, can show higher iron contents (Küsel et al., 2008). Furthermore, the drainage-induced decomposition of peat leads to a proportionally higher content of iron (Litaor et al., 2004). The moderately decomposed peat from the site *Pölchow*, which was primarily used for the K_s tests and the SO_4^{2-} displacement experiment, has a high iron content of 22.7 g kg^{-1} (= 2.27 % dwt). The degraded peat of the overlying horizon has an iron content of 61.6 g kg^{-1} (= 6.16 % dwt), which is a high value for peat (Emsens et al., 2016) and high even compared to common iron contents of 0.2 to 5 % of terrestrial mineral soils (Scheffer and Schachtschabel, 2002). On the contrary, peat samples from the *Hütelmoor* were very low in iron, especially the sea-exposed peat with 1.2 g kg^{-1} (= 0.12 % dwt). This shows the effects of iron-stabilizing oxic conditions like at the site *Pölchow* and iron-mobilizing anoxic conditions like in the *Hütelmoor*. It might explain why only for the sea-exposed peat, which never suffered from drainage, the decreasing DOC release with increasing water salinity was confirmed in this thesis.

In the SO_4^{2-} displacement experiment in Gosch et al. (2019), the anoxic conditions have likely stimulated iron reduction leading to the desorption of organic acids,

which superimposed potential effects of water salinity. For the DOC release in Gosch et al. (2018), the input water was not artificially deoxygenated by argon purge, but deionized water was used, which does have a very low gas content and iron reduction could also have taken place. For the high SO_4^{2-} concentrations in Gosch et al. (2019) also an anion exchange of organic acids by SO_4^{2-} seems possible. Moreover, in all three studies an increased DOC release in the later stages of the experiments was observed in some of the samples. In Gosch et al. (2019) the increased DOC release was clearly related to a beginning SO_4^{2-} reduction, which not only promoted the release of DOC, but also of DIC, TDN and TDP (Figure 3.3 and 3.4). This effect may again be attributed to the interaction with iron compounds since the occurrence of sulfide leads to the formation of iron sulfide and the release of substances previously bound to the iron oxides (Vile et al., 2003).

The peat column in Kreuzburg et al. (2020) showed increased DOC release after the last salinity change from saline to fresh water (~ day 43 of experiment), which was likely induced by a longer time period for the fresh water inflow than for the previous salinity changes. A similar effect was observed during the interval K_s tests in Gosch et al. (2018), where an increased release of CDOM was observed after the last salinity change in Scenario 2 (0.035 % - 3.5 % - 0.035 %) and Scenario 3 (0.035 % - 1.2 % - 0.035 %), while in the control Scenario 1 (0.035 % - 0.035 % - 0.035 %) hardly any CDOM was visible. This might indicate that the negative relationship between EC and DOC may establish with a pronounced time lag for the drained fen peat from *Pölchow.* Seemingly, consecutive salinity changes, flow direction changes and resaturation might ultimately have triggered the effect, since a fluctuating water table is known to stimulate DOC release (Schwalm and Zeitz, 2015).

Furthermore, the impact of water salinity is diminished under more alkaline conditions as shown by the treatment of the peat sample with bicarbonate ($NaHCO_3$) in Ours et al. (1997), after which the previously observed large salinity-related changes of K_s did not reoccur. They attributed this fact to the dissolution of organic acids under alkaline conditions, which then no longer reacted to the changing water salinity. A lower *pH* in the range of 4 to 5.5 of the coastal fen peat studied in Liu and Lennartz (2019b) might explain why the impact of water salinity on DOC release from that peat was stronger than for the fen peat tested in this thesis, for which pore water *pH* ranged between 6.5 and 8.5 (Gosch et al., 2018,

2019). Furthermore, a lower *pH* increases the mobility of aluminum, which can form complexes and co-precipitate with DOC (Jansen et al., 2003).

Effects of *pH* and ionic strength on DOC release can be difficult to disentangle, since they are intercorrelated in peat substrate (Clark et al., 2011). Although ocean water generally has an elevated *pH* of ~ 8.1 (Sigg and Stumm, 2011), saltwater inflow in peat generally leads to a *pH* drop (Clark et al., 2011; Gosch et al., 2018), as H^+ previously bound to the peat is being replaced by Na^+, and a decrease in DOC release. On the other hand, long-term seawater impact and anoxic conditions can increase *pH* due to an H^+-consuming SO_4^{2-} reduction (Clark et al., 2011).

5.2 Long-term seawater effects on peat soil processes

Comparing properties of the submerged peat at the beach of the *Hütelmoor,* which was used in the laboratory experiments in Gosch et al. (2019) and Kreuzburg et al. (2020), to those of similar, but less seawater-affected peat might reveal long-term seawater effects. Table 5.1 summarizes geochemical and physical parameters, which were determined for the sea-exposed peat as well as for the peat of the same soil horizon, but in the hinterland of the coastal protection dune, and for the peat taken at the drained fen in *Pölchow*.

The similar values for ρ_b, Φ and K_s of the sea-exposed and dune-protected peat indicate that the (hydro-)physical properties of the peat did not undergo fundamental changes following long-term seawater impact under the conditions as they prevail in case of the *Hütelmoor*. Similarly, the degree of decomposition and carbon content do not differ between the sea-exposed and dune-protected peat. This implies that, unlike expected, the sea-exposed peat was not subject to a seawater-related enhanced decomposition. As stated in Kreuzburg et al. (2020) the reason might be the low K_s of the peat in the *Hütelmoor*, which reduces the intrusion of O_2 and SO_4^{2-} into the deeper parts of the peat and limits aerobic decomposition to the peat surface. Yet, how long the sampled peat has been exposed to intense seawater impact remains unknown, since erosion of the peat body constantly changes the parts affected by wave action and potential oxygen inflow.

Table 5.1: Comparison of peat properties for sea-exposed, less sea-exposed, i.e. dune-protected, and sea-unaffected peat. The sea-exposed peat from the beach was taken near-surface, while the dune-protected peat was taken ~ 100 m in the hinterland of the dune, but both peats belong to the same soil horizon in an altitude of ~ 0.6 m below sea-level. Parameters were determined as described in Gosch et al. (2019). Additionally, the age of the peat was determined with C-14 dating to verify if the sea-exposed and the dune-protected peat belonged indeed to the same soil horizon. The *CEC* and the exchangeable cations were determined according to DIN EN ISO 13536 (1997). No standard deviation is given due to single or double determination.

Parameter	**Sea-exposed peat (Beach of *Hütelmoor*)**	**Dune-protected peat (*Hütelmoor*)**	**Sea-unaffected peat (*Pölchow*)**
Peat type	reed-sedge fen peat	reed-sedge fen peat	reed-sedge fen peat
Sampling depth (cm)	~10	~115	~50
Age (Years B.P.)	3300 ± 50	3510 ± 50	2280 ± 40
Degree of decomposition (von Post)	H4	H4–5	H6
OM (% dry weight)	85.8	82.2	83.3
ρ_b (g cm^{-3}) ($n \geq 3$)	0.13	0.13	0.19
Φ (-)	0.92	0.92	0.89
K_s (cm d^{-1})	0.97	0.85	34
C (% dry weight)	48.5	48.9	40.4
N (% dry weight)	1.6	2.8	3.1
C/N	30.3	17.5	13.0
S (% dry weight)	3.4	4.4	0.5
Fe (mg kg^{-1})	1173	5409	22730
CEC (mmol$^+$ kg^{-1})	1390	1270	1735
exch. Na (mmol$^+$ kg^{-1})	474.2	177	1.3
exch. K (mmol$^+$ kg^{-1})	12.0	2.9	< 0.6
exch. Mg (mmol$^+$ kg^{-1})	682.8	542.5	63.4
exch. Ca (mmol$^+$ kg^{-1})	513	455	1282
EC_{soil} (mS cm^{-1})	14.4	3.8	0.8
pH_{soil}	6.7	6.4	6.5–6.8

Solute transport in the sea-exposed peat is, like in most peats, characterized by non-equilibrium flow. Br^--pulse input data for three samples of the sea-exposed peat (Figure 5.1) revealed clear early breakthrough with an appearance time of the peak well before 1 PV. Visually, the BTCs of the pulse input resemble the BTCs for the fen peat with an OM content of 47 % measured by Liu et al. (2017) under non-saline conditions, although their OM content of 86 % is substantially higher. However, the BTC parameters in Liu et al. (2017) show that solute transport in peat with a high organic matter content can also be affected by non-equilibrium

flow. Furthermore, the low K_s implies a rather tortuous pore network, which favors dispersion and the presence of immobile zones. The lower β and higher ω for the surface-near sample (Sample Nr. 1), which was the most decomposed, indicate a pronounced immobile zone with small aggregates, where the exchange between mobile and immobile zones is rather quick (Radcliffe and Simunek, 2010). Likely, these conditions benefit the microbial decomposers, which preferably reside in organic-rich microniches (Nunes et al., 2015; Rezanezhad et al., 2016), but rely on solute diffusion towards their niche. This could explain the increased microbial abundance in the upper part of the sea-exposed peat (Figure 4.5).

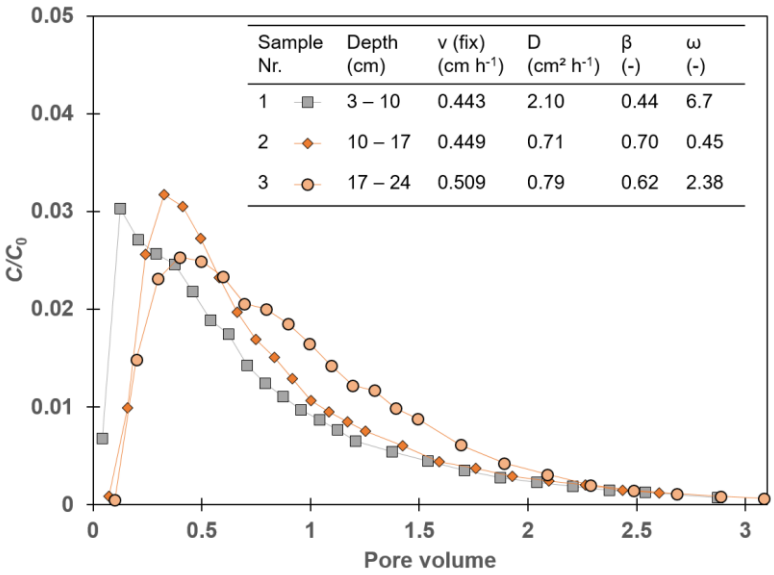

Figure 5.1: Breakthrough curves (3 mL pulse input with 1000 mg Br^- L^{-1}) and parameters for three undisturbed samples (Ø = 4.6 cm, L = 7 cm) of the sea-exposed peat, taken vertically in a depth of 3–24 cm below surface, using the same set-up as in Gosch et al. (2018) (DOC experiment) with a pump-rate of 7.5 mL h^{-1}. The retardation factor *R* was set to 1, i.e. assuming no adsorption occurred.

Conversely, nitrogen, sulfur and iron content of the peat and the exchangeable cations bound to the peat material most likely reflect long-term seawater effects. The sea-exposed peat has a lower nitrogen content (and thus a wider C/N ratio), which can be attributed to a lower proportion of bound NH_4^+ cations, which were replaced by the seawater cations (Na^+, K^+, Mg^{2+}), whose proportion is in turn increased. The *CEC* of the examined peat is in the upper range of the values reported for fen peat by Rydelek et al. (2016) implying a high potential to bind NH_4^+.

Interestingly, the sulfur content is high in both peats from the *Hütelmoor* and even slightly higher in the dune-protected peat, which is likely due to a legacy effect, i.e. the inflow of SO_4^{2-}-enriched seawater in previous times, which was also stated by Koebsch et al. (2019). However, a clear seawater impact-related gradient is indicated for the iron content in the peats. The sea-exposed peat seems to be particularly leached of iron probably due to constant anaerobic conditions paired with pore water flow induced by wave action. The high concentrations of exchangeable Na^+, K^+ and Mg^{2+} also demonstrate the seawater impact on the peats from the *Hütelmoor*. The fact that the sum of exchangeable cations for the sea-exposed peat is higher than its *CEC* is due to salts in the peat sample which were previously dissolved in the pore water (DIN EN ISO 13536, 1997). A high amount of bound Ca^{2+}, as shown in Table 5.1 for the sea-unaffected fen peat from *Pölchow*, is not an indicator for seawater impact, but is based on the fact that peat tends to bind Ca^{2+} strongly, while K^+ and Na^+ can be exchanged easily (Succow and Joosten, 2001).

The results for DOC release in Gosch et al. (2019) and Kreuzburg et al. (2020) show that the sea-exposed peat does represent a long-term carbon source. Under seawater conditions released DOC concentrations ranged in the order of ~ 10 mg L^{-1} for a salinity of ~ 0.4 % (Gosch et al., 2019), which is in the same order of magnitude as a DOC value of 11.7 mg L^{-1} measured on-site in the Baltic Sea (Ibenthal, 2019), and ~ 5 mg L^{-1} for a water salinity of 1.8 % (Kreuzburg et al., 2020). The change towards “fresh water SGD” with a water salinity of 0.16 % in the column experiment in Kreuzburg et al. (2020) led to a pronounced increase of DOC release with an observed maximum of 214 mg L^{-1}. As stated in Chapter 5.1.2 the release is strongly impacted by the duration of water salinity change — the longer the fresh water inflow lasted and thus the lower the water salinity, the higher the DOC concentrations. However, the high OM content of 85.8 %, and thus a large and non-depleted “pool of potential DOC” (Schwalm and Zeitz, 2015), suggests that fresh water-induced mobilization of DOC from the sea-exposed peat in the *Hütelmoor* rarely occurs naturally.

Hypothesis (iv), i.e. the enhanced decomposition of the sea-exposed peat material and the function as long-term carbon source, is partly confirmed. Although the sea-exposed peat from the *Hütelmoor* did not show signs of a pronounced seawater-related decomposition — neither regarding the peat matrix (OM content) nor the pore network (hydrophysical parameters) —

solute transport was characterized by non-equilibrium flow. Furthermore, it can be confirmed that the peat material does represent a long-term carbon source, notably in case of fresh water SGD.

5.3 Implications for coastal freshwater peatlands

Overall, seawater effects in a peatland depend on a variety of factors (Figure 5.2), which are strongly impacted by the land-use history, i.e. if the peatland is pristine, drained or rewetted. The findings of water flow- and solute transport-related studies carried out with bog peat (e.g. Kettridge and Binley, 2010; Tiemeyer et al., 2017b) cannot be directly and entirely transferred to fen peat of (formerly) drained and agriculturally used peatlands. The different response of three wetland soil types to an increase in water salinity in terms of DOC and TDP release in Steinmuller and Chambers (2018) affirms peatland-specific implications. On top of the soil conditions, the salinity regime and the time scale of the seawater exposure have an impact on seawater effects. Therefore, seawater impact may have different consequences for peat bogs at the coast of the oceanic and tidal North Sea than for the fens at the southern coast of the brackish and non-tidal Baltic Sea. In the following, the findings of this thesis are discussed in a broader context, focusing on peatlands in coastal regions, which so far have not been impacted by seawater inflow or — as it is the case for the *Hütelmoor* — have been separated from the sea for a long time period and experienced a strong freshwater impact.

Previous studies like Ours et al. (1997) suggest that in pristine peatlands, notably in bogs, salt water may migrate faster and deeper in the peat body towards the groundwater and the hinterland than fresh water due to the pore dilation effect. Arguably, an increase of K_s of 280 %, as observed for bog peat by van Dijk et al. (2017) for a realistic salinity change from 0.09 to 0.9 %, may lead to a more widespread distribution of seawater ions, including the bioreactive SO_4^{2-}. However, in deeper peat horizons below the root zone, this may only lead to a pronounced SO_4^{2-} reduction and thus OM degradation and enhanced solute release if easily-degradable DOC is supplied concomitantly. Since the DOC concentrations are lowered in saltwater an import of significant amounts of bioavailable DOC with seawater is unlikely, although particulate organic carbon can be (re-)suspended during storm events (Goehrig, 2016). More likely is a salinity-induced dieback of plants and vegetation shift (Herbert et al., 2015), which can especially occur in pristine, previously sea-unaffected peatlands or in coastal peatlands rewetted with

freshwater with a rather salinity-intolerant vegetation (Stofberg et al., 2015), and the following release of bioavailable DOC. Cases of “peat collapse” are often related to vegetation death, which can destabilize peat soils and accelerate mineralization processes (Chambers et al., 2019). However, if an increased seawater impact in fact stimulates OM mineralization is still subject to debate, although organic-rich soils seem to release more carbon when salinized (Herbert et al., 2015).

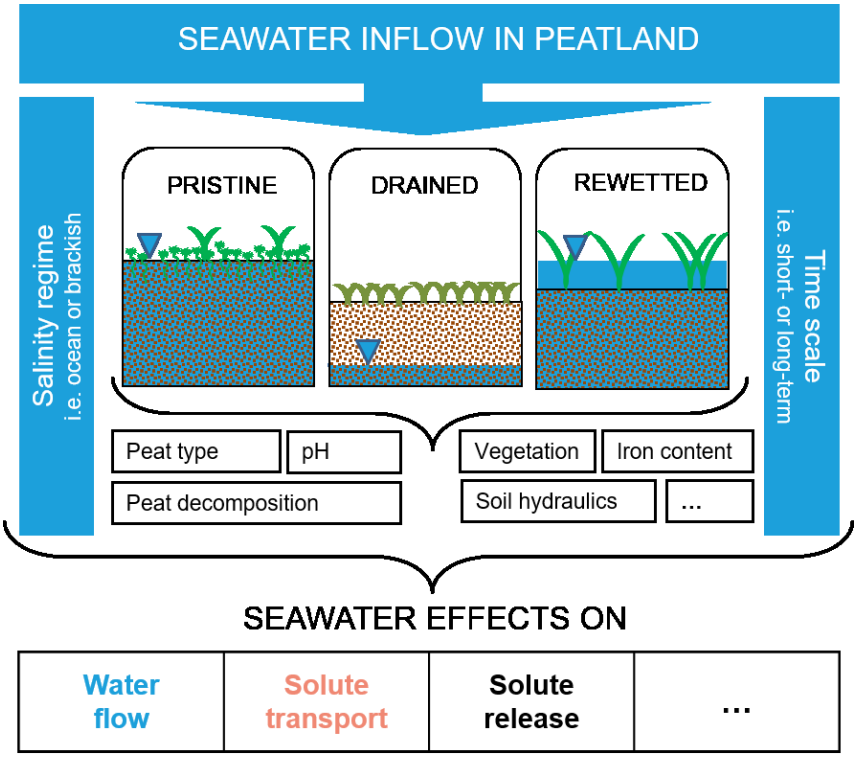

Figure 5.2: Impact factors on seawater effects in peatlands, which determine changes of water flow, solute transport and solute release, but also of other important processes in peat soil such as greenhouse gas emissions and soil accretion.The factors are heavily impacted by the peatland’s land-use history.

The results of this thesis suggest that peat soils in drained fens with a degraded, lowly permeable and iron-enriched top soil will react differently to seawater inflow than those in pristine peatlands. As previously discussed in Section 5.1.4, an elevated iron content may act as “game-changer” in terms of water and matter fluxes during seawater inflow. It may also reduce the risk of vegetation death by binding the phytotoxic sulfide, which is formed during SO_4^{2-} reduction, in form of FeS and FeS_2 (Portnoy and Giblin, 1997). However, the iron impact on the peatland’s response to seawater inflow may only be temporary. As shown in

Figure 3.4 the initial peak and subsequent decrease of concentration in dissolved iron in Gosch et al. (2019) implies that the dominance of iron reduction was limited to the first ~ 20 days of the experiment. This indicates that the iron pool may be quickly depleted unless iron recycling, also referred to as “iron redox wheel” (Li et al., 2012), occurs within the peat.

Due to the low K_s, the seawater may hardly infiltrate into the peat (Ahmad et al., 2020), even in rewetted peatlands, since the peat degradation-induced reduction of K_s is not reversible (Succow and Joosten, 2001). In the *Hütelmoor*, as an example for a formerly drained and nowadays rewetted fen, K_s values seem to be low peatland-wide and regardless of depth, which hinders potential percolation of inflowing seawater into the peat body. The vertical K_s ranged between 0.26 to 2.37 cm d^{-1} for the constantly seawater-exposed peat at the beachside and between 0.07 and 9.35 cm d^{-1} for the superficial muddy peat within the *Hütelmoor*. According to Ad-hoc-Arbeitsgruppe Boden (2005) these K_s values can be classified as “very low to low” and are also lower than the average K_s of fen peat of 22 cm d^{-1} determined by Liu and Lennartz (2019a). Also deeper peat horizons have a low hydraulic conductivity such as the peat in a depth of 1.2 m below ground surface behind the dune with 0.41 to 1.21 cm d^{-1}. These values are confirmed by slug tests carried out in the field, which resulted in K_s values for the peat between 0.09 and 9 cm d^{-1} (= 10^{-6} to 10^{-8} m s^{-1}) (Ibenthal, 2019). For comparison: the K_s of the sandy sediments at the beach of the *Hütelmoor* measured by Schade (2019) ranged between 115 and 9626 cm d^{-1} (≡ k ranging between 1.36 and 113*10^{-12} m²). Generally, in marine benthic sciences sandy sediments with a K_s value below 213 cm d^{-1} (≡ k of 2.5 *10^{-12} m²) are considered impermeable. i.e. with no biogeochemical effects of advective porewater flow (Forster et al., 2003). The peat as a marine sediment must therefore be considered highly impermeable and likely functions as an effective geological barrier for water and solute exchange processes.

Thus, instead of percolating, the superficially inflowing seawater in a (formerly) drained peatland with low K_s values may mobilize organic as well as inorganic solutes at the surface and, in case of the Hütelmoor, may run off rapidly through the ditch system, which pervades the peatland (see Figure 4.1). This was also the conclusion by Koebsch et al. (2019) for the hydraulic conditions in the *Hütelmoor*, who found that only the upper peat horizon (0 – 20 cm) contained fresh water resulting from rewetting while in deeper layers relics of former brackish inflow

characterized by higher pore water *EC* values were preserved. Thus, in regions with predominantly drained peatlands, such as the southern Baltic Sea coast, extended sea water flooding of coastal peatlands may lead to an augmented nutrient release, which may end up in the adjacent aquatic ecosystems.

Due to the constrained percolation, seawater inflow may not cause the desired impedance of methanogenesis by SRB since the SO_4^{2-} is not transported in deeper regions of the peat. In that case, seawater flooding might not contribute as expected to greenhouse gas reductions in the peatland, since the CH_4 emissions are not suppressed efficiently. In the *Hütelmoor* these processes might be mutually dependent since the site has emitted significant amounts of methane after rewetting (Hahn et al., 2015), which means that the formation of methane gas bubbles might contribute to the low K_s of the peat. The methane formation-impeding effect of seawater as stated by van Dijk et al. (2017) and also shown in Kreuzburg et al. (2020) might then be limited to the diffusion of SO_4^{2-} or to a pronounced preferential flow (e.g. by plant roots), which enables a proportion of the seawater with the dissolved SO_4^{2-} to percolate faster than it would be caused by matrix flow determined by the K_s value. Ultimately, low K_s values might reduce the decomposition of the peat since they favor the endurance of anoxic conditions during decreasing water levels and impair the inflow of electron acceptors (Chambers et al., 2014).

Due to the high *CEC* of peat the seawater inflow will in all cases, i.e. for all peat types, lead to a pronounced desorption of cations such as NH_4^+ and thus represent a source for nitrogen. This is also true for less organic wetland soils, such as a mineral marsh, for which Steinmuller and Chambers (2018) observed a clear increase in NH_4^+ release after a rise in water salinity. For coastal peatlands at the Baltic Sea the effect will be less pronounced than for coastal peatlands in other regions due to the lower ionic strength of the brackish Baltic sea water compared to ocean water. To a certain degree, the NH_4^+ release may mitigate the phytotoxicity of sulfide, which hampers the N-uptake of plants (Herbert et al., 2015). Once the peat is permanently exposed to seawater, desorption of NH_4^+ will decrease since the binding places are occupied by seawater cations. Yet, the peat may still act as a long-term source for carbon in form of DOC and dissolved methane and carbon dioxide, especially in case of SGD consisting of fresh water. Although the fresh water-induced dissolution of the OM will most likely have only

local effects on the marine environment since the DOC coagulates once again in the salt water phase (Goehrig, 2016; Liu and Lennartz, 2019b).

5.4 Outlook

Seawater effects on formerly terrestrial ecosystems will continue to increase in the future and represent a threat to freshwater wetlands worldwide (Herbert et al., 2015). For peatland-rich regions, especially those affected by land subsidence such as Northern Germany or the Netherlands, the handling of coastal peatlands will be of great importance for future coastal land management. Günther et al. (2020) recommend extensive and timely rewetting of the drained peatlands for climate change mitigation. Since predicting the consequences of coastal peatland restoration is complicated by the interplay between rewetting and salinization effects, basic coastal research like in *Baltic TRANSCOAST* will ultimately help to address the practical challenges of climate change in the future.

As the current state of research shows that in many cases water salinity affects peat soil processes, further studies on this topic may be required in order to gain a comprehensive understanding of the effects of seawater. Due to the ensemble of pristine, drained and rewetted sites, the seawater inflow-induced biogeochemical conditions will have peat- or site-specific character. Investigations on peat soil functions should contain an extensive chemical analysis of the peat material, including iron content and *pH*, to improve the comparability and transferability of the studies. Ideally, using the same methodology for different peat types and degrees of decomposition should reveal or exclude potential peat-specific characteristics.

Since K_s of peat is a crucial soil parameter, for instance for rewetting projects, and cannot be derived from grain size distribution, like it is the case for mineral soils, it should to be measured. However, in rewetted and inundated peatlands like the *Hütelmoor* taking undisturbed samples for K_s tests is fraught with difficulties and should, if possible, be carried out before the peatland is rewetted. Alternatively, the use of field methods like the direct-push piezometer (Ahmad et al., 2020) might allow a measurement in inundated areas, which are difficult to access. Where possible, the measurement should include a consecutive K_s test with a low and a high water salinity to detect a potential salinity-dependency of K_s. If K_s does show a sensitivity towards a rise of water salinity, it can be expected that this is also the

case for further important hydraulic soil properties such as unsaturated hydraulic conductivity or water retention curve, which has yet to be confirmed.

In rewetted peatlands with a degraded, less permeable top soil and low hydraulic gradients, hydrostatic conditions and thus diffusion-based solute transport may be of increased relevance. In this case, hydrostatic experiments and modelling (Clymo and Williams, 2012) might simulate transport of seawater compounds more realistically than conventional pump-controlled displacement experiments. Furthermore, an advanced interdisciplinarity like in Kreuzburg et al. (2020) for solute transport studies in peat, such as simultaneous greenhouse gas measurements or localization of microbial communities, may help to evaluate the role of Fe^{3+} and SO_4^{2-} reduction during seawater inflow and to better relate peat structure to biogeochemical processes.

The time scale for the enhanced solute release from iron-enriched soils as observed by Emsens et al. (2016), i.e. a potential depletion of the iron poor, should be further investigated. The same holds true for the duration of an increased release of NH_4^+ during seawater inflow. Future laboratory experiments should take this parameter into account, as the peat as a potential source for nitrogen might be relevant for the nutrient balance of the adjacent sea. Generally, long-term studies in coastal peatlands are still scarce but needed for the assessment of permanent seawater inundation. For this, the monitoring of peat soil parameters during rewetting projects may be suited, since this allows “before and after” comparisons.

VI REFERENCES

Aben, R.C.H., Barros, N., van Donk, E., Frenken, T., Hilt, S., Kazanjian, G., Lamers, L.P.M., Peeters, E.T.H.M., Roelofs, J.G.M., de Senerpont Domis, L.N., Stephan, S., Velthuis, M., Van de Waal, D.B., Wik, M., Thornton, B.F., Wilkinson, J., DelSontro, T., Kosten, S., 2017. Cross continental increase in methane ebullition under climate change. Nat. Commun. 8, 1682. doi:10.1038/s41467-017-01535-y

Acreman, M., Holden, J., 2013. How wetlands affect floods. Wetlands 33, 773–786. doi:10.1007/s13157-013-0473-2

Ad-hoc-Arbeitsgruppe Boden, 2005. Bodenkundliche Kartieranleitung, 5. Auflage. ed. Bundesanstalt für Geowissenschaften und Rohstoffe, Hannover.

Ahmad, S., Liu, H., Beyer, F., Kløve, B., Lennartz, B., 2020. Spatial heterogeneity of soil properties in relation to microtopography in a non-tidal rewetted coastal mire. Mires Peat 26, 1–18. doi:10.19189/MaP.2019.GDC.StA.1779

Aitkenhead, J.A., Hope, D., Billett, M.F., 1999. The relationship between dissolved organic carbon in stream water and soil organic carbon pools at different spatial scales. Hydrol. Process. 13, 1289–1302.

Algeo, T.J., Luo, G.M., Song, H.Y., Lyons, T.W., Canfield, D.E., 2015. Reconstruction of secular variation in seawater sulfate concentrations. Biogeosciences 12, 2131–2151. doi:10.5194/bg-12-2131-2015

Andersen, M.S., Nyvang, V., Jakobsen, R., Postma, D., 2005. Geochemical processes and solute transport at the seawater/freshwater interface of a sandy aquifer. Geochim. Cosmochim. Acta 69, 3979–3994. doi:10.1016/j.gca.2005.03.017

Anderson, T.F., Arthur, M.A., 1983. Stable isotopes of oxygen and carbon and their application to sedimentologic and paleoenvironmental problems. SEPM Soc. Sediment. Geol. 1.1–1.151.

Aravena, R., Wassenaar, L.I., 1993. Dissolved organic carbon and methane in a regional confined aquifer, southern Ontario, Canada: Carbon isotope evidence for associated subsurface sources. Appl. Geochemistry 8, 483–493. doi:https://doi.org/10.1016/0883-2927(93)90077-T

Ardón, M., Helton, A.M., Bernhardt, E.S., 2016. Drought and saltwater incursion synergistically reduce dissolved organic carbon export from coastal freshwater wetlands. Biogeochemistry 127, 411–426. doi:10.1007/s10533-016-0189-5

Ardón, M., Morse, J.L., Colman, B.P., Bernhardt, E.S., 2013. Drought-induced saltwater incursion leads to increased wetland nitrogen export. Glob. Chang. Biol. 19, 2976–2985. doi:10.1111/gcb.12287

Badocco, D., Mondin, A., Pastore, P., 2012. Determination of thermodynamic parameters from light intensity signals obtained from oxygen optical sensors. Sensors Actuators B Chem. 163, 165–170. doi:https://doi.org/10.1016/j.snb.2012.01.030

Baird, A.J., Gaffney, S.W., 2000. Solute movement in drained fen peat: a field tracer study in a Somerset (UK) wetland. Hydrol. Process. 14, 2489–2503. doi:10.1002/1099-1085(20001015)14:14<2489::AID-HYP110>3.0.CO;2-Q

Baird, A.J., Waldron, S., 2003. Shallow horizontal groundwater flow in peatlands is reduced by bacteriogenic gas production. Geophys. Res. Lett. 30, 2043. doi:10.1029/2003GL018233

Bange, H.W., 2006. Nitrous oxide and methane in European coastal waters. Estuar. Coast. Shelf Sci. 70, 361–374. doi:https://doi.org/10.1016/j.ecss.2006.05.042

Bange, H.W., Bartell, U.H., Rapsomanikis, S., Andreae, M.O., 1994. Methane in the Baltic and North Seas and a reassessment of the marine emissions of methane. Global Biogeochem. Cycles 8, 465–480. doi:https://doi.org/10.1029/94GB02181

Barlow, P.M., Reichard, E.G., 2010. Saltwater intrusion in coastal regions of North America. Hydrogeol. J. 18, 247–260. doi:10.1007/s10040-009-0514-3

Beetz, S., Liebersbach, H., Glatzel, S., Jurasinski, G., Buczko, U., Höper, H., 2013. Effects of land use intensity on the full greenhouse gas balance in an Atlantic peat bog. Biogeosciences 10, 1067–1082. doi:10.5194/bg-10-1067-2013

Bender, M.L., Heggie, D.T., 1984. Fate of organic carbon reaching the deep sea floor: a status report. Geochim. Cosmochim. Acta 48, 977–986. doi:https://doi.org/10.1016/0016-7037(84)90189-3

Berry, D.F., Zelazny, L.W., Walker Jr, H.L., 1990. Aluminum and organic matter mobilization from forest soil infiltrated with acidified calcium sulfate solutions. Soil Sci. Soc. Am. J. 54, 1757–1762. doi:10.2136/sssaj1990.03615995005400060042x

Bickert, T., 2000. Influence of geochemical processes on stable isotope distribution in marine sediments, in: Schulz, H.D., Zabel, M. (Eds.), Marine Geochemistry. Springer, Berlin Heidelberg, pp. 309–333.

Blodau, C., Mayer, B., Peiffer, S., Moore, T.R., 2007. Support for an anaerobic sulfur cycle in two Canadian peatland soils. J. Geophys. Res. Biogeosciences 112, 1–10. doi:10.1029/2006JG000364

Blume, H.-P., Stahr, K., Leinweber, P., 2011. Bodenkundliches Praktikum. Spektrum Akademischer Verlag, Heidelberg.

Boetius, A., Ravenschlag, K., Schubert, C.J., Rickert, D., Widdel, F., Gieseke, A., Amann, R., Jørgensen, B.B., Witte, U., Pfannkuche, O., 2000. A marine microbial consortium apparently mediating anaerobic oxidation of methane. Nature 407, 623–626. doi:10.1038/35036572

Borch, T., Kretzschmar, R., Kappler, A., 2010. Biogeochemical Redox Processes and their Impact on Contaminant Dynamics - Environmental Science & Technology (ACS Publications). Environ. Sci. Technol. 44, 15–23. doi:10.2136/sssaj1988.03615995005200020032x

Borges, A. V., Champenois, W., Gypens, N., Delille, B., Harlay, J., 2016. Massive marine methane emissions from near-shore shallow coastal areas. Sci. Rep. 6, 2–9. doi:10.1038/srep27908

Boschker, H.T.S., De Graaf, W., Köster, M., Meyer-Reil, L.A., Cappenberg, T.E., 2001. Bacterial populations and processes involved in acetate and propionate consumption in anoxic brackish sediment. FEMS Microbiol. Ecol. 35, 97–103. doi:10.1016/S0168-6496(00)00116-1

Boutton, T.W., 1991. 11 - Stable Carbon Isotope Ratios of Natural Materials: II. Atmospheric, Terrestrial, Marine, and Freshwater Environments, in: Coleman, D.C., Fry, B.B.T.-C.I.T. (Eds.), Carbon Isotope Techniques. Academic Press, pp. 173–185. doi:https://doi.org/10.1016/B978-0-12-179730-0.50016-3

Brouns, K., Verhoeven, J.T.A., Hefting, M.M., 2014. The effects of salinization on aerobic and anaerobic decomposition and mineralization in peat meadows: The roles of peat type and land use. J. Environ. Manage. 143, 44–53. doi:10.1016/j.jenvman.2014.04.009

Bugna, G.C., Chanton, J.P., Cable, J.E., Burnett, W.C., Cable, P.H., 1996. The importance of groundwater discharge to the methane budgets of nearshore and continental shelf waters of the northeastern Gulf of Mexico. Geochim. Cosmochim. Acta 60, 4735–4746. doi:10.1016/S0016-7037(96)00290-6

Burdige, D.J., 2012. Estuarine and Coastal Sediments - Coupled Biogeochemical Cycling, Treatise on Estuarine and Coastal Science. Elsevier Inc. doi:10.1016/B978-0-12-374711-2.00511-8

Burnett, W.C., Aggarwal, P.K., Aureli, A., Bokuniewicz, H., Cable, J.E., Charette, M.A., Kontar, E., Krupa, S., Kulkarni, K.M., Loveless, A., Moore, W.S., Oberdorfer, J.A., Oliveira, J., Ozyurt, N., Povinec, P., Privitera, A.M.G., Rajar, R., Ramessur, R.T., Scholten, J., Stieglitz, T., Taniguchi, M., Turner, J. V., 2006. Quantifying submarine groundwater discharge in the coastal zone via multiple methods. Sci. Total Environ. 367, 498–543. doi:10.1016/j.scitotenv.2006.05.009

Bussmann, I., Suess, E., 1998. Groundwater seepage in Eckernforde Bay (Western Baltic Sea): Effect on methane and salinity distribution of the water column. Cont. Shelf Res. 18, 1795–1806. doi:10.1016/S0278-4343(98)00058-2

Cabrera, R.I., 1998. Monitoring chemical properties of container growing media with small soil solution samplers1The use of trade names in this publication does not imply endorsement of the products used or criticism of similar ones not used.1. Sci. Hortic. (Amsterdam). 75, 113–119. doi:https://doi.org/10.1016/S0304-4238(98)00121-6

Caraco, N.F., Cole, J.J., Likens, G.E., 1989. Evidence for sulphate-controlled phosphorus release from sediments of aquatic systems. Nature 341, 316–318. doi:10.1038/340301a0

Caron, J., Létourneau, G., Fortin, J., 2015. Electrical Conductivity Breakthrough Experiment and Immobile Water Estimation in Organic Substrates : Is R = 1 a Realistic Assumption ? Vadose Zo. J. 14. doi:10.2136/vzj2015.01.0014

Chambers, L.G., Davis, S.E., Troxler, T., Boyer, J.N., Downey-Wall, A., Scinto, L.J., 2014. Biogeochemical effects of simulated sea level rise on carbon loss in an Everglades mangrove peat soil. Hydrobiologia 726, 195–211. doi:10.1007/s10750-013-1764-6

Chambers, L.G., Reddy, K.R., Osborne, T.Z., 2011. Short-Term Response of Carbon Cycling to Salinity Pulses in a Freshwater Wetland. Soil Sci. Soc. Am. J. 75, 2000–2007. doi:https://doi.org/10.2136/sssaj2011.0026

Chambers, L.G., Steinmuller, H.E., Breithaupt, J.L., 2019. Toward a mechanistic understanding of “peat collapse” and its potential contribution to coastal wetland loss. Ecology 100, e02720. doi:https://doi.org/10.1002/ecy.2720

Charman, D., 2002. Peatlands and Environmental Change. John Wiley & Sons, LTD, Chichester.

Chen, C., Dynes, J.J., Wang, J., Sparks, D.L., 2014. Properties of Fe-Organic Matter Associations via Coprecipitation versus Adsorption. Environ. Sci. Technol. 48, 13751–13759. doi:10.1021/es503669u

Cicerone, R.J., Oremland, R.S., 1988. Biogeochemical aspects of atmospheric methane. Global Biogeochem. Cycles 2, 299–327. doi:https://doi.org/10.1029/GB002i004p00299

Clark, J.M., Van Der Heijden, G.M.F., Palmer, S.M., Chapman, P.J., Bottrell, S.H., 2011. Variation in the sensitivity of DOC release between different organic soils following H2SO4 and sea-salt additions. Eur. J. Soil Sci. 62, 267–284. doi:10.1111/j.1365-2389.2010.01344.x

Cline, J.D., 1969. Spectrophotometric determination of hydrogen sulfide in natural waters. Limnol. Oceanogr. 14, 454–458. doi:10.4319/lo.1969.14.3.0454

Clymo, R.S., Williams, M.M.R., 2012. Diffusion of gases dissolved in peat pore water. Mires Peat 10, 1–10.

Comas, X., Slater, L., 2004. Low-frequency electrical properties of peat. Water Resour. Res. 40, 1–9. doi:10.1029/2004WR003534

Cyberski, J., 2011. Climate, hydrology and hydrodynamics of the Baltic Sea., in: Uścinowicz, S. (Ed.), Geochemistry of Baltic Sea Surface Sediments. Polish Geological Institute – National Research Institute, Warszawa, pp. 55–65.

Dahms, P., 1991. Studie Wasserregulierung Hütelmoor.

Dale, A.W., Regnier, P., Knab, N.J., Jørgensen, B.B., Van Cappellen, P., 2008. Anaerobic oxidation of methane (AOM) in marine sediments from the Skagerrak (Denmark): II. Reaction-transport modeling. Geochim. Cosmochim. Acta 72, 2880–2894. doi:https://doi.org/10.1016/j.gca.2007.11.039

Dar, S.A., Kleerebezem, R., Stams, A.J.M., Kuenen, J.G., Muyzer, G., 2008. Competition and coexistence of sulfate-reducing bacteria, acetogens and methanogens in a lab-scale anaerobic bioreactor as affected by changing substrate to sulfate ratio. Appl. Microbiol. Biotechnol. 78, 1045–1055. doi:10.1007/s00253-008-1391-8

Dean, J.F., Middelburg, J.J., Röckmann, T., Aerts, R., Blauw, L.G., Egger, M., Jetten, M.S.M., de Jong, A.E.E., Meisel, O.H., Rasigraf, O., Slomp, C.P., in't Zandt, M.H., Dolman, A.J., 2018. Methane Feedbacks to the Global Climate System in a Warmer World. Rev. Geophys. 56, 207–250. doi:https://doi.org/10.1002/2017RG000559

DeLaune, R.D., Nyman, J.A., Patrick Jr, W.H., 1994. Peat collapse, ponding and wetland loss in a rapidly submerging coastal marsh. J. Coast. Res. 1021–1030.

Deppenmeier, U.B.T.-P. in N.A.R. and M.B., 2002. The unique biochemistry of methanogenesis. Academic Press, pp. 223–283. doi:https://doi.org/10.1016/S0079-6603(02)71045-3

Dikinya, O., Hinz, C., Aylmore, G., 2008. Decrease in hydraulic conductivity and particle release associated with self-filtration in saturated soil columns. Geoderma 146, 192–200. doi:10.1016/j.geoderma.2008.05.014

Dillon, K.S., Corbett, D.R., Chanton, J.P., Burnett, W.C., Furbish, D.J., 1999. The use of sulfur hexafluoride (SF6) as a tracer of septic tank effluent in the Florida Keys. J. Hydrol. 220, 129–140. doi:https://doi.org/10.1016/S0022-1694(99)00073-6

DIN 19683-9 (Deutsches Institut für Normung e.V.), 2012. Soil quality - Physical laboratory tests - Part 9: Determination of the saturated hydraulic water conductivity in the cylindrical core-cutter. Beuth Verlag, Berlin.

DIN EN 15935 (Deutsches Institut für Normung e.V.), 2012. Sludge, treated biowaste, soil and waste - Determination of loss on ignition. Beuth Verlag, Berlin.

DIN EN ISO 11272 (Deutsches Institut für Normung e.V.), 2014. Soil quality - determination of dry bulk density. Beuth Verlag, Berlin.

DIN EN ISO 13536, 1997. Soil quality - Determination of the potential cation exchange capacity and exchangeable cations using barium chloride solution buffered at pH = 8.1. Deutsches Institut für Normung e.V.

Edelstein, M., Ben-Hur, M., Plaut, Z., 2010. Water Salinity and Sodicity Effects on Soil Structure and Hydraulic Properties. Adv. Hortic. Sci. 24, 154–160. doi:10.1400/143516

Emsens, W.J., Aggenbach, C.J.S., Schoutens, K., Smolders, A.J.P., Zak, D., Van Diggelen, R., 2016. Soil iron content as a predictor of carbon and nutrient mobilization in rewetted fens. PLoS One 11, 1–17. doi:10.1371/journal.pone.0153166

EPA, 2002. EPA standard operating procedure for dissolved organic carbon, LG211, Revision 03, December 2002.

Evans, C.D., Jones, T.G., Burden, A., Ostle, N., Zieliński, P., Cooper, M.D.A., Peacock, M., Clark, J.M., Oulehle, F., Cooper, D., Freeman, C., 2012. Acidity controls on dissolved organic carbon mobility in organic soils. Glob. Chang. Biol. 18, 3317–3331. doi:10.1111/j.1365-2486.2012.02794.x

Feistel, R., Weinreben, S., Wolf, H., Seitz, S., Spitzer, P., Adel, B., Nausch, G., Schneider, B., Wright, D.G., 2010. Density and absolute salinity of the baltic sea 2006-2009. Ocean Sci. 6, 3–24. doi:10.5194/os-6-3-2010

Forster, S., Bobertz, B., Bohling, B., 2003. Permeability of Sands in the Coastal Areas of the Southern Baltic Sea: Mapping a Grain-size Related Sediment Property. Aquat. Geochemistry 9, 171–190. doi:10.1023/B:AQUA.0000022953.52275.8b

Freeman, C., Evans, C.D., Monteith, D.T., Reynolds, B., Fenner, N., 2001. Export of organic carbon from peat soils. Nature 412, 785. doi:10.1038/35090628

Gardner, L.R., 1990. Simulation of the diagenesis of carbon, sulfur, and dissolved oxygen in salt marsh sediments. Ecol. Monogr. 60, 91–111. doi:10.2307/1943027

Gatland, J.R., Santos, I.R., Maher, D.T., Duncan, T.M., Erler, D. V., 2014. Carbon dioxide and methane emissions from an artificially drained coastal wetland during a flood: Implications for wetland global warming potential. J. Geophys. Res. Biogeosciences 119, 1698–1716. doi:10.1002/2013JG002544.Received

Gerke, H.H., van Genuchten, M.T., 1993. A dual-porosity model for simulating the preferential movement of water and solutes in structured porous media. Water Resour. Res. 29, 305–319. doi:10.1029/92WR02339

Glatzel, S., Kalbitz, K., Dalva, M., Moore, T., 2003. Dissolved organic matter properties and their relationship to carbon dioxide efflux from restored peat bogs. Geoderma 113, 397–411. doi:https://doi.org/10.1016/S0016-7061(02)00372-5

Goehrig, T.J., 2016. Consequences of salinization on carbon and nutrient release from a restored coastal forested wetland. Master thesis, East Carolina University.

Gorham, E., 1995. The biogeochemistry of northern peatlands and its possible responses to global warming, in: Woodwell, G.M., Mackenzie, F.T. (Eds.), Biotic Feedbacks in the Global Climate System: Will the Warming Feed the Warming? Oxford University Press, Inc, pp. 169–186.

Gosch, L., Janssen, M., Lennartz, B., 2018. Impact of the water salinity on the hydraulic conductivity of fen peat. Hydrol. Process. 32, 1214–1222. doi:10.1002/hyp.11478

Gosch, L., Townsend, H., Kreuzburg, M., Janssen, M., Rezanezhad, F., Lennartz, B., 2019. Sulfate Mobility in Fen Peat and Its Impact on the Release of Solutes. Front. Environ. Sci. 7, 1–13. doi:10.3389/fenvs.2019.00189

Göttlich, K., 1990. Moor- und Torfkunde, 3. neubear. ed. E. Schweizerbart'sche Verlagsbuchhandlung, Stuttgart.

Gu, B., Schmitt, J., Chen, Z., Liang, L., McCarthy, J.F., 1995. Adsorption and desorption of different organic matter fractions on iron oxide. Geochim. Cosmochim. Acta 59, 219–229. doi:https://doi.org/10.1016/0016-7037(94)00282-Q

Günther, A., Barthelmes, A., Huth, V., Joosten, H., Jurasinski, G., Koebsch, F., Couwenberg, J., 2020. Prompt rewetting of drained peatlands reduces climate warming despite methane emissions. Nat. Commun. 11, 1–5. doi:10.1038/s41467-020-15499-z

Hahn, J., Köhler, S., Glatzel, S., Jurasinski, G., 2015. Methane exchange in a coastal fen in the first year after flooding - A systems shift. PLoS One 10, 1–25. doi:10.1371/journal.pone.0140657

Hanin, M., Ebel, C., Ngom, M., Laplaze, L., Masmoudi, K., 2016. New Insights on Plant Salt Tolerance Mechanisms and Their Potential Use for Breeding. Front. Plant Sci. 7, 1–17. doi:10.3389/fpls.2016.01787

Harff, J., Furmańczyk, K., von Storch, H., 2017. Coastline Changes of the Baltic Sea from South to East. Coastal Research Library. Springer International Publishing AG.

Hausmann, B., Knorr, K., Schreck, K., Tringe, S.G., Glavina, T., Loy, A., Pester, M., 2016. Consortia of low-abundance bacteria drive sulfate reduction-dependent degradation of fermentation products in peat soil microcosms. ISME J. 10, 2365–2375. doi:10.1038/ismej.2016.42

Heitmann, T., Blodau, C., 2006. Oxidation and incorporation of hydrogen sulfide by dissolved organic matter. Chem. Geol. 235, 12–20. doi:10.1016/j.chemgeo.2006.05.011

HELCOM, 2018. HELCOM Thematic assessment of eutrophication 2011-2016. Baltic Sea Environment Proceedings No. 156.

Henman, J., Poulter, B., 2008. Inundation of freshwater peatlands by sea level rise: Uncertainty and potential carbon cycle feedbacks. J. Geophys. Res. Biogeosciences 113. doi:https://doi.org/10.1029/2006JG000395

Henrichs, S.M., Reeburgh, W.S., 1987. Anaerobic mineralization of marine sediment organic matter: Rates and the role of anaerobic processes in the oceanic carbon economy. Geomicrobiol. J. 5, 191–237. doi:10.1080/01490458709385971

Herbert, E.R., Boon, P., Burgin, A.J., Neubauer, S.C., Franklin, R.B., Ardon, M., Hopfensperger, K.N., Lamers, L.P.M., Gell, P., Langley, J.A., 2015. A global perspective on wetland salinization: Ecological consequences of a growing threat to freshwater wetlands. Ecosphere 6, 1–43. doi:10.1890/ES14-00534.1

Heyer, J., Berger, U., 2000. Methane Emission from the Coastal Area in the Southern Baltic Sea. Estuar. Coast. Shelf Sci. 51, 13–30. doi:https://doi.org/10.1006/ecss.2000.0616

HFA (Gutachterausschuss Forstliche Analytik), 2014. Handbuch Forstliche Analytik: Eine Loseblatt-Sammlung der Analysemethoden im Forstbereich. Bundesministerium für Ernährung und Landwirtschaft (BMEL), Bonn.

Hillel, D., 1998. Environmental Soil Physics. Academic Press, San Diego.

Holden, J., Chapman, P.J., Labadz, J.C., 2004. Artificial drainage of peatlands: Hydrological and hydrochemical process and wetland restoration. Prog. Phys. Geogr. 28, 95–123. doi:10.1191/0309133304pp403ra

Holmer, M., Kristensen, E., 1994. Coexistence of sulfate reduction and methane production in an organic-rich sediment. Mar. Ecol. Prog. Ser. 107, 177–184. doi:10.3354/meps107177

Hoogland, T., Akker, J.J.H. Van Den, Brus, D.J., 2012. Modeling the subsidence of peat soils in the Dutch coastal area. Geoderma 171–172, 92–97. doi:10.1016/j.geoderma.2011.02.013

Hooijer, A., Page, S., Jauhiainen, J., Lee, W.A., Lu, X.X., Idris, A., Anshari, G., 2012. Subsidence and carbon loss in drained tropical peatlands. Biogeosciences 9, 1053–1071. doi:10.5194/bg-9-1053-2012

Horton, B.P., Khan, N.S., Cahill, N., Lee, J.S.H., Shaw, T.A., Garner, A.J., Kemp, A.C., Engelhart, S.E., Rahmstorf, S., 2020. Estimating global mean sea-level rise and its uncertainties by 2100 and 2300 from an expert survey. npj Clim. Atmos. Sci. 3, 18. doi:10.1038/s41612-020-0121-5

Howarth, R.W., Marino, R., 2006. Nitrogen as the limiting nutrient for eutrophication in coastal marine ecosystems: Evolving views over three decades. Limnol. Oceanogr. 51, 364–376. doi:https://doi.org/10.4319/lo.2006.51.1_part_2.0364

Howarth, R.W., Teal, J.M., 1979. Sulfate reduction in a New England salt marsh1. Limnol. Oceanogr. 24, 999–1013. doi:https://doi.org/10.4319/lo.1979.24.6.0999

Hübner, E., 2013. Küstenhydrologie und -topografie im Naturschutzgebiet Hütelmoor - Projektbericht zum Modul „Geoökologie III“.

Huth, V., Bartel, A., Günther, A., Heinze, S., Hofer, B., Jantz, N., Rosinski, E., Rudolph, J., Schikora, H.-B., Söchting, H.-P., Ullrich, K., Jurasinski, G., 2019. Feldversuch „ OptiMoor “ – Erprobung und Entwicklung der Optimierung von Hochmoor - sanierung auf landwirtschaftlich genutzten Standorten. TELMA 49, 71–88.

Ibenthal, M., 2019. Marine and terrestrial influence on submarine groundwater discharge in coastal waters connected to a peatland. Dissertation. Georg-August-Universität Göttingen.

IPCC, 2013. Climate change 2013: The physical science basis. Contribution of working group I to the fifth assessment report of the Intergovernmental Panel on Climate Change 2013. Cambridge University Press, Cambridge, United Kingdom and New York, NY, USA.

IPS, n.d. What is peat? [WWW Document]. URL https://peatlands.org/peat/peat/ (accessed 9.29.20).

IsoPrime, 2014. IsoPrime100 user’s guide v1.02 for Ionvantage, 2014. Cheadle, UK.

Iversen, N., Blackburn, T.H., 1981. Seasonal Rates of Methane Oxidation in Anoxic Marine Sediments. Appl. Environ. Microbiol. 41, 1295–1300. doi:10.1128/aem.41.6.1295-1300.1981

Jansen, B., Nierop, K.G.J., Verstraten, J.M., 2003. Mobility of Fe(II), Fe(III) and Al in acidic forest soils mediated by dissolved organic matter: influence of solution pH and metal/organic carbon ratios. Geoderma 113, 323–340. doi:https://doi.org/10.1016/S0016-7061(02)00368-3

Johnson, D.W., Todd, D.E., 1983. Relationships Among Iron, Aluminum, Carbon, and Sulfate in a Variety of Forest Soils. Soil Sci. Soc. Am. J. 47.

Joosten, H., Clarke, D., 2002. Wise use of mires and peatlands - background and principles including a framework for decision-making. International Mire Conservation Group and International Peat Society, Saarijärven Offset Oy, Saarijärvi, Finland.

Jørgensen, B.B., Weber, A., Zopfi, J., 2001. Sulphate reduction and anaerobic oxidation in Black Sea sediments. Deep. Res. I 48, 2097–2120.

Jørgensen, N.O., Andersen, M.S., Engesgaard, P., 2008. Investigation of a dynamic seawater intrusion event using strontium isotopes (87Sr/86Sr). J. Hydrol. 348, 257–269. doi:10.1016/j.jhydrol.2007.10.001

Joye, S.B., Hollibaugh, J.T., 1995. Influence of Sulfide Inhibition of Nitrification on Nitrogen Regeneration in Sediments. Science (80-.). 270, 623 LP – 625. doi:10.1126/science.270.5236.623

Jurasinski, G., Janssen, M., Voss, M., Böttcher, M.E.M.E., Brede, M., Burchard, H., Forster, S., Gosch, L., Gräwe, U., Gründling-Pfaff, S., Haider, F., Ibenthal, M., Karow, N., Karsten, U., Kreuzburg, M., Lange, X., Leinweber, P., Massmann, G., Ptak, T., Rezanezhad, F., Rehder, G., Romoth, K., Schade, H., Schubert, H., Schulz-Vogt, H., Sokolova, I.M.I.M., Strehse, R., Unger, V., Westphal, J., Lennartz, B., 2018. Understanding the Coastal Ecocline: Assessing Sea–Land Interactions at Non-tidal, Low-Lying Coasts Through Interdisciplinary Research. Front. Mar. Sci. 5, 1–22. doi:10.3389/fmars.2018.00342

Kalbitz, K., Schmerwitz, J., Schwesig, D., Matzner, E., 2003. Biodegradation of soil-derived dissolved organic matter as related to its properties. Geoderma 113, 273–291. doi:10.1016/S0016-7061(02)00365-8

Kalbitz, K., Solinger, S., Park, J.-H., Michalzik, B., Matzner, E., 2000. Controls on the dynamics of dissolved organic matter in soils: a review. Soil Sci. 165.

Kasimir-Klemedtsson, Å., Klemedtsson, L., Berglund, K., Martikainen, P., Silvola, J., Oenema, O., 1997. Greenhouse gas emissions from farmed organic soils: a review. Soil Use Manag. 13, 245–250. doi:10.1111/j.1475-2743.1997.tb00595.x

Kester, D.R., Duedall, I.W., Connors, D.N., Pytkowicz, R.M., 1967. Preparation of artificial seawater. Limnol. Oceanogr. 12, 176–179. doi:10.4319/lo.1967.12.1.0176

Kettridge, N., Binley, A., 2010. Evaluating the effect of using artificial pore water on the quality of laboratory hydraulic conductivity measurements of peat. Hydrol. Process. 24, 2629–2640. doi:10.1002/hyp.7693

Kettridge, N., Kellner, E., Price, J.S., Waddington, J.M., 2013. Peat deformation and biogenic gas bubbles control seasonal variations in peat hydraulic conductivity. Hydrol. Process. 27, 3208–3216. doi:10.1002/hyp.9369

Kleimeier, C., Karsten, U., Lennartz, B., 2014. Suitability of degraded peat for constructed wetlands — Hydraulic properties and nutrient flushing. Geoderma 228–229, 25–32. doi:10.1016/j.geoderma.2013.12.026

Kleimeier, C., Rezanezhad, F., Cappellen, P. Van, Lennartz, B., 2017. Influence of pore structure on solute transport in degraded and undegraded fen peat soils. Mires Peat 19, 1–9. doi:10.19189/MaP.2017.OMB.282

Knee, K.L., Paytan, A., 2011. 4.08 - Submarine Groundwater Discharge: A Source of Nutrients, Metals, and Pollutants to the Coastal Ocean, in: Wolanski, E., McLusky, D.B.T.-T. on E. and C.S. (Eds.), . Academic Press, Waltham, pp. 205–233. doi:https://doi.org/10.1016/B978-0-12-374711-2.00410-1

Knee, K.L., Street, J.H., Grossman, E.E., Boehm, A.B., Paytan, A., 2010. Nutrient inputs to the coastal ocean from submarine groundwater discharge in a groundwater-dominated system: Relation to land use (Kona coast, Hawaii, U.S.A.). Limnol. Oceanogr. 55, 1105–1122. doi:10.4319/lo.2010.55.3.1105

Knight, B.P., Chaudri, A.M., McGrath, S.P., Giller, K.E., 1998. Determination of chemical availability of cadmium and zinc in soils using inert soil moisture samplers. Environ. Pollut. 99, 293–298. doi:https://doi.org/10.1016/S0269-7491(98)00021-9

Knorr, K.H., 2013. DOC-dynamics in a small headwater catchment as driven by redox fluctuations and hydrological flow paths - are DOC exports mediated by iron reduction/oxidation cycles? Biogeosciences 10, 891–904. doi:10.5194/bg-10-891-2013

Koch, S., Jurasinski, G., Koebsch, F., Koch, M., Glatzel, S., 2014. Spatial Variability of Annual Estimates of Methane Emissions in a Phragmites Australis (Cav.) Trin. ex Steud. Dominated Restored Coastal Brackish Fen. Wetlands 34, 593–602. doi:10.1007/s13157-014-0528-z

Koebsch, F., Jurasinski, G., Koch, M., Hofmann, J., Glatzel, S., 2015. Controls for multi-scale temporal variation in ecosystem methane exchange during the growing season of a permanently inundated fen. Agric. For. Meteorol. 204, 94–105. doi:10.1016/j.agrformet.2015.02.002

Koebsch, F., Winkel, M., Liebner, S., Liu, B., Westphal, J., Spitzy, A., Gehre, M., Jurasinski, G., Köhler, S., Unger, V., Koch, M., Sachs, T., Böttcher, M.E., 2019. Sulfate deprivation triggers high methane production in a disturbed and rewetted coastal peatland. Biogeosciences 16, 1937–1953. doi:10.5194/bg-2018-416

Koehler, A.-K., Murphy, K., Kiely, G., Sottocornola, M., 2009. Seasonal variation of DOC concentration and annual loss of DOC from an Atlantic blanket bog in South Western Ireland. Biogeochemistry 95, 231–242. doi:10.1007/s10533-009-9333-9

Kolp, O., 1957. Die nordöstliche Heide Mecklenburgs : Rostocker Heide, Gelbensander Forst, Forst Alte Heide, Ribnitzer Forst, Abhandlungen / Geographische Gesellschaft in der Deutschen Demokratischen Republik 1. Dt. Verl. der Wiss., Berlin.

Kotwicki, L., Grzelak, K., Czub, M., Dellwig, O., Gentz, T., Szymczycha, B., Böttcher, M.E., 2014. Submarine groundwater discharge to the Baltic coastal zone: Impacts on the meiofaunal community. J. Mar. Syst. 129, 118–126. doi:https://doi.org/10.1016/j.jmarsys.2013.06.009

Kreuzburg, M., Ibenthal, M., Janssen, M., Rehder, G., Voss, M., Naumann, M., Feldens, P., 2018. Sub-marine Continuation of Peat Deposits From a Coastal Peatland in the Southern Baltic Sea and its Holocene Development. Front. Earth Sci. 6. doi:10.3389/feart.2018.00103

Kreuzburg, M., Rezanezhad, F., Milojevic, T., Voss, M., Gosch, L., Liebner, S., Van Cappellen, P., Rehder, G., 2020. Carbon release and transformation from coastal peat deposits controlled by submarine groundwater discharge: a column experiment study. Limnol. Oceanogr. 65, 1116–1135. doi:10.1002/lno.11438

Kruse, J., Lennartz, B., Leinweber, P., 2008. A modified method for measuring saturated hydraulic conductivity and anisotropy of fen peat samples. WETLANDS 28, 527–531.

Küsel, K., Blöthe, M., Schulz, D., Reiche, M., Drake, H.L., 2008. Microbial reduction of iron and porewater biogeochemistry in acidic peatlands. Biogeosciences 5, 1537–1549. doi:10.5194/bg-5-1537-2008

Kuzyakov, Y., Friedel, J.K., Stahr, K., 2000. Review of mechanisms and quantification of priming effects. Soil Biol. Biochem. 32, 1485–1498. doi:https://doi.org/10.1016/S0038-0717(00)00084-5

Lamers, L.P.M., Tomassen, H.B.M., Roelofs, J.G.M., 1998. Sulfate-induced eutrophication and phytotoxicity in freshwater wetlands. Environ. Sci. Technol. 32, 199–205. doi:10.1021/es970362f

Larsen, M., Borisov, S.M., Grunwald, B., Klimant, I., Glud, R.N., 2011. A simple and inexpensive high resolution color ratiometric planar optode imaging approach: application to oxygen and pH sensing. Limnol. Oceanogr. Methods 9, 348–360. doi:https://doi.org/10.4319/lom.2011.9.348

Lasak, S., Hahn, J., Jurasinski, G., Köhler, S., Glatzel, S., 2010. Methanfreisetzungen im Rahmen des Auftauens eines überfluteten Küstenmoors. Aktuelle Probl. im Wasserhaushalt von Nord. Trends, Ursachen, Lösungen. Sci. Tech. Rep. 10, 129–132.

Laverman, A.M., Pallud, C., Abell, J., Cappellen, P. Van, 2012. Comparative survey of potential nitrate and sulfate reduction rates in aquatic sediments. Geochim. Cosmochim. Acta 77, 474–488. doi:10.1016/j.gca.2011.10.033

Li, L., Barry, D.A., Stagnitti, F., Parlange, J.Y., 1999. Submarine groundwater discharge and associated chemical input to a coastal sea. Water Resour. Res. 35, 3253–3259. doi:10.1029/1999WR900189

Li, Y., Yu, S., Strong, J., Wang, H., 2012. Are the biogeochemical cycles of carbon, nitrogen, sulfur, and phosphorus driven by the “FeIII–FeII redox wheel” in dynamic redox environments? J. Soils Sediments 12, 683–693. doi:10.1007/s11368-012-0507-z

Limpens, J., Berendse, F., Blodau, C., Canadell, J.G., Freeman, C., Holden, J., Roulet, N., Rydin, H., Schaepman-Strub, G., 2008. Peatlands and the carbon cycle: From local processes to global implications - A synthesis. Biogeosciences 5, 1475–1491. doi:10.5194/bg-5-1475-2008

Litaor, M.I., Reichmann, O., Auerswald, K., Haim, A., Shenker, M., 2004. The Geochemistry of Phosphorus in Peat Soils of a Semiarid Altered Wetland. Soil Sci. Soc. Am. J. 68, 2078–2085. doi:10.2136/sssaj2005.0068

Liu, D.Y., Ding, W.X., Jia, Z.J., Cai, Z.C., 2011. Relation between methanogenic archaea and methane production potential in selected natural wetland ecosystems across China. Biogeosciences 8, 329–338. doi:10.5194/bg-8-329-2011

Liu, H., Forsmann, D.M., Kjærgaard, C., Saki, H., Lennartz, B., 2017. Solute Transport Properties of Fen Peat Differing in Organic Matter Content. J. Environ. Qual. 46, 1106–1113. doi:10.2134/jeq2017.01.0031

Liu, H., Janssen, M., Lennartz, B., 2016. Changes in flow and transport patterns in fen peat following soil degradation. Eur. J. Soil Sci. 67, 763–772. doi:10.1111/ejss.12380

Liu, H., Lennartz, B., 2019a. Hydraulic properties of peat soils along a bulk density gradient—A meta study. Hydrol. Process. 33, 101–114. doi:10.1002/hyp.13314

Liu, H., Lennartz, B., 2019b. Short Term Effects of Salinization on Compound Release from Drained and Restored Coastal Wetlands. Water 11.

Luo, M., Huang, J.-F., Zhu, W.-F., Tong, C., 2019. Impacts of increasing salinity and inundation on rates and pathways of organic carbon mineralization in tidal wetlands: a review. Hydrobiologia 827, 31–49. doi:10.1007/s10750-017-3416-8

Lyman, J., 1969. Redefinition of salinity and chlorinity. Limnol. Oceanogr. 14, 928–929. doi:https://doi.org/10.4319/lo.1969.14.6.0928

Mandernack, K.W., Lynch, L., Krouse, H.R., Morgan, M.D., 2000. Sulfur cycling in wetland peat of the New Jersey Pinelands and its effect on stream water chemistry. Geochim. Cosmochim. Acta 64, 3949–3964.

Marschner, B., Kalbitz, K., 2003. Controls of bioavailability and biodegradability of dissolved organic matter in soils. Geoderma 113, 211–235. doi:10.1016/S0016-7061(02)00362-2

Martinez, C.E., Kleinschmidt, A.W., Tabatabai, M.A., 1998. Sulfate adsorption by variable charge soils: Effect of low-molecular-weight organic acids. Biol. Fertil. Soils 26, 157–163. doi:10.1007/s003740050361

McCarter, C.P.R., Weber, T.K.D., Price, J.S., 2018. Competitive transport processes of chloride, sodium, potassium, and ammonium in fen peat. J. Contam. Hydrol. 217, 17–31. doi:10.1016/j.jconhyd.2018.08.004

Meier-Uhlherr, R., Schulz, C., Luthardt, V., 2011. Steckbriefe Moorsubstrate. HNE Eberswalde, Berlin.

Meyer-Jacob, C., Michelutti, N., Paterson, A.M., Cumming, B.F., Keller, W., Smol, J.P., 2019. The browning and re-browning of lakes: Divergent lake-water organic carbon trends linked to acid deposition and climate change. Sci. Rep. 9, 1–10. doi:10.1038/s41598-019-52912-0

Meyers, P.A., 1997. Organic geochemical proxies of paleoceanographic, paleolimnologic, and paleoclimatic processes. Org. Geochem. 27, 213–250. doi:https://doi.org/10.1016/S0146-6380(97)00049-1

Miegel, K., Graeff, T., Selle, B., Salzmann, T., Franck, C., Bronstert, A., 2016. Untersuchung eines renaturierten Niedermoores an der mecklenburgischen Ostseeküste – Teil I: Systembeschreibung und hydrologische Grundcharakterisierung (Investigation of a renatured fen on the Baltic Sea coast of Mecklenburg – Part I: System description . Hydrol. und Wasserbewirtschaftung 60. doi:10.5675/HyWa

Montanarella, L., Jones, R.J.A., Hiederer, R., 2006. The distribution of peatland in Europe. Mires Peat 1, 1–10.

Monteith, D.T., Stoddard, J.L., Evans, C.D., De Wit, H.A., Forsius, M., Høgåsen, T., Wilander, A., Skjelkvåle, B.L., Jeffries, D.S., Vuorenmaa, J., Keller, B., Kopécek, J., Vesely, J., 2007. Dissolved organic carbon trends resulting from changes in atmospheric deposition chemistry. Nature 450, 537–540. doi:10.1038/nature06316

Moore, T.R., Dalva, M., 1993. The influence of temperature and water table position on carbon dioxide and methane emissions from laboratory columns of peatland soils. J. Soil Sci. 44, 651–664. doi:10.1111/j.1365-2389.1993.tb02330.x

Moore, W.S., 2009. The Effect of Submarine Groundwater Discharge on the Ocean. Ann. Rev. Mar. Sci. 2, 59–88. doi:10.1146/annurev-marine-120308-081019

Moore, W.S., 1999. The subterranean estuary: a reaction zone of ground water and sea water. Mar. Chem. 65, 111–125. doi:https://doi.org/10.1016/S0304-4203(99)00014-6

Mulholland, P.J., 2003. 6 - Large-Scale Patterns in Dissolved Organic Carbon Concentration, Flux, and Sources, in: Findlay, S.E.G., Sinsabaugh, R.L.B.T.-A.E. (Eds.), Aquatic Ecology. Academic Press, Burlington, pp. 139–159. doi:https://doi.org/10.1016/B978-012256371-3/50007-X

Münch, J.M., Totsche, K.U., Kaiser, K., 2002. Physicochemical factors controlling the release of dissolved organic carbon from columns of forest subsoils. Eur. J. Soil Sci. 53, 311–320. doi:10.1046/j.1365-2389.2002.00439.x

Nerem, R.S., Beckley, B.D., Fasullo, J.T., Hamlington, B.D., Masters, D., Mitchum, G.T., 2018. Climate-change–driven accelerated sea-level rise detected in the altimeter era. Proc. Natl. Acad. Sci. U. S. A. 115, 2022–2025. doi:10.1073/pnas.1717312115

Neubauer, S.C., 2013. Ecosystem Responses of a Tidal Freshwater Marsh Experiencing Saltwater Intrusion and Altered Hydrology. Estuaries and Coasts 36, 491–507. doi:10.1007/s12237-011-9455-x

Neubauer, S.C., Craft, C.B., 2009. Global Change and Tidal Freshwater Wetlands: Scenarios and Impacts, Tidal Freshwater Wetlands.

Nicholls, R.J., Cazenave, A., 2010. Sea-level rise and its impact on coastal zones. Science (80-.). 328, 1517–1520. doi:10.1126/science.1185782

Nieuwenhuis, H.S., Schokking, F., 1997. Land subsidence in drained peat areas of the Province of Friesland, The Netherlands. Q. J. Eng. Geol. Hydrogeol. 30, 37–48. doi:10.1144/GSL.QJEGH.1997.030.P1.04

Nieuwenhuize, J., Maas, Y.E.M., Middelburg, J.J., 1994. Rapid analysis of organic carbon and nitrogen in particulate materials. Mar. Chem. 45, 217–224. doi:https://doi.org/10.1016/0304-4203(94)90005-1

Nunes, F.L.D., Aquilina, L., de Ridder, J., Francez, A.-J., Quaiser, A., Caudal, J.-P., Vandenkoornhuyse, P., Dufresne, A., 2015. Time-scales of hydrological forcing on the geochemistry and bacterial community structure of temperate peat soils. Sci. Rep. 5, 14612. doi:10.1038/srep14612

Oremland, R.S., Marsh, L.M., Polcin, S., 1982. Methane production and simultaneous sulphate reduction in anoxic, salt marsh sediments. Nature 296, 143–145.

Ostrovsky, I., 2003. Methane bubbles in Lake Kinneret: Quantification and temporal and spatial heterogeneity. Limnol. Oceanogr. 48, 1030–1036. doi:https://doi.org/10.4319/lo.2003.48.3.1030

Ostseestiftung, 2016. Entwicklung eines Leitbildes und Differenzierung von umsetzungsbezogenen Zielzuständen für Küstenüberflutungsräume zwischen Rostock und Westrügen (Hotspot-29-Gebiet des Bundesprogramms Biologische Vielfalt). Greifswald.

Ottow, J.C.G., 2011. Mikrobiologie von Böden - Biodiversität, Ökophysiologie und Metagenomik. Springer-Verlag, Heidelberg.

Ours, D.P., Siegel, D.I., Glaser, P.H., 1997. Chemical dilation and the dual porosity of humified bog peat. J. Hydrol. 196, 348–360.

Ozuolmez, D., Na, H., Lever, M., Kjeldsen, K., Jørgensen, B., Plugge, C., 2015. Methanogenic archaea and sulfate reducing bacteria co-cultured on acetate: teamwork or coexistence? Front. Microbiol.

Pallud, C., Meile, C., Laverman, A.M., Abell, J., Cappellen, P. Van, 2007. The use of flow-through sediment reactors in biogeochemical kinetics: Methodology and examples of applications. Mar. Chem. 106, 256–271. doi:10.1016/j.marchem.2006.12.011

Pallud, C., Van Cappellen, P., 2006. Kinetics of microbial sulfate reduction in estuarine sediments. Geochim. Cosmochim. Acta 70, 1148–1162. doi:10.1016/j.gca.2005.11.002

Paul, E.A., 2016. The nature and dynamics of soil organic matter: Plant inputs, microbial transformations, and organic matter stabilization. Soil Biol. Biochem. 98, 109–126. doi:https://doi.org/10.1016/j.soilbio.2016.04.001

Peltonen, L., Koistinen, P., Karjalainen, M., Häkkinen, A., Hirvonen, J., 2002. The effect of cosolvents on the formulation of nanoparticles from low-molecular-weight poly(l)lactide. AAPS PharmSciTech 3, 52. doi:10.1208/pt030432

Plag, H.-P., Jules-Plag, S., 2013. Sea-Level Rise and Coastal Ecosystems. Clim. Vulnerability Underst. Addressing Threat. to Essent. Resour. 4, 163–184. doi:10.1016/B978-0-12-384703-4.00419-6

Plaut, Z., Edelstein, M., Ben-Hur, M., 2013. Overcoming Salinity Barriers to Crop Production Using Traditional Methods. CRC. Crit. Rev. Plant Sci. 32, 250–291. doi:10.1080/07352689.2012.752236

Portnoy, J.W., Giblin, A.E., 1997. Biogeochemical effects of seawater restoration to diked salt marshes. Ecol. Appl. 7, 1054–1063. doi:https://doi.org/10.1890/1051-0761(1997)007[1054:BEOSRT]2.0.CO;2

Porubsky, W.P., Weston, N.B., Moore, W.S., Ruppel, C., Joye, S.B., 2014. Dynamics of submarine groundwater discharge and associated fluxes of dissolved nutrients, carbon, and trace gases to the coastal zone (Okatee River estuary, South Carolina). Geochim. Cosmochim. Acta 131, 81–97. doi:10.1016/j.gca.2013.12.030

Radcliffe, D.E., Simunek, J., 2010. Soil Physics with HYDRUS: Modelling and Applications. Taylor & Francis.

Ramaswamy, V., 2001. Radiative forcing of climate change, in: Houghton, J.T., Ding, Y., Griggs, D.J., Noguer, M., Linden, P.J. van der, Dai, X., Maskell, K., Johnson, C.A. (Eds.), Climate Change 2001: The Scientific Basis. Contribution of Working Group I to the Third Assessment Report of the Intergovernmental Panel on Climate Change. Cambridge University Press, Cambridge, UK, pp. 349–416.

Rapaglia, J., 2005. Submarine groundwater discharge into Venice Lagoon, Italy. Estuaries 28, 705–713. doi:10.1007/BF02732909

Rasband, W.S., 2015. ImageJ. US National Institutes of Health, Bethesda, USA.

Rath, K.M., Rousk, J., 2015. Salt effects on the soil microbial decomposer community and their role in organic carbon cycling: A review. Soil Biol. Biochem. 81, 108–123. doi:https://doi.org/10.1016/j.soilbio.2014.11.001

Reeburgh, W.S., 1980. Anaerobic methane oxidation: Rate depth distributions in Skan Bay sediments. Earth Planet. Sci. Lett. 47, 345–352. doi:https://doi.org/10.1016/0012-821X(80)90021-7

Reeburgh, W.S., Alperin, M.J., 1988. Studies on anaerobic methane oxidation. Scope/Unep 66, 367–375.

Reemtsma, T., Bredow, A., Gehring, M., 1999. The nature and kinetics of organic matter release from soil by salt solutions. Eur. J. Soil Sci. 50, 53–64. doi:10.1046/j.1365-2389.1999.00212.x

Rezanezhad, F., Couture, R., Kovac, R., Connell, D.O., Cappellen, P. Van, 2014. Water table fluctuations and soil biogeochemistry : An experimental approach

using an automated soil column system. J. Hydrol. 509, 245–256. doi:10.1016/j.jhydrol.2013.11.036

Rezanezhad, F., Kleimeier, C., Milojevic, T., Liu, H., Weber, T.K.D., Van Cappellen, P., Lennartz, B., 2017. The Role of Pore Structure on Nitrate Reduction in Peat Soil: A Physical Characterization of Pore Distribution and Solute Transport. Wetlands 37, 951–960. doi:10.1007/s13157-017-0930-4

Rezanezhad, F., Price, J.S., Craig, J.R., 2012. The effects of dual porosity on transport and retardation in peat: A laboratory experiment. Can. J. Soil Sci. 92, 723–732. doi:10.4141/cjss2011-050

Rezanezhad, F., Price, J.S., Quinton, W.L., Lennartz, B., Milojevic, T., Van Cappellen, P., 2016. Structure of peat soils and implications for water storage, flow and solute transport: A review update for geochemists. Chem. Geol. 429, 75–84. doi:10.1016/j.chemgeo.2016.03.010

Rezanezhad, F., Quinton, W.L., Price, J.S., Elrick, D., Elliot, T.R., Heck, R.J., 2009. Examining the effect of pore size distribution and shape on flow through unsaturated peat using computed tomography. Hydrol. Earth Syst. Sci. 13, 1993–2002.

Ritson, J.P., Bell, M., Graham, N.J.D., Templeton, M.R., Brazier, R.E., Verhoef, A., Freeman, C., Clark, J.M., 2014. Simulated climate change impact on summer dissolved organic carbon release from peat and surface vegetation: Implications for drinking water treatment. Water Res. 67, 66–76. doi:10.1016/j.watres.2014.09.015

Robinson, C., Li, L., Barry, D.A., 2007. Effect of tidal forcing on a subterranean estuary. Adv. Water Resour. 30, 851–865. doi:10.1016/j.advwatres.2006.07.006

Roulet, N., Moore, T., Bubier, J., Lafleur, P., 1992. Northern fens: methane flux and climatic change. Tellus, Ser. B 44 B, 100–105. doi:10.3402/tellusb.v44i2.15429

Roulet, N., Moore, T.R., 2006. Browning the waters. Nature 444, 283–284.

Rydelek, P., Bąkowska, A., Zawrzykraj, P., 2016. Variability of cation-exchange capacity (CEC) of fen peats in vertical profiles from eastern and central poland in relation to function of Peatlands as natural geological barriers. Stud. Quat. 33, 111–116. doi:10.1515/squa-2016-0011

Sahrawat, K.L., 2003. Organic matter accumulation in submerged soils. Adv. Agron. 81, 169–201. doi:https://doi.org/10.1016/S0065-2113(03)81004-0

Santos, I.R., Eyre, B.D., Huettel, M., 2012. The driving forces of porewater and groundwater flow in permeable coastal sediments: A review. Estuar. Coast. Shelf Sci. 98, 1–15. doi:10.1016/j.ecss.2011.10.024

Säurich, A., Tiemeyer, B., Dettmann, U., Don, A., 2019. How do sand addition, soil moisture and nutrient status influence greenhouse gas fluxes from drained organic soils? Soil Biol. Biochem. 135, 71–84. doi:https://doi.org/10.1016/j.soilbio.2019.04.013

Schade, H., 2019. Respiration of sandy Baltic Sea sediments. Dissertation. University of Rostock.

Scheffer, F., Schachtschabel, P., 2002. Lehrbuch der Bodenkunde, 15th ed. Spektrum Akademischer Verlag, Heidelberg.

Schlüter, M., Sauter, E.J., Andersen, C.E., Dahlgaard, H., Dando, P.R., 2004. Spatial distribution and budget for submarine groundwater discharge in Eckernförde Bay (Western Baltic Sea). Limnol. Oceanogr. 49, 157–167. doi:10.4319/lo.2004.49.1.0157

Schmaljohann, R., 1996. Methane dynamics in the sediment and water column of Kiel Harbour (Baltic Sea). Mar. Ecol. Prog. Ser. 131, 263–273. doi:10.3354/meps131263

Schwalm, M., Zeitz, J., 2015. Concentrations of dissolved organic carbon in peat soils as influenced by land use and site characteristics - A lysimeter study. Catena 127, 72–79. doi:10.1016/j.catena.2014.12.007

Seeberg-Elverfeldt, J., Schlüter, M., Feseker, T., Kölling, M., 2005. Rhizon sampling of porewaters near the sediment-water interface of aquatic systems. Limnol. Oceanogr. Methods 3, 361–371. doi:https://doi.org/10.4319/lom.2005.3.361

Seitzinger, S.P., Harrison, J.A., 2008. Chapter 9 - Land-Based Nitrogen Sources and Their Delivery to Coastal Systems, in: Capone, D.G., Bronk, D.A., Mulholland, M.R., Carpenter, E.J.B.T.-N. in the M.E. (Second E. (Eds.), . Academic Press, San Diego, pp. 469–510. doi:https://doi.org/10.1016/B978-0-12-372522-6.00009-8

Sela-Adler, M., Ronen, Z., Herut, B., Antler, G., Vigderovich, H., Eckert, W., Sivan, O., 2017. Co-existence of Methanogenesis and Sulfate Reduction with Common Substrates in Sulfate-Rich Estuarine Sediments. Front. Microbiol.

Senesi, N., Loffredo, E., 1999. The Chemistry of Soil Organic Matter, in: Sparks, D.L. (Ed.), Soil Physical Chemistry. CRC Press, Boca Raton, pp. 239–370.

Sergeev, A., Sivkov, V., Zhamoida, V., Ryabchuk, D., Bitinas, A., Mažeika, J., 2015. Holocene organic-rich sediments within the curonian spit coast, the south-eastern baltic sea. Baltica 28, 41–50. doi:10.5200/baltica.2015.28.05

Sharp, E.L., Parsons, S.A., Jefferson, B., 2006. The impact of seasonal variations in DOC arising from a moorland peat catchment on coagulation with iron and aluminium salts. Environ. Pollut. 140, 436–443. doi:10.1016/j.envpol.2005.08.001

Sherif, M.M., Singh, V.P., 1999. Effect of climate change on sea water intrusion in coastal aquifers. Hydrol. Process. 13, 1277–1287. doi:10.1002/(SICI)1099-1085(19990615)13:8<1277::AID-HYP765>3.0.CO;2-W

Sholkovitz, E.R., 1976. Flocculation of dissolved organic and inorganic matter during the mixing of river water and seawater. Geochim. Cosmochim. Acta 40, 831–845. doi:10.1016/0016-7037(76)90035-1

Sigg, L., Stumm, W., 2011. Aquatische Chemie. vdf Hochschulverlag AG an der ETH Zürich, Zürich.

Simhayov, R.B., Weber, T.K.D., Price, J.S., 2018. Saturated and unsaturated salt transport in peat from a constructed fen. Soil 4, 63–81. doi:10.5194/soil-4-63-2018

Sirianni, M.J., Comas, X., 2020. Changes in Physical Properties of Everglades Peat Soils Induced by Increased Salinity at the Laboratory Scale: Implications for Changes in Biogenic Gas Dynamics. Water Resour. Res. 56, e2019WR026144. doi:https://doi.org/10.1029/2019WR026144

Sirin, A., Laine, J., 2008. Peatlands and greenhouse gases, in: Assessment on Peatlands, Biodiversity, and Climate Change: Main Report. Kuala Lumpur : Global Environment Centre & Wetlands International, Wageningen, pp. 118–138.

Slomp, C.P., Van Cappellen, P., 2004. Nutrient inputs to the coastal ocean through submarine groundwater discharge: Controls and potential impact. J. Hydrol. 295, 64–86. doi:10.1016/j.jhydrol.2004.02.018

St-Jean, G., 2003. Automated quantitative and isotopic (13C) analysis of dissolved inorganic carbon and dissolved organic carbon in continuous-flow using a total organic carbon analyser. Rapid Commun. Mass Spectrom. 17, 419–428. doi:https://doi.org/10.1002/rcm.926

Stadtman, T.C., Barker, H.A., 1949. Studies on the methane fermentation; tracer experiments on the mechanism of methane formation. Arch. Biochem. 21, 256–264.

Stainton, M., Capel, M.J., Armstrong, F.A., 1977. The chemical analysis of fresh water. Fish. Environ. Canada, Fish. Mar. Serv. Misc. Spec. Publ. No. 25.

Stam, M.C., Mason, P.R.D., Pallud, C., Van Cappellen, P., 2010. Sulfate reducing activity and sulfur isotope fractionation by natural microbial communities in sediments of a hypersaline soda lake (Mono Lake, California). Chem. Geol. 278, 23–30. doi:10.1016/j.chemgeo.2010.08.006

Stein, R. (Ed.), 1991. Accumulation of organic carbon in Baffin Bay and Labrador Sea sediments (ODP-Leg 105) BT - Accumulation of Organic Carbon in Marine Sediments: Results from the Deep Sea Drilling Project/Ocean Drilling Program (DSDP/ODP). Springer Berlin Heidelberg, Berlin, Heidelberg, pp. 40–84. doi:10.1007/BFb0010387

Steinmuller, H.E., Chambers, L.G., 2018. Can Saltwater Intrusion Accelerate Nutrient Export from Freshwater Wetland Soils? An Experimental Approach. Soil Sci. Soc. Am. J. 82, 283–292. doi:https://doi.org/10.2136/sssaj2017.05.0162

Sterr, H., 2008. Assessment of vulnerability and adaptation to sea-level rise for the coastal zone of Germany. J. Coast. Res. 24, 380–393. doi:10.2112/07A-0011.1

Stofberg, S.F., Klimkowska, A., Paulissen, M.P.C.P., Witte, J.-P.M., van der Zee, S.E.A.T.M., 2015. Effects of salinity on growth of plant species from terrestrializing fens. Aquat. Bot. 121, 83–90. doi:https://doi.org/10.1016/j.aquabot.2014.12.004

Strack, M., 2008. Peatlands and climate change. International Peat Society, Jyväskylä.

Strehse, R., Bohne, H., Amha, Y., Leinweber, P., 2018. The influence of salt on dissolved organic matter from peat soils. Org. Geochem. 125, 270–276. doi:10.1016/J.ORGGEOCHEM.2018.10.001

Stutter, M.I., Lumsdon, D.G., Cooper, R.J., 2007. Temperature and soil moisture effects on dissolved organic matter release from a moorland Podzol O horizon under field and controlled laboratory conditions. Eur. J. Soil Sci. 58, 1007–1016. doi:10.1111/j.1365-2389.2006.00880.x

Succow, M., Joosten, H., 2001. Landschaftsökologische Moorkunde, 2nd ed. E. Schweizerbart'sche Verlagsbuchhandlung, Stuttgart.

Taffs, K.H., Logan, B., Parr, J.F., Jacobsen, G.E., 2012. The evolution of a coastal peatland at Byron Bay, Australia: multi-proxy evidence from the microfossil record, in: Haberle, S., David, B. (Eds.), Terra Australis 34: Peopled Landscapes: Archaeological and Biogeographic Approaches to Landscapes. ANU E-press, Canberra, ACT, Australia, pp. 429–442.

Tanneberger, F., Tegetmeyer, C., Busse, S., Barthelmes, A., Shumka, S., Mariné, A.M., Jenderedjian, K., Steiner, G.M., Essl, F., Etzold, J., Mendes, C., Kozulin, A., Frankard, P., Milanović, Ganeva, A., Apostolova, I., Alegro, A., Delipetrou, P., Navrátilová, J., Risager, M., Leivits, A., Fosaa, A.M., Tuominen, S., Muller, F., Bakuradze, T., Sommer, M., Christanis, K., Szurdoki, E., Oskarsson, H., Brink, S.H., Connolly, J., Bragazza, L., Martinelli, G., Aleksāns, O., Priede, A., Sungaila, D., Melovski, L., Belous, T., Saveljić, D., De Vries, F., Moen, A., Dembek, W., Mateus, J., Hanganu, J., Sirin, A., Markina, A., Napreenko, M., Lazarević, P., Stanová, V.Š., Skoberne, P., Pérez, P.H., Pontevedra-Pombal, X., Lonnstad, J., Küchler, M., Wüst-Galley, C., Kirca, S., Mykytiuk, O., Lindsay, R., Joosten, H., 2017. The peatland map of Europe. Mires Peat 19, 1–17. doi:10.19189/MaP.2016.OMB.264

Tiemeyer, B., Albiac Borraz, E., Augustin, J., Bechtold, M., Beetz, S., Beyer, C., Drösler, M., Ebli, M., Eickenscheidt, T., Fiedler, S., Förster, C., Freibauer, A., Giebels, M., Glatzel, S., Heinichen, J., Hoffmann, M., Höper, H., Jurasinski, G., Leiber-Sauheitl, K., Peichl-Brak, M., Roßkopf, N., Sommer, M., Zeitz, J., 2016. High emissions of greenhouse gases from grasslands on peat and other organic soils. Glob. Chang. Biol. 22, 4134–4149. doi:10.1111/gcb.13303

Tiemeyer, B., Bechtold, M., Belting, S., Freibauer, A., Förster, C., Schubert, E., Dettmann, U., Frank, S., Fuchs, D., Gelbrecht, J., Jeuther, B., Laggner, A., Rosinski, E., Leiber-sauheitl, K., Sachteleben, J., Zak, D., Drösler, M., 2017a. Moorschutz in Deutschland – Optimierung des Moormanagements in Hinblick auf den Schutz der Biodiversität und der Ökosystemleistungen. doi:10.19217/skr462

Tiemeyer, B., Pfaffner, N., Frank, S., Kaiser, K., Fiedler, S., 2017b. Pore water velocity and ionic strength effects on DOC release from peat-sand mixtures: Results from laboratory and field experiments. Geoderma 296, 86–97. doi:10.1016/j.geoderma.2017.02.024

Tipping, E., Hurley, M.A., 1988. A model of solid-solution interactions in acid organic soils, based on the complexation properties of humic substances. J. Soil Sci. 39, 505–519. doi:https://doi.org/10.1111/j.1365-2389.1988.tb01235.x

Toride, N., Leij, F.J., van Genuchten, M.T., 1999. The CXTFIT Code for Estimating Transport Parameters from Laboratory or Field Tracer Experiments. Version 2.1. Research Report 137, US Salinity Laboratory, Agricultural Research Service, US Department of Agriculture, Riverside, California.

Tully, K., Gedan, K., Epanchin-Niell, R., Strong, A., Bernhardt, E.S., Bendor, T., Mitchell, M., Kominoski, J., Jordan, T.E., Neubauer, S.C., Weston, N.B., 2019. The invisible flood: The chemistry, ecology, and social implications of coastal saltwater intrusion. Bioscience 69, 368–378. doi:10.1093/biosci/biz027

Upstill-Goddard, R.C., 2006. Air–sea gas exchange in the coastal zone. Estuar. Coast. Shelf Sci. 70, 388–404. doi:https://doi.org/10.1016/j.ecss.2006.05.043

van der Welle, M.E.W., Smolders, A.J.P., Op Den Camp, H.J.M., Roelofs, J.G.M., Lamers, L.P.M., 2007. Biogeochemical interactions between iron and sulphate in freshwater wetlands and their implications for interspecific competition between aquatic macrophytes. Freshw. Biol. 52, 434–447. doi:10.1111/j.1365-2427.2006.01683.x

van Diggelen, J.M.H., Lamers, L.P.M., Loermans, J.H.T., Rip, W.J., Smolders, A.J.P., 2020. Towards more sustainable hydrological management and land use of drained coastal peatlands-a biogeochemical balancing act. Mires Peat 26, 1–12. doi:10.19189/MaP.2019.APG.StA.1771

van Dijk, G., Nijp, J.J., Metselaar, K., Lamers, L.P.M., Smolders, A.J.P., 2017. Salinity-induced increase of the hydraulic conductivity in the hyporheic zone of coastal wetlands. Hydrol. Process. 31, 880–890. doi:10.1002/hyp.11068

van Genuchten, M.T., Wierenga, P.J., 1976. Mass Transfer Studies in Sorbing Porous Media I. Analytical Solutions. Soil Sci. Soc. Am. J. 40, 473–480. doi:10.2136/sssaj1976.03615995004000040011x

van Winden, J.F., Reichart, G.-J., McNamara, N.P., Benthien, A., Damsté, J.S.S., 2012. Temperature-Induced Increase in Methane Release from Peat Bogs: A Mesocosm Experiment. PLoS One 7, e39614.

Vile, M.A., Bridgham, S.D., Wieder, R.K., 2003. Response of Anaerobic Carbon Mineralization Rates to Sulfate Amendments in a Boreal Peatland. Ecol. Appl. 13, 720–734.

Voigtländer, U., Schmidt, J., Scheller, W., 1996. Pflege- und Entwicklungsplan Naturschutzgebiet Heiligensee und Hütelmoor.

von Post, L., 1922. Sveriges Geologiska Undersöknings torvinventering och några av dess hittills vunna resultat. Sven. Mosskulturfören. Tidskr. 36, 1–27.

Vuillemin, A., Horn, F., Friese, A., Winkel, M., Alawi, M., Wagner, D., Henny, C., Orsi, W.D., Crowe, S.A., Kallmeyer, J., 2018. Metabolic potential of microbial communities from ferruginous sediments. Environ. Microbiol. 20, 4297–4313. doi:https://doi.org/10.1111/1462-2920.14343

Wang, H., Richardson, C.J., Ho, M., Flanagan, N., 2016. Drained coastal peatlands: A potential nitrogen source to marine ecosystems under prolonged drought and heavy storm events—A microcosm experiment. Sci. Total Environ. 566–567, 621–626. doi:10.1016/j.scitotenv.2016.04.211

Wang, M., Liu, H., Zak, D., Lennartz, B., 2020. Effect of anisotropy on solute transport in degraded fen peat soils. Hydrol. Process. 34, 2128–2138. doi:10.1002/hyp.13717

Watt, M., Silk, W.K., Passioura, J.B., 2006. Rates of root and organism growth, soil conditions, and temporal and spatial development of the rhizosphere. Ann. Bot. 97, 839–855. doi:10.1093/aob/mcl028

Weber, T., Wiseman, N.A., Kock, A., 2019. Global ocean methane emissions dominated by shallow coastal waters. Nat. Commun. 10, 1–10. doi:10.1038/s41467-019-12541-7

Wen, X., Unger, V., Jurasinski, G., Koebsch, F., Horn, F., Rehder, G., Sachs, T., Zak, D., Lischeid, G., Knorr, K.-H., Böttcher, M., Winkel, M., Liebner, S., 2018. Predominance of methanogens over methanotrophs contributes to high methane emissions in rewetted fens. Biogeosciences Discuss. 1–37. doi:10.5194/bg-2018-184

Wen, Y., Bernhardt, E.S., Deng, W., Liu, W., Yan, J., Baruch, E.M., Bergemann, C.M., 2019. Salt effects on carbon mineralization in southeastern coastal wetland soils of the United States. Geoderma 339, 31–39. doi:https://doi.org/10.1016/j.geoderma.2018.12.035

Weston, N.B., Dixon, R.E., Joye, S.B., 2006. Ramifications of increased salinity in tidal freshwater sediments: Geochemistry and microbial pathways of organic matter mineralization. J. Geophys. Res. Biogeosciences 111, 1–14. doi:10.1029/2005JG000071

Weston, N.B., Vile, M.A., Neubauer, S.C., Velinsky, D.J., 2011. Accelerated microbial organic matter mineralization following salt-water intrusion into tidal freshwater marsh soils. Biogeochemistry 102, 135–151. doi:10.1007/s10533-010-9427-4

Whiticar, M.J., Faber, E., Schoell, M., 1986. Biogenic methane formation in marine and freshwater environments: CO2 reduction vs. acetate fermentation-Isotope evidence. Geochim. Cosmochim. Acta 50, 693–709. doi:10.1016/0016-7037(86)90346-7

Wieder, R.K., Lang, G.E., 1988. Cycling of inorganic and organic sulfur in peat from Big Run Bog, West Virginia. Biogeochemistry 5, 221–242.

Worrall, F., Gibson, H.S., Burt, T.P., 2007. Modelling the impact of drainage and drain-blocking on dissolved organic carbon release from peatlands. J. Hydrol. 338, 15–27. doi:10.1016/j.jhydrol.2007.02.016

Zak, D., Gelbrecht, J., 2007. The mobilisation of phosphorus, organic carbon and ammonium in the initial stage of fen rewetting (a case study from NE Germany). Biogeochemistry 85, 141–151. doi:10.1007/s10533-007-9122-2

Zak, D., Goldhammer, T., Cabezas, A., Gelbrecht, J., Gurke, R., Wagner, C., Reuter, H., Augustin, J., Klimkowska, A., McInnes, R., 2018. Top soil removal reduces water pollution from phosphorus and dissolved organic matter and lowers methane emissions from rewetted peatlands. J. Appl. Ecol. 55, 311–320. doi:10.1111/1365-2664.12931

Zak, D., Wagner, C., Payer, B., Augustin, J., Gelbrecht, J., 2010. Phosphorus mobilization in rewetted fens: The effect of altered peat properties and implications for their restoration. Ecol. Appl. 20, 1336–1349. doi:10.1890/08-2053.1

Zauft, M., Fell, H., Glasser, F., Rosskopf, N., Zeitz, J., 2010. Carbon storage in the peatlands of Mecklenburg-Western Pomerania , north-east Germany. Mires Peat 6, 1–12.

Zehnder, A.J.B., Mitchell, R., 1978. Ecology of methane formation. Water Pollut. Microbiol. 2, 349–376.

Zeitz, J., Velty, S., 2002. Soil properties of drained and rewetted fen soils. J. Plant Nutr. Soil Sci. 165, 618–626. doi:10.1002/1522-2624(200210)165:5<618::AID-JPLN618>3.0.CO;2-W

Zhang, B., Tian, H., Lu, C., Chen, G., Pan, S., Anderson, C., Poulter, B., 2017. Methane emissions from global wetlands: An assessment of the uncertainty associated with various wetland extent data sets. Atmos. Environ. 165, 310–321. doi:https://doi.org/10.1016/j.atmosenv.2017.07.001